Spatially-Informed Demand-Side Policies for Green Hydrogen Diffusion in Europe - Supplementary Notes

Contents

Contents

1 Supplementary Notes to Diffusion, Cost Competitiveness and Spatial Spillovers

1.1 SN1: European H_2 policy landscape

The EU has set ambitious targets for green H_2 deployment. By 2030, it aims to produce 10 Mt domestically and import an additional 10 Mt from outside the EU.[1] To advance these objectives, the EU and 18 of its 27 Member States have adopted dedicated green H_2 strategies.[1,2] These strategies are supported by a portfolio of policy instruments. To establish the institutional context necessary for interpreting our results, we provide an overview of these policies (as of February 2026) in Supplementary Table 1.

Supplementary Table 1 Overview of policy instruments relevant for green H_2 (structured into EU and member state level, and H_2 vs technology neutral; then sorted by funding volume)

Instrument	Level	Technology	Description	Type	Sector-based	Place-based	Allocation mechanism	Funding	Source
European Hydrogen Bank (EHB)	EU	H_2	Fixed-premium auctions supporting renewable H_2 production projects to reduce the cost gap between H_2 and fossil incumbents.	Supply	Partly[i]	No	Competitive auction; pass/fail eligibility screening (financial maturity, "do-no-harm", additionality); qualified projects ranked by bid price until budget exhaustion.	EUR 3.3 bn total (EUR 1.3 bn in 3rd 2025 auction) funded through the Innovation Fund.	3,4
European Hydrogen Valleys	EU	H_2	Portfolio of grant-based instruments intended to create regional H_2 ecosystems covering the full H_2 value chain, including production, infrastructure and end-use.	Mixed	No	Yes	Multi-criteria evaluation (project scale, value chain integration, geographic scope, sector diversity)	EUR 250 mn total (EUR 80 mn in 2025 call) under Horizon Europe / Hydrogen Joint Undertaking.	5
Innovation Fund (regular calls)	EU	Neutral	Competitive support for innovative early-stage decarbonization projects (H_2 projects are eligible).	Supply	No	No	Composite scoring reflecting cost efficiency, abatement potential, innovation, maturity and scalability; funding allocated to highest-scoring projects.	EUR 40bn between 2020-2030, 2.9 bn in 2025 funded by ETS revenues; $\sim$1/3 to green H_2.	6
EU Just Transition Fund	EU	Neutral	Regional grants supporting economic restructuring in regions disproportionately affected by the energy transition; H_2 eligible if aligned with territorial plan objectives.	Mixed	No	Yes	Allocation via approved territorial just transition plans and associated project pipelines.	EUR 19.7 bn total (not specific to green H_2).	7
Mandatory portfolio standards	EU	Neutral[iii]	Regulatory obligations mandating minimum shares for low-carbon fuels and energy carriers in aviation, maritime and industrial H_2 use.	Demand	Yes	No	Quota or intensity mandates.	Regulatory instrument (no budget).	8–10
IPCEI Hydrogen	Member state	H_2	State-aid framework enabling member states to support strategically relevant H_2 value-chain projects.	Mixed	Partly	No	Assessed under IPCEI compatibility rules and strategic relevance; no single EU-wide ranking procedure.	Approved state aid EUR 5.4 bn (Hy2Tech), EUR 7 bn (Hy2Use), EUR 5.4 bn (Hy2Infra), EUR 1.4 bn (Hy2Move).	11,12
Klimaschutzverträge (German CCfDs)	Member state (DE)	Neutral	Fixed CO_2 price for verified emissions reductions over a defined period, with payments adjusted to the EU ETS price, thereby compensating the incremental cost of technology switching and reducing investment uncertainty.	Demand	Yes	No	Ranked by cost per ton CO_2 avoided.	EUR 6 bn (2026 budget).	13
H2Global	Member state (DE, NL)	H_2	Double-auction mechanism that matches long-term supply contracts with shorter-term offtake tenders and bridges price gaps to enable market formation and improve H_2 bankability.	Supply	Partly[ii]	No	Weighted bid score (90% price, 10% delivery quantity) with additional qualification criteria.	Germany: EUR 3 bn (2026); Netherlands: EUR 33 mn.	14

Notes: [i] 3rd auction is structured into three topics: Renewable Fuel from Non-Biological Origin (RFNBO)-General, RFNBO and Electrolytic Low-carbon H_2-General, and Maritime and Aviation. [ii] Structured by H_2 derivative or product category.[iii] ReFuelEU Aviation mandates a minimum share of RFNBO e-fuels (35%). Note that this table does not aim to be fully exhaustive with respect to member state-level policies under which H_2 may be eligible.

The largest share of EU-level public funding is allocated through supply-side measures, most notably the European Hydrogen Bank (EHB) auctions funded through the Innovation Fund. At the same time, several instruments – such as the European Hydrogen (EU H_2) Valleys and member state-level programs – are mixed or incorporate demand-side elements. Germany's H_2 Global program, for example, is designed to match long-term supply contracts with shorter-term offtake agreements, which reduces offtake risk and the price gap with respect to fossil incumbents. As offtake risk is an important barrier to financing H_2 projects,[15] this is a highly relevant aspect of policy-making: in the second EHB auction (grant agreements completed in January 2026), signed contracts amounted to only EUR 271 mn, compared to a budget of EUR 1.2 bn (22.5%). The attrition partially reflects uncertainty with regard to size and structure of demand.[16]

While the highest-volume instruments, most notably the EHB auctions, allocate support almost exclusively on the basis of subsidy requirements, several programs incorporate additional criteria aligned with broader strategic objectives. In particular, the EU H_2 Valleys initiative explicitly seeks to create regional institutional capacity and "anchor" demand and supply, closely related to the concept of spatial spillovers explored in this paper (see Supplementary Note 2).[5] IPCEI Hydrogen aims to strengthen European competitiveness in strategic sectors and establish integrated value chains. The EU Just Transition Fund, in turn, emphasizes regional resilience and structural transformation.[11]

Our research design reflects the existing European policy landscape in three ways. First, we examine whether, controlling for sector, cost competitiveness and size, directing support towards green H_2 offtakers that are spatially central leads to more favorable policy outcomes, in terms of policy cost competitiveness, than a spatially-neutral allocation. In other words, we assess whether instruments that allocate support primarily on the basis of cost competitiveness could yield superior outcomes if they incorporated qualitative demand-side considerations such as spatial centrality, as is routinely done, for example, in offshore wind auctions.[17,18] Second, while the empirical focus of our research lies on demand-side interventions, our results are directly transferable to supply-side instruments, most notably EHB auctions: to this purpose, we assess whether incorporating demand-side elements, in the present case a demand-side spatial spillover criterion, into an EHB-style supply-side auction improves policy cost effectiveness, the key EHB policy objective, compared to an award mechanism based solely on subsidy requirements. Third, we assess whether policy instruments that already incorporate spatial considerations, such as the EU H_2 Valleys program, whose stated objective is to "kickstart" a low-carbon H_2 economy, target regions with high spatial spillover potential. This approach enables us to formulate policy recommendations that connect explicitly to the existing European policy framework (see the Discussion in the main article).

1.2 SN2: Defining spatial spillovers

The rate of diffusion of energy technologies reflects a trade-off between cost and risk for entrants relative to incumbent technologies, but it is also shaped by factors that extend beyond techno-economic considerations. This includes a broader set of technology- and system-specific characteristics that affect the perceived risk and feasibility of technology adoption. Technology-specific characteristics include modularity, that is, the extent to which a technology is composed of self-contained and standardized units, and retrofitability, or the degree to which a technology can be integrated into existing assets. Another important factor is whether the technology depends on a new system that entails new infrastructure, related technologies and institutions, such as established market arrangements and legal frameworks that enable trade in the technology.[19,20] The relative importance of these factors may depend on the stage of technology diffusion.[20]

In this context, spatial spillovers are defined as demand-side interdependencies where the presence of existing adopters increases the likelihood of adoption for installations in geographic proximity. In economic terms, spatial spillovers can be interpreted as positive spatial externalities that affect adoption probabilities through non-price channels. These spillovers can occur both on a firm or individual level[21–23] and on a regional level, where a high level of adoption in one geography has a positive effect on adoption in a neighboring region.[24–26]

The economic geography literature and the literature on the diffusion of energy technologies document several possible parallel mechanisms that support the presence of spatial spillovers. In the

case of green H_2 demand, these include shared infrastructure, supply-chain materialization, knowledge spillovers, peer and neighborhood effects and policy spillovers. Below, we summarize the most relevant mechanisms and explain how they are relevant for the diffusion of green H_2 demand.

Shared infrastructure: Energy technologies that are not fully modular and retrofittable often depend on the concurrent development of complementary infrastructure, including supply, transmission, distribution, storage, and associated market arrangements.[20,27] This was the case, for example, for the diffusion of natural gas-based power generation, which required the scale-up of upstream gas extraction, pipeline transmission and distribution networks and gas markets.[20] A similar logic applies to green H_2 demand, which depends on the expansion of renewable generation and electrolysis capacity and, depending on the production configuration, transmission, distribution, and storage infrastructure, as well as markets for trade.[28] In both cases, infrastructure investments are spatially concentrated and generate benefits for nearby adopters, making shared infrastructure a central source of spatial spillovers.

Supply-chain materialization: Beyond shared infrastructure, technology diffusion relies on the local presence of equipment and raw material suppliers, as well as specialized engineering and installation capabilities (e.g., for setting up shared infrastructure or retrofitting production facilities for the use of a new energy technology). Spatial spillovers can result from the co-location of these suppliers and service providers and industrial users. In the case of heat pumps, for example, spatial spillovers have been linked to supply-chain materialization in installation capabilities.[21] While demand for green H_2 is heterogeneous, as processes differ across sectors (Supplementary Note 6), similarities remain in the need for equipment, engineering, and installation capabilities, at least with respect to shared supply, transmission, distribution, and storage infrastructure. Further, co-location of suppliers and service providers often occurs across different components or technologically related industries, which makes it possible for supply chain materialization to occur even for distinct green H_2 demand applications.[29–31]

Knowledge spillovers: Diffusion also depends on tacit knowledge that is not fully codified and is transmitted through direct interaction, learning-by-doing, and repeated project development. Even where technical knowledge is largely codified, tacit knowledge often remains important for system integration, retrofitting, and operational learning: in renewable energy generation, spatial spillovers have been linked to localized knowledge stocks, proximity to research institutions, and regionally targeted public research support.[24] As with supply-chain materialization, similar dynamics are plausible for green H_2 demand.

Peer and neighborhood effects: Spatial spillovers may arise through imitation and neighborhood effects, whereby actors update beliefs and expectations based on observed adoption by peers. Such effects have been documented for a range of energy technologies, including rooftop photovoltaics[22,23] and electric vehicles.[32] Notably, these studies focus on consumer-facing technologies. While peer and neighborhood effects are likely to operate differently in firm or industrial settings, we cannot exclude that they may still condition adoption decisions.

Policy spillovers: Diffusion can be shaped by geographically bounded policies and regulations. "Policy spillovers" can arise, for example, when the success of a policy in one jurisdiction induces adoption of similar policies in neighboring jurisdictions.[33] Although many green H_2 support programs are administered at the EU level (Supplementary Table 1), similar mechanisms remain plausible in the case of green H_2.

Much of the existing literature on spatial spillovers in green energy technologies focuses on consumer-facing technologies, including rooftop photovoltaics,[23] electric vehicles,[32] solar-battery integration[34] and heat pumps[21] and often emphasizes peer and neighborhood effects as well as supply-chain materialization. Spillovers have also been documented beyond consumer-facing technologies, for example for renewable portfolio standards[26]. We posit that in the case of green H_2, spatial spillovers will partly follow those observed for consumer-facing technologies but operate primarily through the first three mechanisms listed above, shared infrastructure, supply-chain materialization, and knowledge spillovers. This mirrors the structure of spatial spillovers in natural gas power generation (see Supplementary Note 3 for a detailed discussion of these parallels).

1.3 SN3: Natural gas power generation as historical analogue for green H_2 demand

To guide our choice of historical analogue and document it transparently, we draw on Roberts and Nemet's Systematic Historical Analogue Research for Decision-making (SHARD) approach.[35] SHARD offers a structured and theory-informed framework to identify historical cases that exhibit structural similarity to a target technology. Rather than requiring similarity across all dimensions, the approach prioritizes alignment along those characteristics that are central to the analytical objective.

To select the most appropriate analogue, we proceed in four steps, where the first three steps follow the SHARD procedure and the fourth includes additional considerations on the robustness of our analogue choice. First, we clarify the objective of the historical analogue search. Second, we define a set of target characteristics for green H_2 demand based on the SHARD dimensions and, to reflect the core of our study, spatial spillover mechanisms (Supplementary Note 2). Third, we select an analogue from a broad set of available technology datasets based on the closest analytical fit to green H_2 demand, again considering both the SHARD dimensions and spatial spillover mechanisms. Finally, we address specific considerations that are critical for assessing the fit between green H_2 and natural gas power plants, our selected historical analogue.

Step 1: Clarification of research objective

We begin by clarifying the research objective. In our study, the historical analogue provides the empirical foundation to construct a model of green H_2 demand that is driven primarily by cost competitiveness and spatial spillovers. We then use forward-looking projections from this model as a baseline for policy evaluation. Therefore, the central requirement for the historical analogue is that its historical diffusion process structurally resembles that expected for green H_2. In particular, the spatial spillovers observed in the analogue context must be transferable to green H_2 demand. Concretely, the analogue must exhibit the core spatial spillover mechanisms identified for green H_2 in Supplementary Note 2, namely shared infrastructure, supply chain materialization and knowledge spillovers.

Step 2: Assessment of target characteristics for green H_2 demand

Target characteristics based on the SHARD method

For identifying target characteristics, Roberts and Nemets propose structuring the analysis across five domains: technological and infrastructural characteristics, economic and financial characteristics, policy and political characteristics, social and cultural characteristics and user and consumption characteristics.[35] Importantly, the focus of our research is green H_2 *demand* and not production. Many important characteristics of H_2 production – such as siting flexibility or feedstock variability – are therefore not directly relevant to this exercise.

Technological and infrastructural characteristics: Malhotra and Schmidt propose evaluating technological characteristics with particular attention to design complexity and the need for customization.[36] H_2 is of low volumetric energy density and specific handling requirements, rendering it technically more complex than conventional fuels. Although green H_2 demand spans multiple use cases, these are characterized by similarly high levels of complexity, with multiple sub-components integrated into complex processes and systems, as well as significant customization needs driven by site-specific conditions such as access to H_2 infrastructure. This infrastructure, encompassing supply, transport, storage, and delivery, is consistent and shared across all green H_2 demand applications. Storage plays a central role in smoothing load profile variability; salt caverns are promising but geographically constrained, while above-ground tanks are costly and limited in scale.[37] Adoption frequently requires partial or complete redesign of existing processes or equipment, and modularity and standardization remain limited across sectors.[37,38] In addition, many offtake sectors require high purity and pressure levels, which further increase complexity at the interface between supply and demand.[38]

The spatial distribution of demand reflects existing industrial structures, for example for refining, steel, and chemicals (such as ammonia or methanol), although it may somewhat shift when additional demand sources, where green H_2 is less competitive to other decarbonization options (such as heating,

see Supplementary Note 6), are considered. Infrastructure interdependencies are extensive: demand-side adoption is often conditional on concurrent progress in H_2 delivery and storage infrastructure. Leveraging existing natural gas infrastructure could ease build-out requirements,[39] but requires the resolution of technical challenges related to structural integrity and safety of operations.[40,41]

Economic and financial characteristics: Green H_2 to date remains economically uncompetitive with fossil incumbents (1-5 times more expensive) depending on the sector and geography, even though costs are expected to decrease significantly.[42] Still, green H_2 costs and pricing are highly uncertain, and dependent on the trajectory of several uncertain input components, including renewable electricity, electrolyzer costs and carbon prices.[43] Capital intensity is high for conversion and retrofit of demand-side assets, with long payback periods and high sensitivity to utilization rates.[38] Offtake agreements are closely tied to financing conditions and usually long term. Bloomberg New Energy Finance's (BNEF) offtaker database reports a median contract length of 15 years, with a range between 7 and 30 years.[44] Similarly, existing policy support measures including CfD regimes typically range between 10 and 15 years.[45]

Policy and political characteristics: The EU as well as 18 of its national governments have adopted green H_2 strategies.[1,2] Existing policy measures include primarily supply-side auctions administered by the European H_2 bank[46] and demand-side portfolio standards for industrial H_2,[10] aviation[8] and shipping.[9] Eligibility for incentives is often tied to stringent certification criteria (e.g. additionality)[47] increasing complexity. A detailed overview of policy instruments is provided in Supplementary Table 1. In the context of policy and political characteristics, the purpose of the empirical model is to provide a projection that can serve as a baseline for subsequent policy evaluation. Accordingly, the technology analogue should, as far as possible, abstract from current policy support mechanisms while still reflecting the structural features that condition H_2 demand adoption in key sectors.

Social and cultural characteristics: Social acceptance of green H_2 varies by sector and end use. It is seen as a high-credibility solution for hard-to-abate industrial applications but faces skepticism in low-temperature heat or passenger transport.[48]

User and consumption characteristics: Green H_2 competes not only with fossil incumbents but also with alternative low-carbon options such as direct electrification, and carbon capture, utilization and storage (CCUS).[37] Demand potential is concentrated with large customers in sectors where these other decarbonization technologies are either technically unfeasible or economically less competitive. These include high-temperature industrial heat (e.g., steel, ceramics, glass), chemical feedstocks (e.g., ammonia, methanol), and selected transport modes (aviation, maritime, heavy duty transport) (see Supplementary Note 6). Retail offtake is limited to a narrow range of applications (heat, road transport), where technical efficiency and cost competitiveness typically fall short of other decarbonization alternatives.[49,50]

Target characteristics based on spatial spillover mechanisms

In addition to the dimensions proposed in the SHARD process, our historical analogue assessment also incorporates the structure of spatial spillovers, following the mechanisms identified in Supplementary Note 2. In the case of green H_2, we expect spatial spillovers to occur primarily through shared infrastructure, supply chain materialization and knowledge spillovers.

Green H_2 demand relies strongly on the concurrent scale-up of infrastructure that connects demand to supply, including transmission, distribution and storage infrastructure. This induces strong spatial interdependencies in the adoption of green H_2 by installations in geographic proximity, related to the presence and the possibility to share the cost for this infrastructure.

Green H_2 demand covers several processes across transport, heating, and industry. These include fuel and fuel cell applications in transport, process heat, and the use of green H_2 as a feedstock in refining, chemicals, and iron & steel. While this diversity may somewhat moderate spillovers arising from highly specialized supply chains and sector-specific knowledge, significant spatial spillovers from supply chain development and knowledge diffusion can still be expected (see Step 4 – special considerations for further detail). Importantly, green H_2 demand applications and technologies are structurally comparable in terms of complexity and customization needs. This supports cross-sector

linkages, including shared requirements for equipment manufacturing, engineering services, and installation capabilities. Since all applications rely on common green H_2 supply infrastructure, spillovers linked to both supply chain materialization and knowledge exchange are also likely to arise through shared infrastructure development (see Supplementary Note 2).

The intensity of spatial spillovers depends on the overall extent of diffusion. If a technology diffuses only marginally, the resulting spillovers are likely to be limited. Importantly, in the present setting this does not affect the selection of a historical analogue. We control for these feedback mechanisms through the choice of saturation rates in the main analysis (see Methods and Supplementary Note 6). Lower saturation rates mechanically result in lower spillover pressure, whereas higher saturation rates imply stronger spillover pressure, irrespective of the saturation level observed for the historical analogue. We therefore focus exclusively on structural comparability.

Step 3: Selection of natural gas power plants as historical analogue from a technology long list

Next, we evaluate a long list of potential technology analogues against the characteristics outlined above, as well as our study objectives. A common starting point for creating such a list is the Historical Adoption of Technologies (HATCH) database, which aggregates data from sources including peer-reviewed literature, the International Energy Agency, and the U.S. Energy Information Administration, to provide time series characterizing the diffusion of technologies in native units.[51] An important requirement for our analysis is the availability of high-quality data that is both longitudinal and spatially explicit, enabling the study of spatial technology diffusion. The HATCH dataset is aggregated at the regional or national level and does not provide sub-national or installation-level information. In line with our research focus, it is therefore not suitable as a long list for analogue selection. However, it can serve as an initial screening tool to assess technology fit and to identify candidate technologies for which high-quality, longitudinal, and spatially explicit data may be available from other sources.

In its 1.5 version, the HATCH database includes 202 technologies. As a first step, we make a broad selection based on sector, excluding technologies related to consumer demand (42), healthcare (15), digital (14), agriculture (10), machinery (5), and the public sector (3). These are not comparable to H_2 in terms of basic technology and infrastructure characteristics, and their dispersed nature makes the availability of spatial diffusion data unlikely. We also eliminate technologies that are "pure" infrastructure such as road, rail, pipeline, and water infrastructure (6). For the remaining 120 technologies, we review data availability.

S&P Capital IQ provides detailed data on power plants, including capacity, service years, and locations. Similar data exists for mining operations, though coverage is partial, with service years missing for around 4,000 of 9,700 installations. Global Energy Monitor provides open datasets on oil and gas infrastructure and steel plants, including operation dates and geo-location. The EU ETS and the European Pollutant Release and Transfer Register (E-PRTR) cover a wide range of industrial emitters, but data availability is limited to post-2005 (ETS) and post-2007 (E-PRTR), making them unsuitable for modelling full diffusion processes. We are not aware of other technologies for which spatially explicit, longitudinal data is publicly available.

This yields the following long list of technologies that combine a broad sectoral match with data availability:

- Power plants: Biogas, coal, geothermal, hydro, marine, natural gas, nuclear, pumped hydro, solar (CSP, PV, thermal), wind (offshore, onshore)
- Oil and gas production: Natural gas, oil (conventional, shale)
- Metals and mining: Coal, cobalt, copper, gold, graphite, iron, lead, lithium, magnesium, rare earths, silver, steel production, tin, titanium sponge, zinc

While data is available for all of these technologies, data coverage and sample size vary substantially. For example, in the case of biogas or coal plants, the number of plants that could be considered are less than 100. Similarly, steel production plants are limited to around 80 across all production

routes. This limits their applicability for use in an empirical model of technology adoption. Based on the characteristics of green H_2 demand outlined above, we identify natural gas power plants and renewable power plants (e.g., wind) as the most promising candidates. While renewable power plants have been used as analogues for green H_2 supply,[52] we consider natural gas power plants the more appropriate analogue for green H_2 demand. Natural gas power plants closely match the basic technological, economic, policy, social, user and cultural characteristic dimensions of the SHARD framework, and align well with the structural diffusion mechanics expected for green H_2, in particular with regard to spatial spillover mechanisms (see detailed considerations below).

Analytical fit between green H_2 demand and natural gas power generation along SHARD characteristics

Green H_2 demand and natural gas power plants are similar in terms of technological and infrastructure characteristics. H_2 and natural gas share key physical attributes: both are gaseous and fugitive, with similar characteristics for transport, transmission, and storage.[40] Natural gas power plants and green H_2 demand are also comparable in terms of technological complexity and the need for customization.[36] In both cases, technologies can be characterized as relatively complex systems with significant system integration requirements, where multiple interacting design elements and site-specific conditions necessitate project-level customization and infrastructure access. Importantly, both exhibit interdependencies between demand and infrastructure. This is less pronounced for renewable generation, which is connected to existing electricity grids, even though grid upgrades and additional reserves are likely required[53] and securing grid connections can be challenging.[54] Green H_2 demand and natural gas power plants also show similar spatial patterns, which broadly track industrial activity and population centers (see Step 4 – additional considerations for further details on parallels in siting).

Economically, both natural gas and renewables were emerging technologies at the time of adoption, with negative cost spreads to incumbents and rapidly falling cost curves.[55]

From a policy and political perspective, in Europe, renewable power, in contrast to natural gas power plants, has received extensive policy support, extensive subsidies under feed-in tariffs and auction regimes. In 2021, the year before the start of the war in Ukraine, renewables subsidies amounted to EUR 83bn, versus EUR 10bn for natural gas.[56] While H_2 is also likely to require policy support,[42] the aim of our model is to establish a policy-neutral baseline. Using renewable power as an analogue risks embedding policy effects in the baseline. Natural gas power, by contrast, was subject to more limited direct support. A potential caveat is that natural gas prices and availability are partially shaped by geopolitics.[57] However, this also applies to H_2 (see, e.g., Van de Graaf et al[58] for a qualitative assessment of the interplay between H_2 trade and international relations), which is expected to rely heavily on imports under EU 2030 targets.[1]

In terms of user and consumption characteristics, both green H_2 and natural gas power plants partly share a common user base: both are, to a significant degree, used by large-scale customers in industrial sectors – green H_2 as fuel and feedstock and natural gas power in the context of cogeneration plants. In the power sector and in some cogeneration plants, green H_2 can even be considered a substitute for natural gas.[59] There is no similar common user base for renewable generation.

Analytical fit between green H_2 demand and natural gas power generation along spatial spillover mechanisms

Natural gas power plants closely match the spatial spillover mechanisms expected for green H_2 (see above and Supplementary Note 2). The spatial patterns of natural gas power plants reflect technical and system-level characteristics such as electricity grid topology, shared supply infrastructure and proximity to demand centers, especially for cogeneration plants.[60,61] These demand centers, including large-scale industrial installations in sectors such as iron & steel, refining, chemicals and non-metallic minerals[62] or district heating,[61,63] are structurally comparable to green H_2 demand.[62,63] While site selection does not necessarily depend on the presence of prior plants per se, these characteristics generate strong spatial interdependencies, particularly through shared infrastructure and demand proximity. In some cases, green H_2 can even directly substitute for natural gas as a fuel.[64]

In terms of shared infrastructure, the expansion of natural gas power generation in Europe between 1963 and today coincided with the development of gas extraction, pipeline networks, LNG terminals, and market institutions. This co-evolution of infrastructure and demand created spatial interdependencies, as early infrastructure investments reduced adoption barriers for subsequent plants in nearby locations.[28] This dynamic resembles the expected evolution of green H_2 demand, where adoption decisions depend on the parallel development of production, transport, distribution, and storage infrastructure (Supplementary Note 2). Shared infrastructure therefore represents a central and transferable mechanism underlying spatial spillovers in both contexts.

Although green H_2 demand spans several use cases they remain structurally comparable to each other and to natural gas power plants with regard to design complexity and need for customization, indicating similar dynamics with regard to supply chain materialization and knowledge spillovers. For more details on how the presence of multiple H_2 demand use cases affect comparability, see additional considerations below.

Summary

Based on our rigorous, formal selection process, along the SHARD framework and HATCH technology database routinely used in the feasibility space literature,[65] natural gas power plants emerge as the closest available match to green H_2 demand from a structural and modeling perspective. This provides a rigorous foundation for our empirical analysis and forward-looking analysis.

Beyond matching structural characteristics, natural gas power plants also offer a key technical advantage over renewable generation: the diffusion curve for EU countries approaches saturation and shows a well-defined s-shape consistent with the typical shape of technology diffusion curves[66] (Supplementary Figure 1), while renewables remain subject to strong growth. This makes calibration on natural gas power plants more straightforward, as it can be based on a full diffusion curve.

Step 4: Special considerations on the analytical fit between green H_2 demand and natural gas power plants

Siting of green H_2 demand relative to natural gas power plants

Although the siting of natural gas power plants can depend on many aspects, including access to natural gas supply, grid bottlenecks or proximity to demand centers,[60,61] siting decisions are structurally comparable to green H_2 and empirically correlated with the presence of other natural gas power plants. This reinforces the comparability of natural gas power plants and green H_2 demand, and the presence of spatial spillovers in both contexts.

Natural gas power plants frequently co-locate with large and steady demand sources, with a substantial share operating as cogeneration facilities. In our dataset, approximately 75% of natural gas power plants, accounting for roughly one third of installed capacity, are combined heat and power plants supplying industrial facilities or district heating networks (see Supplementary Figure 1).[61–63] These plants are embedded in industrial clusters and co-located with concentrated demand, generating spatial interdependencies through shared infrastructure, supply chains and knowledge exchange. In terms of spatial footprint and system integration, such cogeneration plants are comparable to green H_2 demand locations, which are likewise concentrated in industrial clusters.

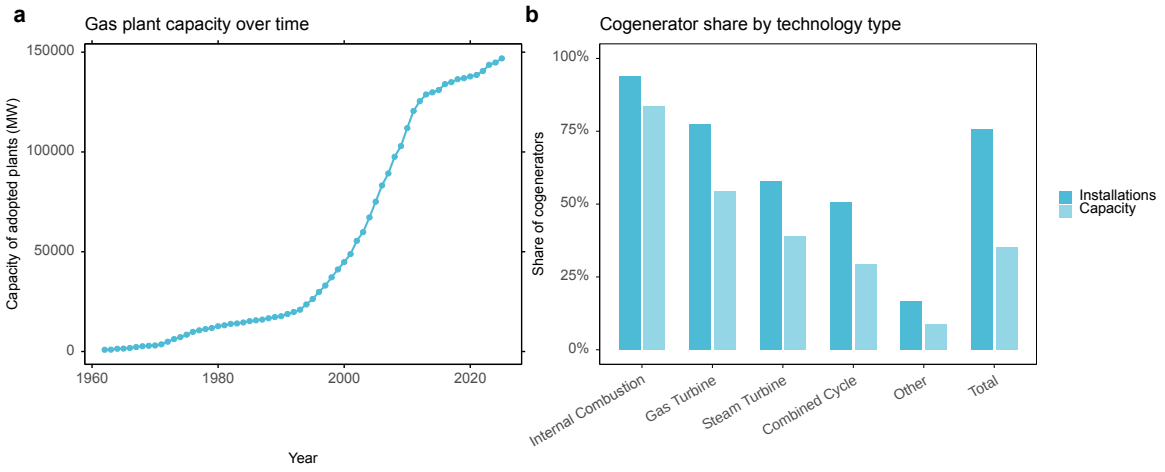

Supplementary Figure 1 Natural gas power plants in the EU 1962-2024. a Build-up of natural gas power plant capacity in the EU in MW. The dataset includes all operating and out-of-service natural gas power plants in the EU as of 31 December 2024. Observations with missing values in geographic coordinates and commissioning year are excluded; the capacity of power plant units in the same location is aggregated. This results in a total of 3493 power plants considered in the sample. **b** Share of natural gas power plants classified as cogeneration plants. Over 75% of installations, and over a third of capacity are cogeneration plants, with particular concentration in internal combustion and gas turbine plants.

We also find empirical evidence that new natural gas plants tend to be commissioned in clusters of existing plants. To demonstrate this, we divide natural gas power plants by decade of commissioning. For installations newly commissioned in each decade, we compute kernel densities based on the existing natural gas power generation footprint, using the locations of the new plants and 5,000 reference points across the EU land mass, and sort them into percentiles. The median local density percentile of newly commissioned plants consistently exceeds the 80th percentile in all decades, indicating that new installations are strongly correlated with the location of existing plants (Supplementary Figure 2).

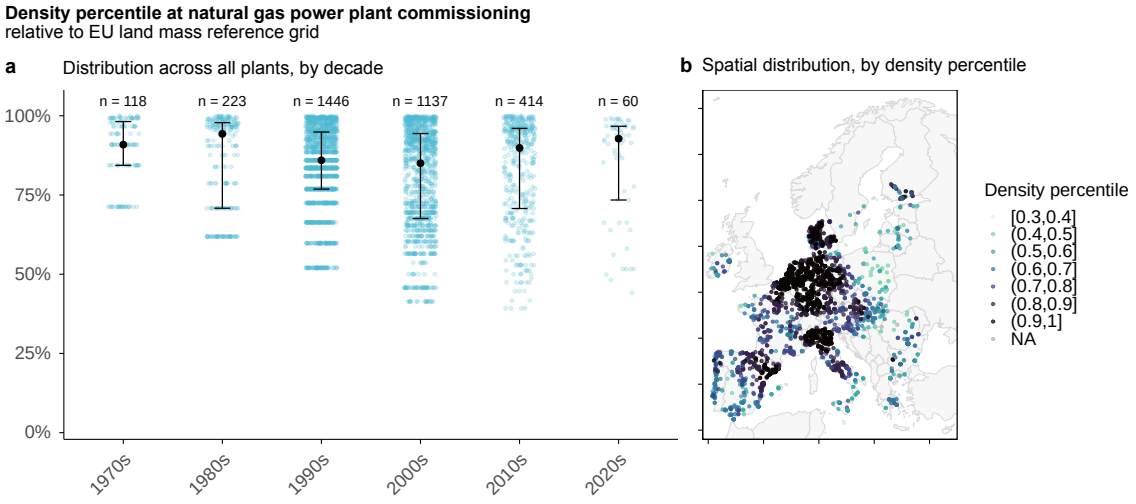

Supplementary Figure 2 Spatial dependency of natural gas power plant siting over time a Distribution of kernel density percentiles for the locations of newly commissioned plants by decade. Density percentiles are calculated relative to the spatial distribution of existing plants at the time of commissioning and benchmarked against 5,000 reference points across the European Union land mass. Blue points represent individual observations, black points the median and whiskers the interquartile distance. The median percentile exceeds 80% in every decade, indicating that at least half of all new plants are sited within the 20% most densely occupied locations based on the prior footprint, indicating spatial correlation over time. **b** Spatial distribution of natural gas power plants and corresponding density percentiles.

Considerations on the heterogeneity of green H_2 demand applications

Green H_2 demand spans multiple use cases across transport, heating and industry. Despite this heterogeneity, these applications share structural characteristics that enable spatial spillovers through supply chain materialization and knowledge exchange, extending beyond shared fuel and infrastructure.

Structural similarity between technologies can be assessed by comparing their relative design complexity and need for customization.[36] Green H_2 end-use technologies are best characterized as complex products and systems (CoPS) rather than mass-produced commodities. CoPS technologies exhibit high design complexity, strong interdependencies between components, and substantial requirements for system integration and site-specific adaptation.[36,67] Innovation in such technologies typically proceeds through iterative improvements at the component and subsystem level rather than through standardized mass production.[30,31] This innovation process relies on project-based engineering capabilities and specialized supplier networks that integrate multiple technical subsystems.

These characteristics have clear spatial implications. In CoPS industries, technological learning and innovation frequently emerge from close interaction between lead users and specialized suppliers. Empirical research shows that geographic proximity between component suppliers and lead users facilitates iterative problem solving, tacit knowledge exchange, and the accumulation of engineering capabilities.[29,68] In the context of green H_2, lead users are typically large industrial installations in sectors such as iron & steel, chemicals, refining, and non-metallic minerals. The co-location of suppliers and industrial users can therefore reinforce spatial clustering and generate localized spillovers that lower adoption barriers for subsequent projects.

Evidence from other CoPS in the energy sector illustrates similar patterns across components. Wind turbines are customized, engineering-intensive systems in which innovation and cost reductions occur primarily at the component level rather than in the final assembly.[30] The manufacturing value chain consequently involves hundreds of specialized suppliers producing towers, blades, gearboxes, and control systems for a relatively small number of turbine manufacturers. Empirical analyses further document geographically concentrated supplier–manufacturer relationships, reflecting the importance of localized manufacturing capabilities and specialized engineering expertise within wind energy supply chains.[30]

Many specialized suppliers in green H_2-related value chains operate across multiple technologically related industries. Firms producing compressors, turbines, high-pressure piping, cryogenic equipment, catalysts, and engineering services frequently serve power generation, chemicals, refining, and heavy industry. These overlapping capabilities create opportunities for cross-sector knowledge spillovers and reinforce spatial clustering in regions with strong engineering and industrial capabilities. For example, Rolls-Royce serves defense, civil aerospace, and power systems markets; within power systems it supplies marine, governmental, industrial, and power generation applications, often holding significant market shares.[69] GE Vernova manufactures equipment for major forms of power generation, including natural gas, H_2 combustion solutions, and several direct electrification technologies for industry.[70]

Beyond supply chain materialization and knowledge spillovers, one of the primary mechanism driving spatial spillovers in green H_2 demand – shared infrastructure for supply, transmission, storage, and delivery – is largely independent of end-use heterogeneity and closely comparable to the infrastructure requirements of natural gas.

Finally, natural gas power generation has itself historically exhibited substantial technological heterogeneity. Since initial deployment, it has undergone several technological waves, from steam turbines to gas turbines and internal combustion units to combined cycle gas turbines (see Supplementary Figure 3). These waves reflect learning processes, knowledge spillovers, and supply chain materialization specific to each configuration that can be viewed as similar to that of green H_2 demand.

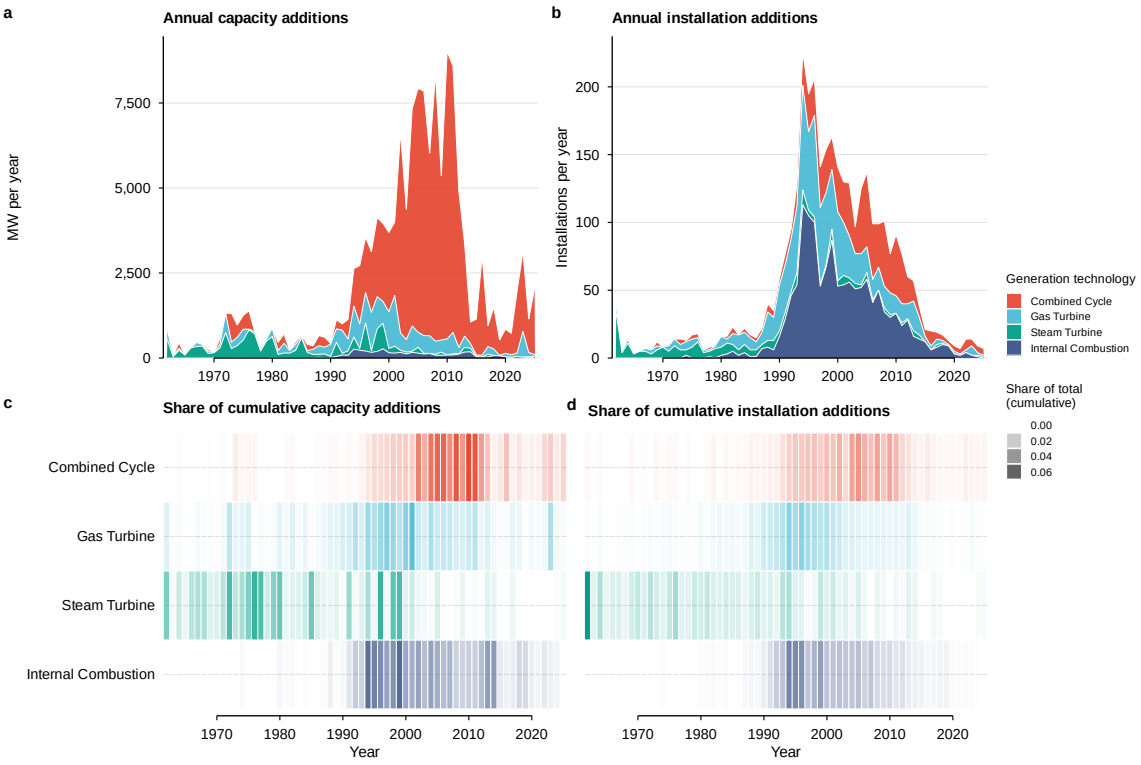

Supplementary Figure 3 Natural gas power plant additions by year and generation technology. a Capacity additions of natural gas power plants by year and generation technology (combined cycle, gas turbine, internal combustion, and steam turbine). **b** Additions of natural gas power plants measured by number of installations. **c** Share of capacity additions within a generation technology in a given year, expressed as a share of total capacity additions across all years. Results indicate distinct technology waves, from steam turbines to gas turbines and internal combustion plants, and subsequently to combined cycle turbines. **d** Share of installation additions within a generation technology in a given year, expressed as a share of total installation additions across all years.

Considerations on central versus decentral green H_2 supply

In our analysis, we focus on green H_2 demand rather than supply, irrespective to whether it is supplied through centralized or on-site production. We follow the literature in assuming that infrastructure, which can include renewable generation, transmission, distribution and storage systems, is required to support green H_2 demand.[39] At a minimum, generation and storage infrastructure are also required in a fully decentralized system, and benefit from infrastructure sharing, supply chain materialization and local knowledge build-up. Spatial spillovers in the case of green H_2 are thus robust across different supply configurations.

SN4: Robustness tests on the empirical model

Empirical identification with alternative historical analogues

The structured analysis of historical analogues in Supplementary Note 3 demonstrates that natural gas power plants are the most suitable historical analogue to build a spatially explicit model of green H_2 diffusion over time. Still, as a robustness test, we explore to which degree our results and conclusions hold for different definitions of historical analogues.

First, we restrict the sample of natural gas power plants to cogeneration plants only. Cogeneration plants follow the structure of green H_2 demand, for example in terms of spatial patterns, even more closely than natural gas power plants at large (see Supplementary Note 3). Second, we test an empirical identification based on wind power plants, which have been proposed as a historical analogue in

the case of green H_2 supply.[52] Data source (S&P Capital IQ), model specification and estimation procedures remain unchanged (see Methods).

Natural gas cogeneration plants

Results for cogeneration plants (Supplementary Table 2) are fully consistent with the results for natural gas power plants at large reported in the main article (Extended Data Table 1). In the second pass regression, the coefficient on spatial spillovers is slightly higher (11.1 versus 10.7) and the coefficient on distance of natural gas transmission corridors is significant and negative, albeit at an extremely low magnitude (-0.0055). The remaining coefficients are materially unchanged.

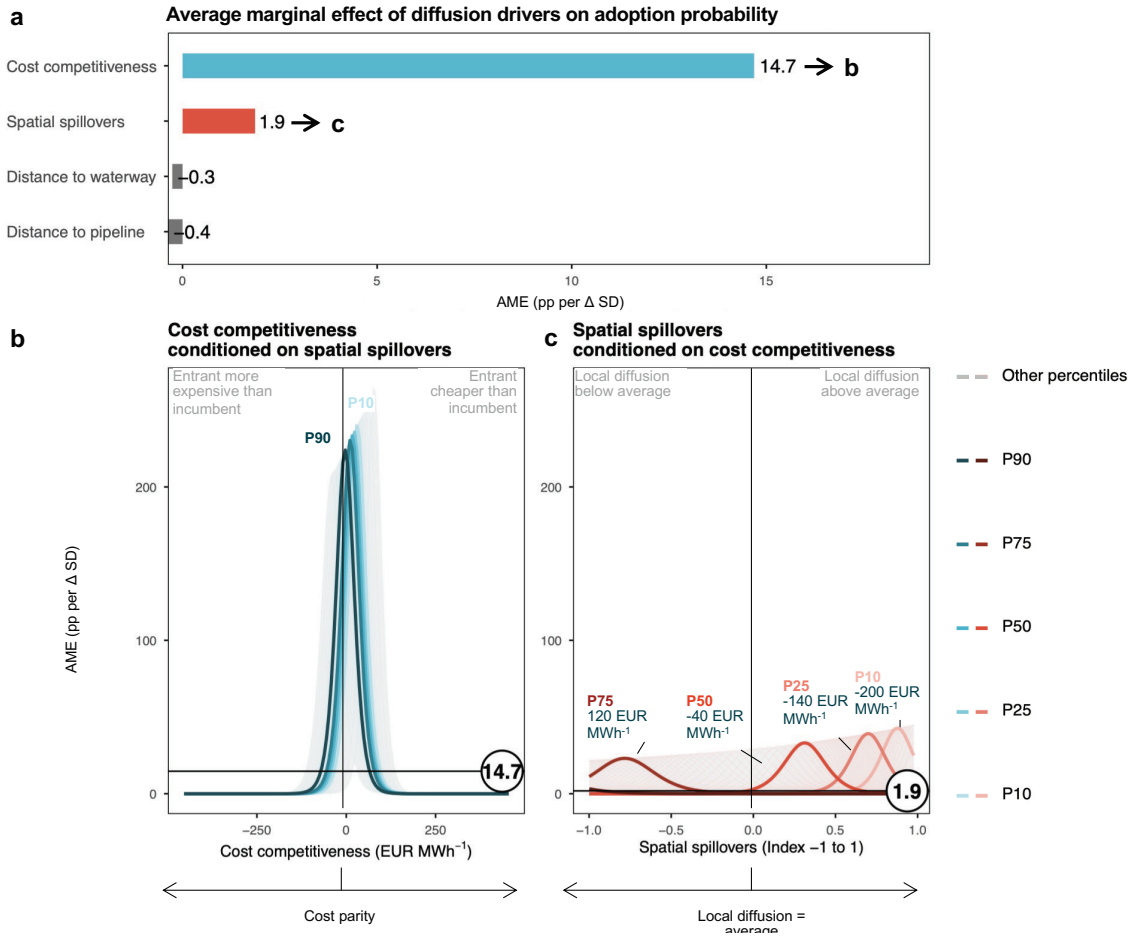

Supplementary Figure 4 Average marginal effects of cost competitiveness and spatial spillovers on adoption using cogeneration plants as historical analogue. a Average marginal effect (AME) of all independent variables. Cost competitiveness and spatial spillovers are the primary drivers of diffusion, with an AME of cost competitiveness (blue bar) approximately 8-times the AME of spatial spillovers (red bar).
b-c AME of cost competitiveness (**b**) and spatial spillovers (**c**), conditioned on each other. Colored lines denote the AME across the predictor's range for selected percentiles of the conditioning variable. The grey ribbon indicates the overall range of AMEs across all possible values of the conditioning variable. Horizontal black lines and annotations denote the overall AME. Vertical black lines denote zero values (cost parity and local diffusion = average diffusion). AMEs are derived from the logistic regression model in Supplementary Table 2 using a finite difference approximation and normalized using the variables' standard deviations.

The estimated marginal effect of spatial spillovers increasing slightly from 1.7 to 1.9 percentage points per standard deviation (see Supplementary Figure 4a). The main results can therefore be

Supplementary Table 2 GEE logistic regression estimates of adoption probability (AR(1) correlation structure)

Variable	First pass				Second pass			
	Est.	SE	Wald	p	Est.	SE	Wald	p
Intercept	-0.143	0.0304	22.02	2.7e-06***	-0.784	0.0406	373.4	<2e-16***
Cost competitiveness ($C_{i,t}$)	—	—	—	—	0.0622	0.000694	8037.1	<2e-16***
Spatial spillovers ($S_{i,t}$)	2.159	0.125	297.93	<2e-16***	11.092	0.402	760.8	<2e-16***
Distance to waterways (D_i^{water})	-0.000483	0.000178	7.39	0.00656**	-0.002580	0.000437	34.9	3.5e-09***
Distance to pipeline corridors (D_i^{pipe})	-0.002207	0.001610	1.88	0.1706	-0.005511	0.001233	20.0	7.8e-06***
Interaction: $C_{i,t} \times S_{i,t}$	—	—	—	—	-0.02210	0.00388	32.5	1.2e-08***

Notes: Output from two generalized estimating equation (GEE) logistic regression models with an AR(1) correlation structure. The first-pass model includes spatial spillovers and distances to waterways and pipeline corridors. The second-pass model additionally includes cost competitiveness and its interaction with spatial spillovers. Standard errors are clustered at the installation level. Wald statistics equal $(\hat{\beta}/\text{SE})^2$. First-pass: AR(1) $\hat{\alpha} = 0.8707$ (SE = 0.0203), scale = 1.005 (SE = 0.2109). Second-pass: AR(1) $\hat{\alpha} = 0.0185$ (SE = 0.166), scale = 1.02 (SE = 9.14). Clusters: 2,647. Maximum cluster size: 53. Significance: ***p<0.001, **p<0.01, *p<0.05, .p<0.1. n= 111,147.

interpreted as slightly conservative with respect to spillover magnitudes relevant for green H_2 demand. Supplementary Figure 5 reports baseline green H_2 demand projections (including carbon pricing, but no other policy interventions) for the cogeneration plants analogue. The projections are consistent with those reported in the main article with only immaterial differences.

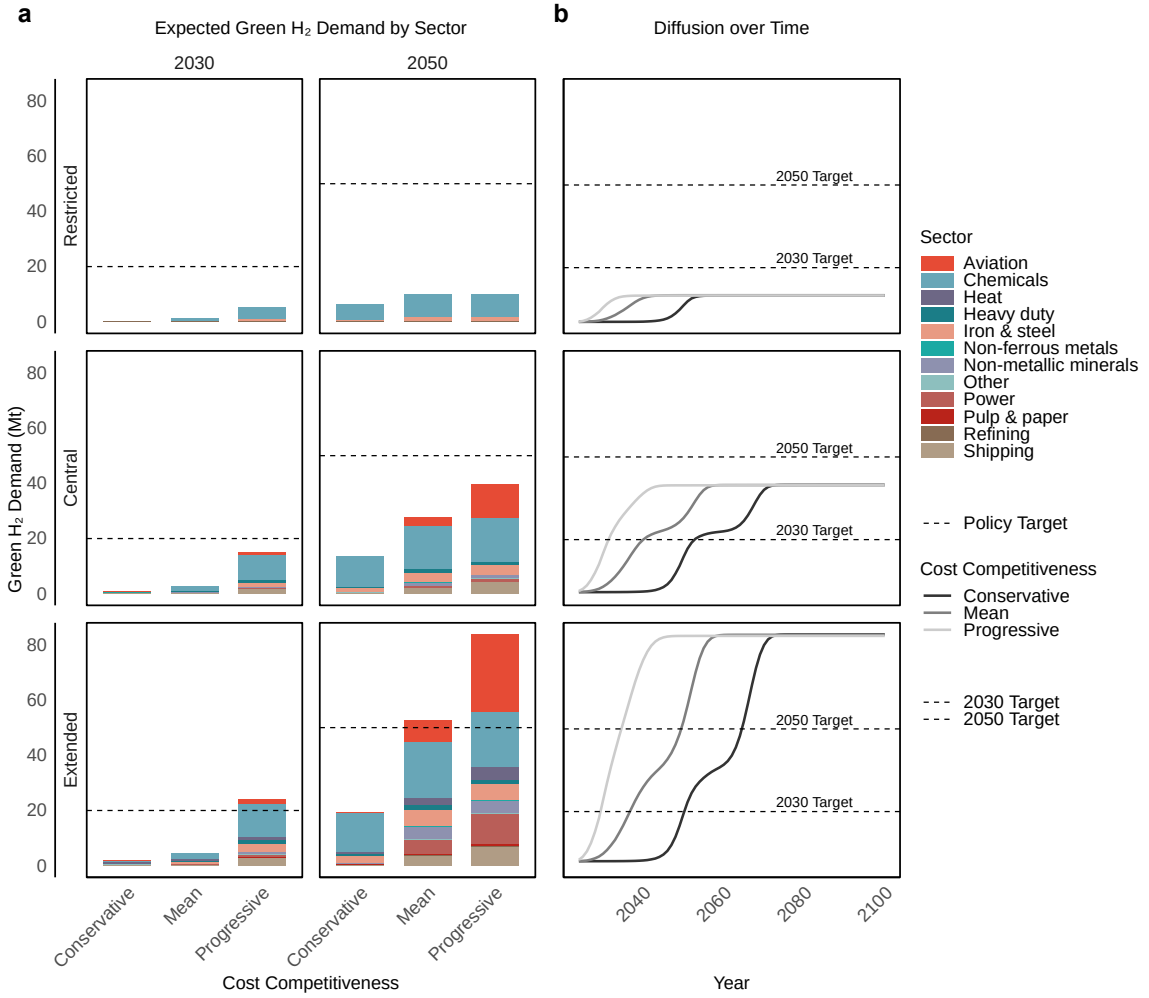

Supplementary Figure 5 Baseline projections of expected green H_2 demand before policy intervention using cogeneration plants as historical analogue
a Expected green H_2 demand in 2030 and 2050 under combinations of green H_2 cost trajectories (conservative, mean, progressive) and saturation assumptions (restricted, central, extended), broken down by sector. Dashed lines indicate policy targets of 20 Mt green H_2 demand by 2030, and 50 Mt (10% of final energy demand as per the EU's SAM GEM E3 model)[71] by 2050. Projections still fall short of policy targets in most cases, but show a higher rate of diffusion compared to the main model. **b** Time series of green H_2 diffusion between 2024 and 2100 disaggregated by saturation case. Green H_2 cost trajectories are shown in varying shades of grey. Diffusion curves follow the typical S-shape of technology diffusion.[66]

Empirical identification with wind power plants

For wind power plants, results are similarly consistent (see Supplementary Table 3). Results are structurally consistent with the natural gas power plant results: the coefficient on spatial spillovers is even higher than in the model calibrated on natural gas power plants; the coefficients on cost competitiveness (12 and the interaction term are somewhat lower, and the coefficients on the infrastructure variables are materially unchanged.

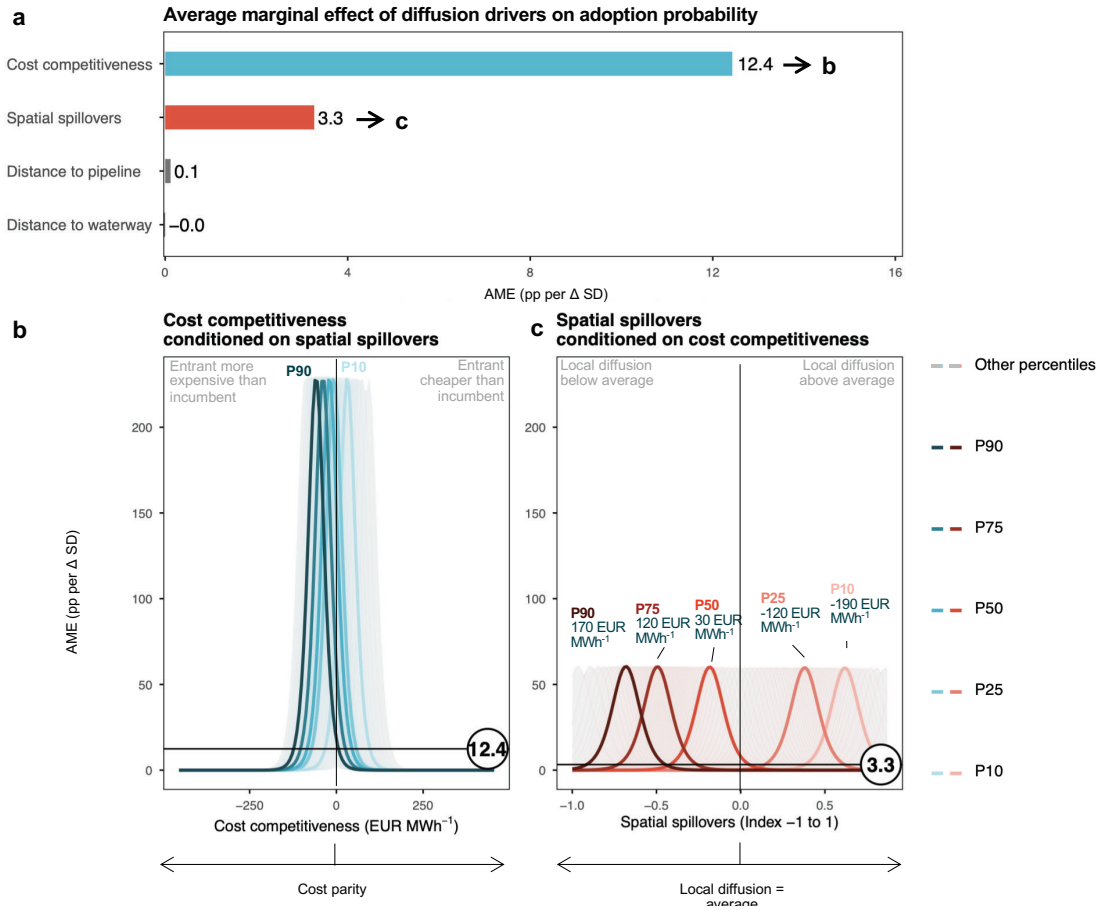

Supplementary Figure 6 Average marginal effects of cost competitiveness and spatial spillovers on adoption using wind as historical analogue. a Average marginal effect (AME) of all independent variables. Cost competitiveness and spatial spillovers are the primary drivers of diffusion, with an AME of cost competitiveness (blue bar) approximately 4-times the AME of spatial spillovers (red bar).
b-c AME of cost competitiveness (**b**) and spatial spillovers (**c**), conditioned on each other. Colored lines denote the AME across the predictor's range for selected percentiles of the conditioning variable. The grey ribbon indicates the overall range of AMEs across all possible values of the conditioning variable. Horizontal black lines and annotations denote the overall AME. Vertical black lines denote zero values (cost parity and local diffusion = average diffusion). AMEs are derived from the logistic regression model in Supplementary Table 3 using a finite difference approximation and normalized using the variables' standard deviations.

Supplementary Figure 6a reports the average marginal effects of all diffusion drivers on green H_2 adoption probability. Consistent with the results from the regression, cost competitiveness and spatial spillovers are the main drivers of diffusion, with an average marginal effect of cost competitiveness of approximately 12.6 pp per SD, compared to 3.3 pp per SD for spatial spillovers. Compared to natural gas power plants, the average marginal effect of cost competitiveness is thus slightly lower (12.6 versus 14.5), the average marginal effect of spatial spillovers higher (3.3 vs 1.7).

Supplementary Table 3 GEE logistic regression estimates of adoption probability (AR(1) correlation structure)

Variable	First pass				Second pass			
	Est.	SE	Wald	p	Est.	SE	Wald	p
Intercept	0.2301	0.0161	205.34	<2e-16***	1.1693	0.0319	1344.07	<2e-16***
Cost competitiveness ($C_{i,t}$)	—	—	—	—	0.0662	0.00054	15055.50	<2e-16***
Spatial spillovers ($S_{i,t}$)	3.6256	0.0777	2179.66	<2e-16***	18.1901	0.2349	5994.56	<2e-16***
Distance to waterways (D_i^{water})	-0.00030	0.00021	1.96	0.161	-0.00038	0.00036	1.13	0.287
Distance to pipeline corridors (D_i^{pipe})	0.00011	0.00007	2.29	0.130	0.00061	0.00019	10.98	0.00092***
Interaction: $C_{i,t} \times S_{i,t}$	—	—	—	—	0.00069	0.00300	0.05	0.817

Notes: Output from two generalized estimating equation (GEE) logistic regression models with an AR(1) correlation structure. The first-pass model includes spatial spillovers and distances to waterways and pipeline corridors. The second-pass model additionally includes cost competitiveness and its interaction with spatial spillovers. Standard errors are clustered at the installation level. Wald statistics equal $(\hat{\beta}/\text{SE})^2$.
First-pass: AR(1) $\hat{\alpha} = 0.7885$ (SE = 0.00343), scale = 0.9873 (SE = 0.0154).
Second-pass: AR(1) $\hat{\alpha} = 0.0234$ (SE = 0.0348), scale = 0.472 (SE = 0.702).
Clusters: 10,019. Maximum cluster size: 30. Significance: ***p<0.001, **p<0.01, *p<0.05, .p<0.1.
$n = 213{,}788$.

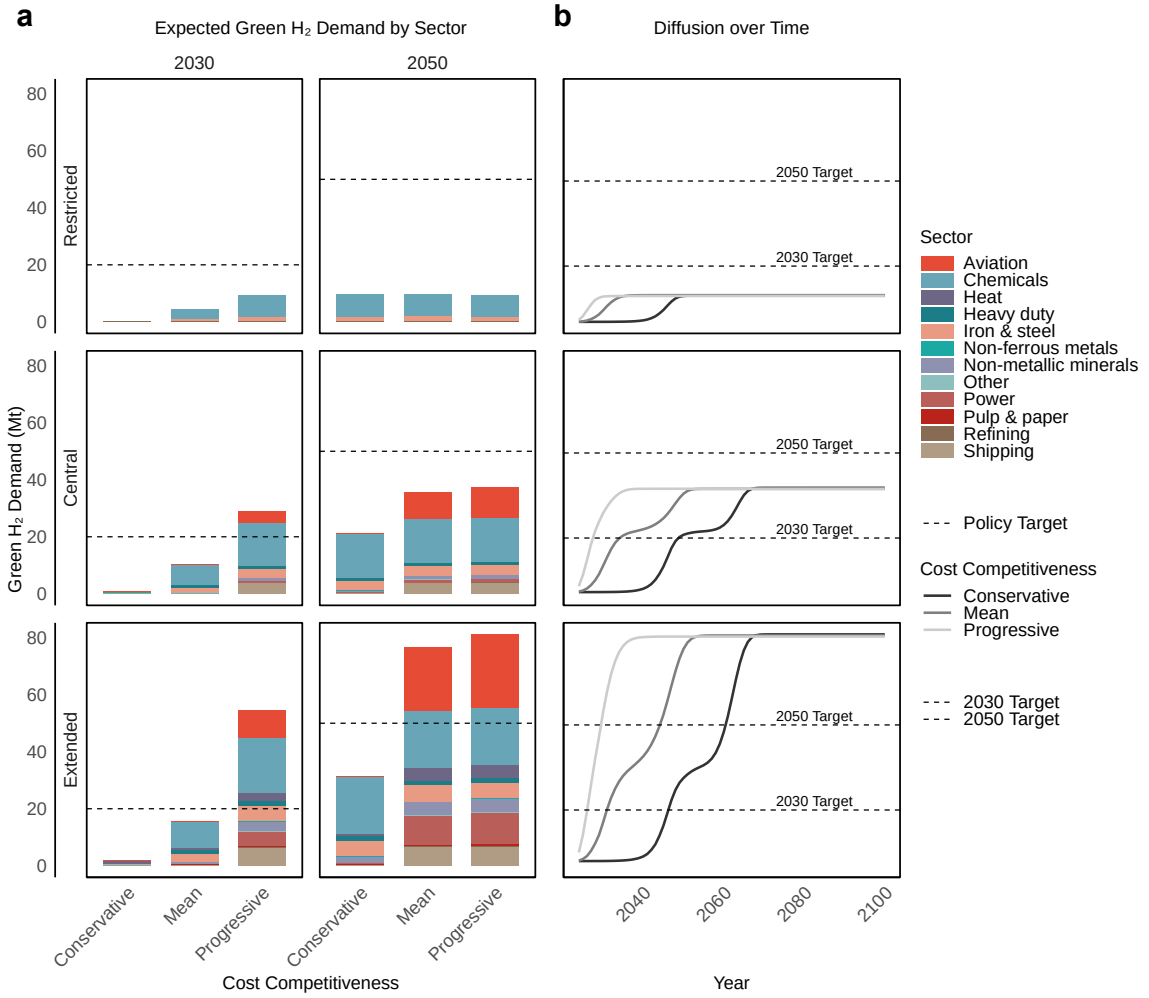

Supplementary Figure 7 Baseline projections of expected green H_2 demand before policy intervention using wind as historical analogue
a Expected green H_2 demand in 2030 and 2050 under combinations of green H_2 cost trajectories (conservative, mean, progressive) and saturation assumptions (restricted, central, extended), broken down by sector. Dashed lines indicate policy targets of 20 Mt green H_2 demand by 2030, and 50 Mt (10% of final energy demand as per the EU's SAM GEM E3 model)[71] by 2050. Projections still fall short of policy targets in most cases, but show a higher rate of diffusion compared to the main model. **b** Time series of green H_2 diffusion between 2024 and 2100 disaggregated by saturation case. Green H_2 cost trajectories are shown in varying shades of grey. Diffusion curves follow the typical S-shape of technology diffusion.[66]

Supplementary Figure 6b and c report the average marginal effects of cost competitiveness and spatial spillovers, conditioned on each other. The average marginal effect of cost competitiveness, conditioned on spatial spillovers, behaves similarly to the main model but peaks at lower levels of cost competitiveness. Relative to the main model's range of approximately –35 EUR MWh^{-1} to 75 EUR MWh^{-1}, the peaks now begin at –90 EUR MWh^{-1} and extend to 95 EUR MWh^{-1}. We interpret this as evidence that adoption of wind plants starts earlier, at lower levels of cost competitiveness. The average marginal effect of spatial spillovers, conditioned on cost competitiveness, again shows consistent behavior but with less variation in level. Spatial spillovers remain influential even at higher cost competitiveness levels (up to the 90th percentile), reinforcing their stronger role in the diffusion of wind respective to natural gas power plants.

We interpret this as evidence that adoption of wind plants starts earlier, at lower levels of cost competitiveness. The average marginal effect of spatial spillovers, conditioned on cost competitiveness, again shows consistent behavior but with less variation in level. Spatial spillovers remain influential even at higher cost competitiveness levels (up to the 90th percentile), reinforcing their stronger role in the diffusion of wind respective to natural gas power plants.

Supplementary Figure 7 reports baseline green H_2 demand projections (including carbon pricing, but no other policy interventions) for a wind power plant analogue. The projections are consistent with those reported in the main article but show a faster rate of diffusion. For example, in the extended saturation case, the 2030 policy target is (almost) achieved in the mean cost competitiveness trajectory in addition to the progressive one. This is consistent with the notion, presented in the main article and in Supplementary Note 3, that wind power plants were historically subject to substantially higher levels of policy support compared to natural gas power plants, making them less suitable for constructing an intervention-free baseline of green H_2 demand.

Empirical identification with external levelized cost of electricity (LCOE) measures

We operationalize cost competitiveness using a two-step regression approach, where cost competitiveness is identified from the residuals of a first-pass regression of adoption on spatial spillovers and physical distance to natural gas transmission pipelines and navigable waterways. As explained in Methods, residuals-based measurement is common practice when direct measurement is challenging and is regularly applied in energy research. [72]

A residuals-based approach is valid when the residual is dominated by the latent variable of interest—in this case, cost competitiveness. The literature on energy technology diffusion suggests that cost competitiveness plays a major role in diffusion. [20,27,55] There is therefore a strong theoretical argument that, after partialling out spatial dependencies and distances to physical infrastructure, cost accounts for a large share of the remaining variation.

We use external measures of cost competitiveness to further test this assumption. In the case of natural gas power generation, cost competitiveness can be defined broadly as the spread between the LCOE of natural gas and the LCOE of alternative generation technologies, such as coal. As explained in Methods, historical time series for both natural gas and coal LCOEs are extremely limited in availability and quality. To our knowledge, the most comprehensive dataset on historical LCOEs reports coal LCOEs starting in the 1920s, with several gaps, and natural gas LCOEs only from 1982. [55] We refrain from using these values for our main analysis for several reasons. First, LCOEs are composites of different sources, which do not always fully disclose their underlying assumptions and can be internally inconsistent. Second, they are US-based, whereas our analysis is EU-focused, which can lead to significant differences, particularly due to fuel cost differences. [73] Third, LCOEs are aggregate measures and therefore fail to account for spatial heterogeneity in costs. Fourth, a cost competitiveness measure based on LCOEs is necessarily pairwise, for example natural gas versus coal, which substantially simplifies actual competition dynamics in electricity markets, where different generation sources, including coal, natural gas, nuclear, hydro, wind, and solar, compete contemporaneously. Finally, availability does not cover the full natural gas power plant diffusion process: in 1982, the first year with available natural gas LCOEs, deployed capacity already amounted to 14 GW, or 8% of cumulative diffusion.

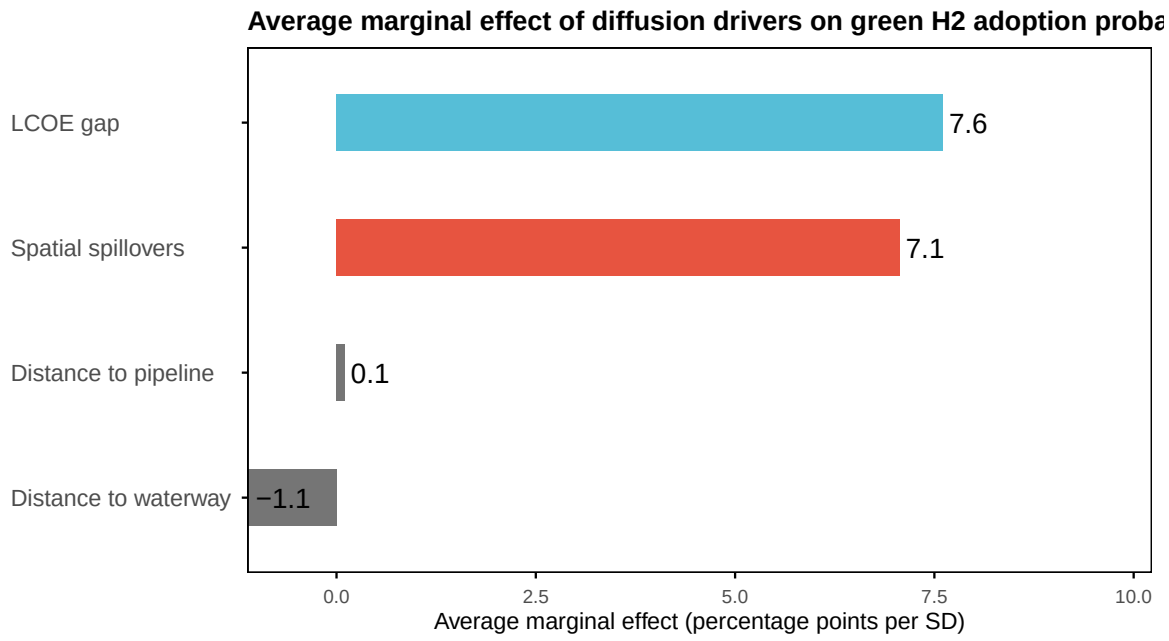

Supplementary Figure 8 Average marginal effects of cost competitiveness and spatial spillovers on adoption using external LCOE measures. Average marginal effect (AME) of all independent variables. Cost competitiveness and spatial spillovers are the primary drivers of diffusion, with an AME of cost competitiveness (blue bar, measured as gap between external measurements of natural gas and coal LCOEs[55]) slightly larger than the AME of spatial spillovers (red bar

. Effects are consistent with the main model.

While we caution against using these LCOEs in the main analysis, they provide a useful benchmark for assessing whether our empirical measure captures cost competitiveness dynamics. Our latent measure of cost competitiveness is reasonably strongly linked to the external LCOE time series, with a correlation coefficient of 0.7 and an R^2 of 0.47. Given the limitations of the LCOE time series, this suggests a robust conceptual link.

As a further robustness test, we re-estimate marginal effects using the external LCOE time series rather than the latent cost competitiveness measure. Results remain robust, with both the LCOE gap and spatial spillovers being positively and statistically significantly associated with diffusion. The average marginal effect of spatial spillovers, which is central to our results and most relevant to our policy implications, increases to 7.1 percentage points Supplementary Figure 8. This suggests that the spillover effects reported in the main article are conservative relative to an alternative model using external LCOE measures. The average marginal effect of cost competitiveness is lower, at 7.6 percentage points, but remains the most prominent driver of diffusion.

Statistical robustness tests

To test whether our specification and implementation of the empirical model is appropriate from a statistical perspective, we assess it for potential issues related to multicollinearity and autocorrelation. The independent variables do not present problematic multicollinearity, with variance inflation factors only slightly exceeding one (see Supplementary Table 4).

Through the spatial spillover variable, we control for spatial autocorrelation directly in the model specification. We confirm this using a Moran plot (see Supplementary Figure 9) placing the model residuals on the x axis, and their spatial lag on the y axis. A positive slope, or global Moran I, indicates spatial autocorrelation. The distribution of the observations does not indicate spatial autocorrelation, which is consistent with the model specification.

Supplementary Table 4 Collinearity statistics from the first and second pass of model specification.

Term	VIF (CI)	SE Factor	Tolerance (CI)
First pass			
Spatial spillovers ($S_{i,t}$)	1.00 (1.00–1.01)	1.00	0.996 (0.986–0.999)
Distance to waterways (D_i^{water})	1.32 (1.32–1.33)	1.15	0.755 (0.750–0.760)
Distance to pipeline corridors (D_i^{pipe})	1.32 (1.31–1.33)	1.15	0.756 (0.751–0.761)
Second pass			
Cost competitiveness ($C_{i,t}$)	1.10 (1.09–1.10)	1.05	0.911 (0.905–0.916)
Spatial spillovers ($S_{i,t}$)	1.25 (1.24–1.25)	1.12	0.802 (0.797–0.807)
Distance to waterways (D_i^{water})	1.21 (1.21–1.22)	1.10	0.825 (0.820–0.830)
Distance to pipeline corridors (D_i^{pipe})	1.21 (1.20–1.22)	1.10	0.826 (0.821–0.831)
Interaction: $C_{i,t}S_{i,t}$	1.15 (1.14–1.16)	1.07	0.869 (0.864–0.874)

Note: Variance inflation factors (VIFs) measure multicollinearity among regressors and are defined as $\text{VIF}_j = (1 - R_j^2)^{-1}$, where R_j^2 is obtained from regressing regressor j on all other regressors. SE factors correspond to $\sqrt{\text{VIF}}$; tolerance is defined as 1/VIF. Confidence intervals are based on repeated resampling. All VIF values remain below conventional thresholds (e.g. VIF < 5), indicating low multicollinearity.

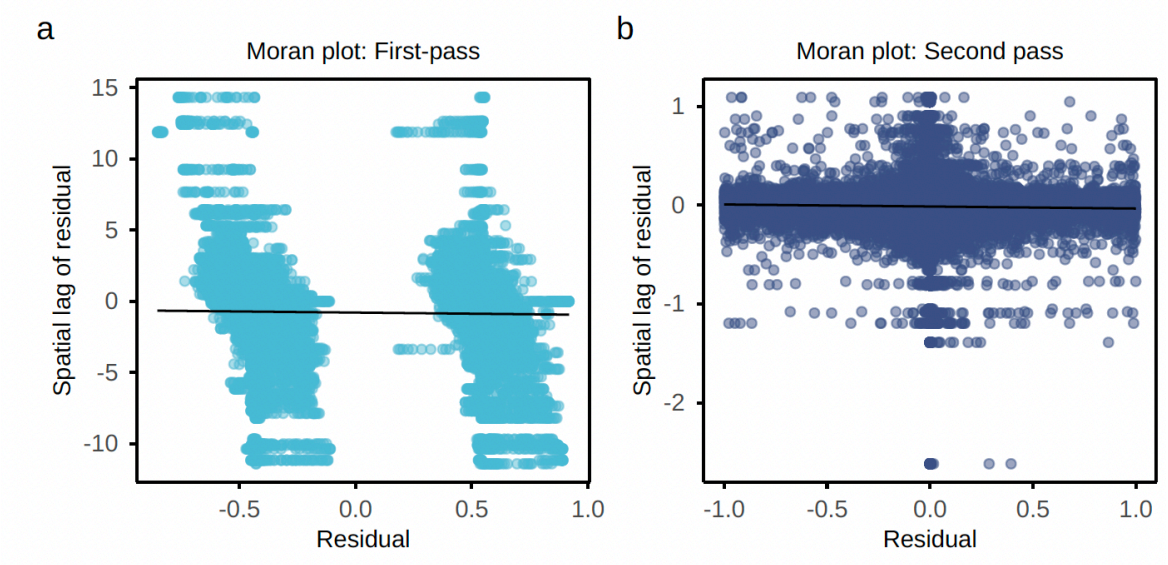

Supplementary Figure 9 Spatial autocorrelation in the residuals of the empirical adoption model The plot relates residuals of first and second pass of the model to their spatial lag. The slope, represented as a black line, is equivalent to Global Moran's I, a measure of spatial autocorrelation. Since the slope is close to zero, the plot suggests a lack of spatial autocorrelation.

In our model we use a cumulative irreversible measure of adoption as a dependent variable($A_{i,t}$). This results, by definition, in serial autocorrelation. This is evident from an ACF plot (Supplementary Figure 10), which shows the correlation of residuals with lagged residuals over 17 time periods (years). For all but the last lag, the plot indicates serial autocorrelation significant at a 5% level.

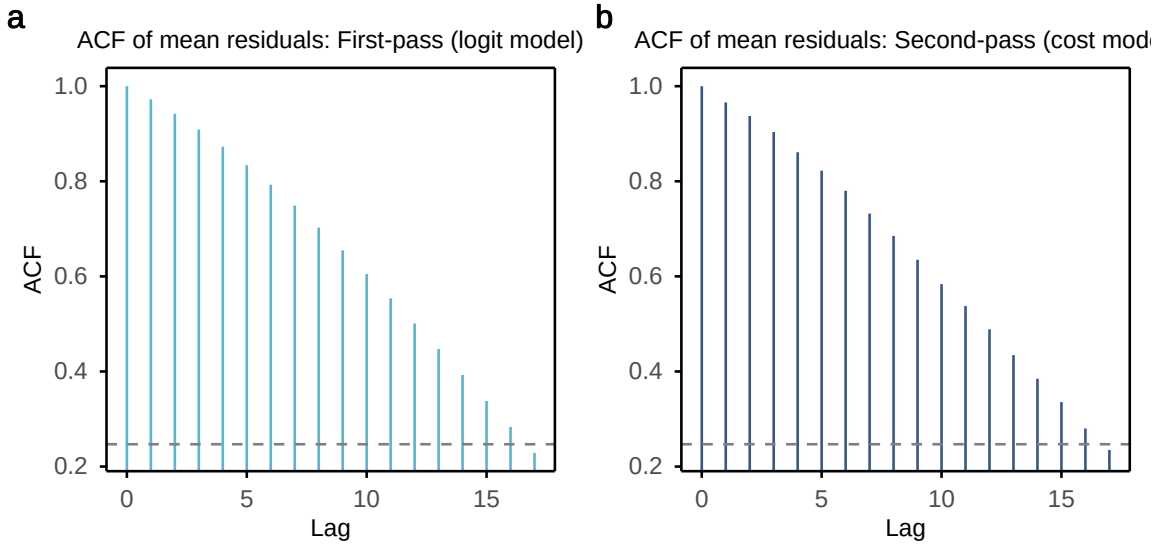

Supplementary Figure 10 Serial autocorrelation in the residuals of the empirical adoption model The plot shows the correlation between residuals of first and second pass of the model to their temporal lags. The dashed horizontal lines represent the 95% confidence bands for the null hypothesis of no serial correlation. For all but the last lag, the correlation exceeds this line, indicating significant autocorrelation at a 5% significance level.

One way to control for autocorrelation would be to include the lagged adoption term $A_{i,t-1}$ as a predictor. In the present set-up, we refrain from doing so because $A_{i,t-1}$ is highly correlated with the cost competitiveness variable, which is itself a function of $A_{i,t}$, leading to multicollinearity. Instead, we estimate the logit model using Generalized Estimating Equations (GEE) rather than a Generalized Linear Model (GLM). GEE yields consistent and unbiased coefficient estimates even in the presence of autocorrelation.[74] We specify a one-lag auto-regressive correlation structure within installations. Importantly, in GEE the choice of correlation structure affects efficiency but not consistency – estimates remain valid even if the structure is mis-specified. Reported p-values are based on the Wald Z-statistic and robust (sandwich) standard errors, which are also robust to autocorrelation within clusters.

2 Supplementary Notes to Spatial Spillover Potentials for informing H_2 Policymaking

2.1 SN5: Projection of future cost competitiveness

For the purpose of this paper, cost competitiveness is defined as the difference between the cost of green H_2 (or its derivatives, such as e-methanol or e-kerosene) and the cost of the incumbent fossil energy carrier used in each sector. Cost estimates up to 2050 are taken from Odenweller and Ueckerdt,[42] and subsequently extended to 2100, which aligns with the time horizon of the IPCC 1.5 °C target. Extending the projections beyond 2050 is necessary, as previous research indicates that neither technology adoption nor cost structures are expected to have reached saturation by mid-century.[52]

Green H_2 costs are extrapolated beyond 2050 using a Wright's Law formulation anchored at their estimated 2050 values. The rate of cost decline implied by this formulation is estimated from observed values between 2023 and 2050 using nonlinear least-squares methods, implemented via R's *minpack.lm* package. This procedure yields deterministic cost trajectories for each green H_2 cost scenario. In line with the objective of providing internally consistent scenario pathways to the simulation, we do not introduce stochastic uncertainty into the learning rate.

Fossil-cost trajectories depend on the assumed carbon-price pathway (Supplementary Note 7). Under a flat carbon-price setting, we follow Way et al in estimating a first-order autoregressive model, in which costs in each year depend on the preceding year and a random disturbance.[55] The autoregressive parameter is obtained by maximum likelihood under stationarity constraints. For the default (escalating) carbon price scenario, fossil costs are projected using autoregressive integrated moving-average (ARIMA) models, to account for the non-stationarity introduced by changing carbon prices. The appropriate model specification, including the autoregressive order, the degree of differencing, and the moving-average order, is selected using R's *auto.arima* package, which minimizes the Akaike Information Criterion over the available cost projections (2023-2050).

The extended green H_2 and fossil cost trajectories provide sector-specific cost levels and cost differentials for the period 2024–2100. These values enter directly into the simulation framework and serve as dynamic cost inputs to the adoption decision function in the simulation.

We broadly follow Odenweller and Ueckerdt[42] in the choice of technology pairings (see Supplementary Table 5), while adding e-methanol – diesel for shipping, and e-methane – natural gas for power and heat. For other industries we assume that the relevant competition occurs between green H_2 and natural gas.

Supplementary Table 5 Technology mapping by sector.

Sector	Green H_2 and Derivatives	Fossil Technology
Aviation	E-Kerosene	Kerosene
Chemicals	Green H_2	Grey H_2
Heat	E-Methane	Natural Gas
Heavy-duty trucks	Green H_2	Diesel
Iron & steel	Green H_2	Natural Gas
Non-ferrous metals	Green H_2	Natural Gas
Non-metallic minerals	Green H_2	Natural Gas
Other	Green H_2	Natural Gas
Power	E-Methane	Natural Gas
Pulp & paper	Green H_2	Natural Gas
Refining	Green H_2	Grey H_2
Shipping	E-Methanol	Diesel

The development of future cost, in particular for green H_2 and derivatives, is subject to substantial uncertainty. We therefore use a range of H_2 cost estimates that include the mean, progressive and conservative H_2 cost scenarios presented by Odenweller and Ueckerdt.[42] H_2 cost estimates are reported in Supplementary Figure 11. Green H_2 costs for iron & steel are adjusted for differences in technical efficiencies between natural gas and H_2 (20 %).[42]

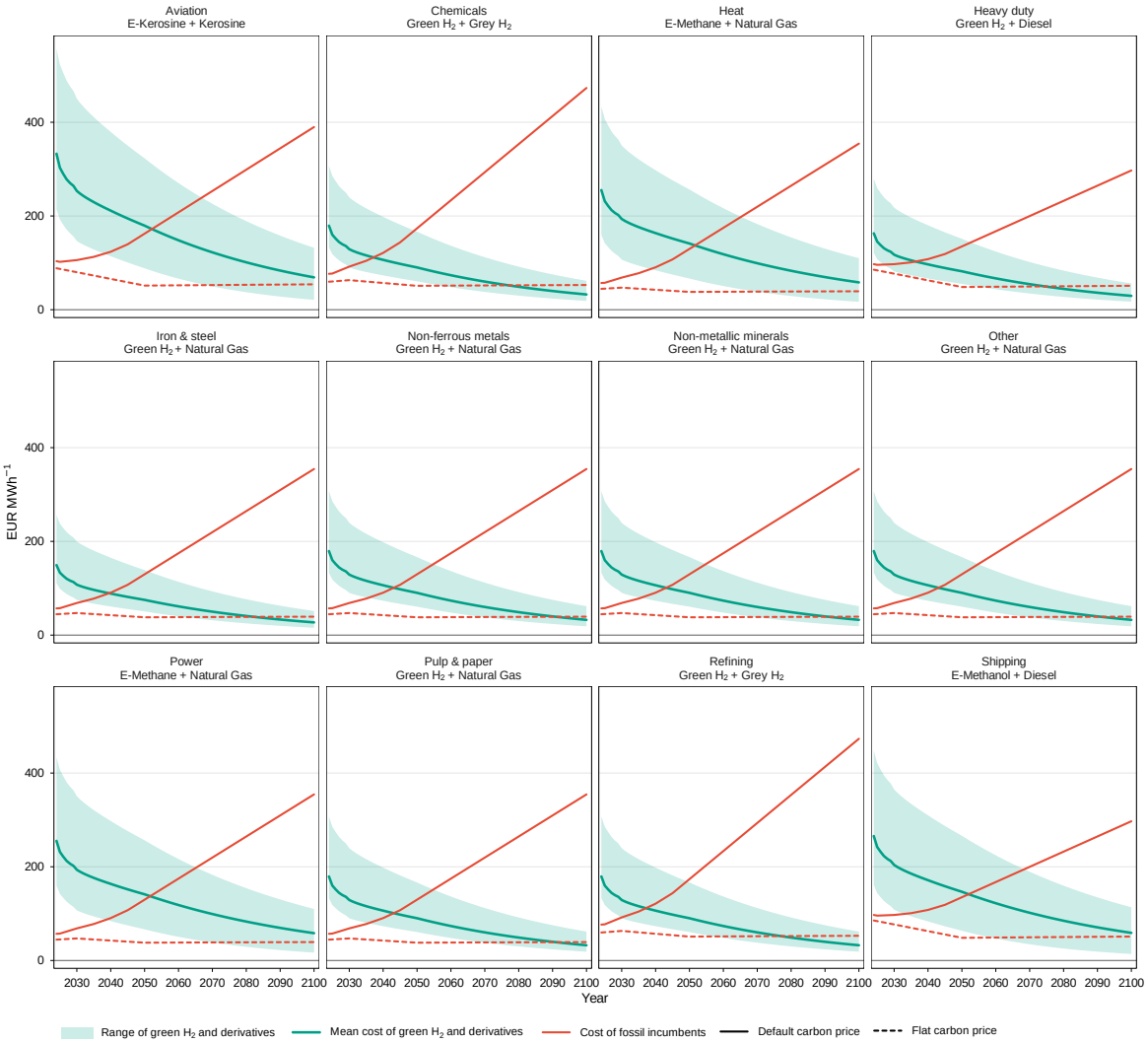

Supplementary Figure 11 Cost trajectories for green H_2, derivatives and fossil incumbents by sector. Projections up to 2050 are based on Odenweller and Ueckerdt [42] and extended to 2100 using an auto-regressive specification for fossil cost trajectories, and a Wright's law specification for the cost trajectories of green H_2 and its derivatives. For green H_2 costs, the solid green line illustrates the mean cost scenario; the green ribbon illustrates the potential range of green costs between progressive and conservative cost scenario. For fossil costs, the solid red line shows the cost trajectory under default (escalating) carbon prices; [75] the dashed line the cost trajectory under flat carbon price assumptions.

Note that our definition of cost competitiveness is necessarily simplifying. We rely on sector-level technology pairings that reflect the most commonly employed incumbent fossil energy source. Yet, we acknowledge that within each sector, incumbent fossil energy sources can to a certain degree differ, based on production process and plant configuration. For instance, in the iron & steel sector, the raw material for downstream steel processing can be produced either through a direct reduction route (using natural gas) or through a blast furnace route (using coke). [76] Similarly, coal rather than natural gas is often used in the smelting and roasting of non-ferrous metals like copper, zinc or lead, or for the production of rotary klins in the cement value chain. [77] As the purpose of this paper is to assess the role of geography and spatial spillovers in the diffusion process rather than making exact, plant-level predictions of cost competitiveness and adoption, we deliberately abstract from these granularities.

Similarly, we choose to define cost competitiveness as cost competitiveness versus fossil incumbents, and reflect alternative decarbonization technologies like direct electrification (e.g., using scrap

electric arc furnaces for steel production, heat pumps for heating, or batteries for heavy-duty transport) through sectoral green H_2 saturation rates. We believe that given the focus and emphasis of this paper this is an adequate approach, given the elevated uncertainty on the cost trajectories of these alternative technologies, and the heterogeneity of these costs across sub-sectors and installations. Further details on the rationale of this modeling choice and the derivation of saturation rates is provided in Supplementary Note 6

2.2 SN6: Competition for alternative decarbonization technologies and saturation rates

Green H_2 competes not only with fossil incumbents such as natural gas, diesel, or kerosene, but also with alternative decarbonization technologies. These include direct electrification, carbon capture, storage and utilization (CCUS), and biomass-based solutions, whose applicability varies across sectors and processes. In some applications, these alternatives offer technological advantages, including higher technical efficiency or lower cost.

Conceptually, there are two ways to reflect this competition in our model. The first involves constructing a cost competitiveness measure that integrates cost estimates for alternative decarbonization technologies into a single metric. The second involves introducing sector-specific saturation rates that cap the diffusion of green H_2. In the present setting, the first approach is likely to yield misleading results (as described in the following), making saturation rates the more appropriate representation.

Reflecting cost competitiveness requires deriving the cost projections for a broad range of decarbonization technologies. Based on capital and operating cost inputs from the Danish Energy Agency, [78] and on the electricity and carbon price assumptions underlying the construction of green H_2 cost projections (Supplementary Note 5), we compute levelized cost estimates for a set of direct electrification, CCUS, and biomass technologies relevant to the sectors examined in this analysis (see Supplementary Figure 12). Although these projections remain subject to considerable uncertainty, they allow us to approximate plausible cost trajectories and relative competitiveness over time.

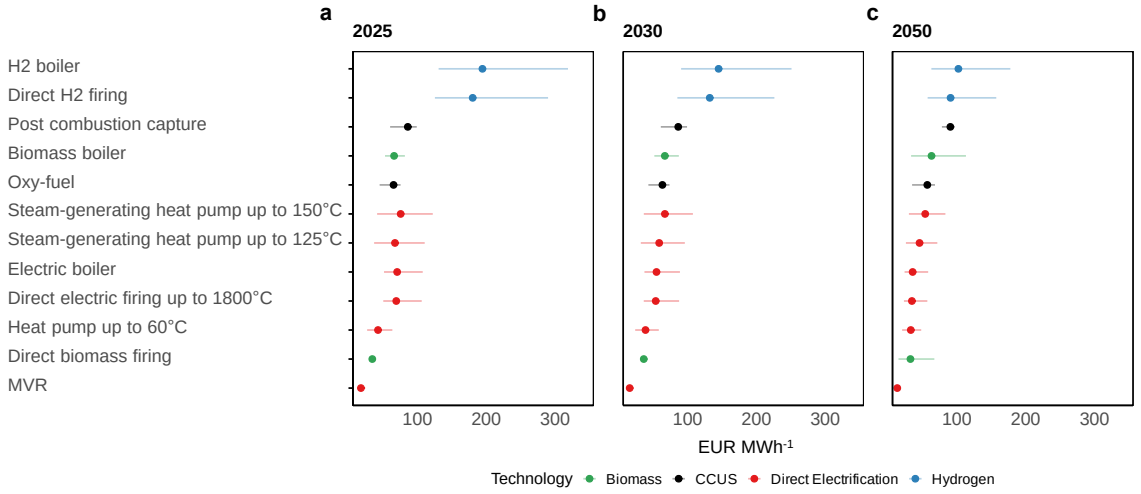

Supplementary Figure 12 Levelized cost of direct electrification, CCUS and biomass technologies. Levelized cost estimates include energy costs as well as levelized capital and operating expenditures based on inputs from the Danish National Energy Agency. [78] Electricity, natural gas and carbon price assumptions are aligned with those used for the green H_2 cost projections in our analysis. The upper bound of natural gas prices is fixed to 6-month TTF natural gas futures as of March 2026, representing constrained natural gas markets. To enable comparability, we construct green H_2 costs by combining H_2 production costs with levelized capital and operating expenditures for natural gas firing, as the Danish National Agency does not provide dedicated assumptions for H_2 firing in industrial contexts. While direct electrification, CCUS and biomass solutions appear to outperform green H_2 in some cases, both costs and applicability vary substantially across industries and production processes. Note that for CCUS pathways, transport and storage costs are not includes, so in reality these costs can be expected to be somewhat higher than suggested.

These estimates could, in principle, be incorporated directly into the model's cost competitiveness variable, thereby extending the framework from a two-way comparison between green H_2 and a fossil incumbent to a multi-way comparison that includes green H_2, the fossil incumbent, direct electrification, CCUS and biomass. However, this approach is problematic for three reasons.

First, we define cost competitiveness at the sector level and do not distinguish between individual activities or processes within sectors. While this simplification is defensible when comparing two energy carriers, namely green H_2 and fossil incumbents, it becomes problematic when extending the comparison to heterogeneous decarbonization technologies. Many alternatives, such as mechanical vapor recompression in pulp & paper, apply only to specific production steps or configurations.[78] They may appear more competitive than green H_2, yet they are not directly comparable because they often address different parts of the value chain.

Second, alternative technologies exhibit fundamentally different cost structures. Green H_2 can, in some cases, substitute for natural gas with limited additional capital expenditure. By contrast, direct electrification technologies such as steam heat pumps for process heat up to 150°C, direct electric firing for higher temperatures, or CCUS solutions typically require substantial upfront capital investment to modify production facilities, even if recurring energy and operating costs are lower. A comparison based solely on energy costs would therefore be biased.[78] To reflect this, the cost projections shown in Supplementary Figure 12 include levelized capital and operating costs in addition to energy costs (the calculations are available on the paper's Github repository). These are based on generic applications and are thus highly stylized, which makes them useful for qualitative comparisons but unsuitable as model inputs. A comprehensive assessment of levelized capital and operating expenditures is not feasible in the present context, given the heterogeneity of production processes and differences in value chain coverage across technologies, even within a single sector.

Third, cost projections for direct electrification, CCUS and biomass, like those for green H_2, remain highly uncertain. Collapsing multiple technologies into a single cost competitiveness metric complicates the representation of this uncertainty. Even if we specified cost ranges for each technology, we would also need to define their correlation structure. For example, declining renewable electricity costs would simultaneously improve the competitiveness of green H_2 and direct electrification.

In light of these considerations, we represent competition between green H_2, direct electrification, and CCUS through sector-level saturation rates rather than a single multi-way cost competitiveness metric. This approach allows us to specify broad saturation ranges across three scenarios (restricted, central, and extended), thereby capturing uncertainty in technical applicability and cost development separately from competition between green H_2 and fossil incumbents. Operationally, we define saturation relative to the sector's relevant energy or feedstock base as specified in each sector subsection.

In defining saturation rates, we proceed as follows:

1. **Process assessment:** For each sector, we first assess the production process and identify which energy inputs are technically substitutable with green H_2. In this step, we exclude process components that are already decarbonized, for example through biomass, or fully electrified. For the transport and heating sectors, which do not feature a discrete production process, we omit this step.
2. **Assessment of decarbonization options:** We then identify the set of alternative decarbonization technologies that compete with green H_2. Across sectors, we distinguish four broad pathways for replacing fossil feedstocks, fuels and process heat: direct electrification, including direct electric firing, electric boilers and batteries; green H_2 and its derivatives, such as e-kerosene or green methanol; CCUS, including blue H_2 produced from natural gas via steam methane reforming with CCUS; and biomass-based solutions, such as biofuels, biomass boilers and biomass gasification.
3. **Derivation of saturation rates:** We assess the relative competitiveness of green H_2 within this technology portfolio and derive sector-specific saturation rates for the restricted, central and extended scenarios. Where possible, we anchor these rates in EU policy targets or projections from institutions such as the International Energy Agency (IEA) or BNEF. To reflect substantial uncertainty, we deliberately select saturation rates that span a wide range of plausible outcomes,

thereby covering a broad solution space that captures most competitive constellations between green H_2, direct electrification and CCUS.

Although saturation rates are defined at the sectoral level, the scenarios share a common underlying rationale, which we summarize below:

- **Restricted case:** Direct electrification technologies are technologically mature across most applications. Low- and medium-temperature process heat is almost fully decarbonized through electrification and partially electrified even in selected high-temperature processes, such as non-metallic minerals or iron & steel. Biomass supply remains unconstrained, and regulatory treatment of indirect land-use change emissions [79] and carbon debt [80] is not tightened further. CCUS technologies mature substantially, CO_2 removal becomes more effective, and transport and storage infrastructure is deployed at scale. Methane emissions remain unpriced. In this setting, biomass and CCUS outcompete green H_2 in most applications, except for selected core uses in iron, steel and chemicals.
- **Central case:** Direct electrification is widely deployed for low- and medium-temperature process heat but remains technologically constrained in high-temperature applications. Supply chain bottlenecks and stricter scrutiny of life-cycle emissions limit biomass use to core applications, notably aviation, pulp and cement. CCUS technologies improve, but their competitiveness is reduced by pricing residual emissions and more limited CO_2 infrastructure. At the same time, declining electrolysis costs improve the relative position of green H_2. As a result, green H_2 is widely adopted as a feedstock and competes on roughly equal footing with CCUS, biomass and, where technically feasible, direct electrification for high-temperature process heat.
- **Extended case:** Direct electrification remains broadly deployed for low- and medium-temperature heat but does not achieve at-scale deployment in more demanding high-temperature processes. Biomass availability becomes severely constrained, preventing expansion beyond existing applications in pulp and cement as well as limited aviation use. CCUS fails to achieve substantial improvements in technological maturity and carbon removal effectiveness. Methane emissions are priced, further eroding the competitiveness of fossil-based CCUS pathways. CO_2 infrastructure does not materialize at scale. Under these conditions of weakened competition, green H_2 attains a dominant position in the provision of low-carbon feedstocks, high-temperature process heat and transport fuels.

It is important to note that the saturation rates are designed to reflect the competition between green H_2 and alternative decarbonization technologies for a given level of industrial activity. We account for expected changes in industrial activity – for example, a decline in refining due to the phase-out of fossil transport fuels, or a reduction in chemicals production resulting from higher imports – by adjusting sectoral activity levels using EU-27 energy balance projections from the European Commission's Global Energy and Climate Outlook (see Methods). This outlook builds on the SAM GEM E3 general equilibrium model, which the European Commission employs to construct baseline scenarios for policy impact assessments, including those underpinning the EU Fit for 55 package. [71]

Finally, we emphasize that the primary purpose of the saturation rates is to generate a transparent projection of green H_2 demand that serves as an input for subsequent policy evaluation. Although these rates are relevant, particularly when benchmarking against policy targets, they remain secondary to the central contribution of the paper, which is to demonstrate the importance of spatially-informed demand-side policies. A detailed structural analysis of technology competition, and of how spatial patterns shape this competition, constitutes a promising avenue for future research but lies beyond the scope of the present study.

Aviation

Decarbonizing the aviation sector is structurally challenging because aircraft exhibit long technical lifetimes and slow fleet turnover, [81] while aviation fuels require exceptionally high volumetric energy

density. Conventional jet fuel provides approximately 23 MJ/l,[82] which constrains the feasibility of alternative energy carriers.

The principal low-carbon options include:[81]

- Direct electrification via batteries
- E-fuels (e.g., e-kerosene) or cryogenic fuels synthesized from green H_2
- E-fuels (e.g., e-kerosene) or cryogenic fuels synthesized from blue H_2
- Biofuels

Direct electrification in aviation is more constrained than in ground transport. Despite higher drivetrain efficiencies and expected improvements in battery technology, the gravimetric energy density of batteries remains insufficient for medium- and long-haul aviation. The battery mass required to provide an energy-equivalent amount of drop-in fuel is approximately 28 times higher.[82,83] This weight penalty renders large-scale battery-electric aviation infeasible beyond short-range applications.

Drop-in e-fuels such as e-kerosene are produced via reverse water-gas shift and Fischer-Tropsch synthesis using H_2 and captured or biogenic CO_2. These fuels are compatible with existing aircraft and refueling infrastructure, implying that a substitution of conventional jet fuel by 2050 is technically feasible without premature asset scrapping.[81] However, as in other end uses of green H_2, large-scale deployment requires a substantial expansion of renewable electricity generation and electrolysis capacity.[84] Cryogenic fuels such as liquid H_2 eliminate carbon at the point of use but face structural constraints related to volumetric energy density and storage requirements. Liquid H_2 has a lower volumetric energy density than drop-in fuels and requires cryogenic storage systems, introducing safety and engineering challenges associated with volatility and flammability.[83]

For both drop-in fuels and cryogenic fuels, green H_2 can be replaced with blue H_2 that is generated from natural gas using CCUS. The competitiveness of this CCUS pathway depends strongly on the relative pricing of natural gas, the effectiveness of carbon removal and the pricing of residual carbon and methane emissions.[43]

At present, most commercially available sustainable aviation fuels are bio-based and produced through hydrotreating oils, fats, and residues.[83] While lifecycle emissions are lower than for conventional jet fuel, residual carbon intensities remain significant and vary widely by feedstock. Biofuels derived from waste oils exhibit lifecycle emissions of approximately 14–23 g CO_2/MJ, whereas fuels produced from virgin oils range between 65–99 g CO_2/MJ. Although improved agricultural practices and biogenic carbon sequestration in soils could reduce these emissions, such measures primarily mitigate rather than eliminate residual emissions and add additional cost layers.[83] In the short term, biofuels can contribute to emission reductions given their technical maturity and compatibility with existing assets. In the long term, however, constrained sustainable biomass availability is likely to limit production volumes and increase marginal costs.[81]

The European Union's ReFuelEU Aviation regulation establishes binding targets for sustainable aviation fuel deployment, requiring a 70% share of sustainable aviation fuels overall and a 35% share of e-fuels by 2050.[8] These targets reflect both climate neutrality objectives and expected constraints on biomass availability. The 35% target is also consistent with the IEA's net zero projections for 2050.[85]

Supplementary Table 6 reports the saturation rates and assumptions based on this analysis (assuming e-kerosene rather than liquid H_2 is the baseline carrier for aviation fuels).

Chemicals

The Chemicals sector encompasses a heterogeneous portfolio of products and processes, including nitrogen-based chemicals (such as ammonia, 35% of estimated energy consumption in 2050 as recorded

Supplementary Table 6 Saturation assumptions for green H_2 in aviation

Saturation scenario	Saturation rate	Rationale
Restricted	0%	Biofuels remain persistently cheaper than e-fuels in the long term; sustainable biomass supply is sufficient, and residual lifecycle emissions are mitigated (e.g., via carbon sequestration).
Central	35%	The EU 2050 target of 35% e-fuel penetration is achieved but not exceeded in the long term.
Extended	80%	E-fuels exceed the EU 2050 target and largely displace biofuels in the long term as biomass constraints and residual emissions reduce biofuel competitiveness.

Note: Saturation values rounded to 5% increments.

in our database), industrial H_2 and synthetic gas (8%), organic chemicals and polymers (46%), and other inorganic chemicals (12%).

Across these subsectors, emissions result from high-temperature process heat and process emissions. The relative importance of these elements differs across subsectors, which in turn shapes the relative role of green H_2 in deep decarbonization pathways.

Nitrogen-based chemicals

Nitrogen-based chemicals comprise primarily ammonia, which is used as an input for nitric acid and other downstream products within the fertilizer value chain.

The conventional nitrogen chemicals value chain involves several stages. First, H_2 is produced from fossil feedstocks via steam reforming. The resulting H_2 is then combined with nitrogen in the Haber-Bosch process to synthesize ammonia. This synthesis step is exothermic; electricity input for nitrogen separation and the Haber-Bosch process is negligible.[86] In subsequent steps, ammonia can be reacted with CO_2 to produce urea, with phosphoric acid to produce phosphate-based fertilizers, or oxidized to nitric acid, which serves as an input for fertilizers and explosives. Energy use and emissions are concentrated almost entirely in the steam reforming step that generates H_2, which in the conventional production process relies predominantly on fossil feedstocks.[86] In our analysis of decarbonization options, we therefore focus on this value chain step.

Decarbonization options include:[86]

- Electrolytic H_2 (green H_2)
- CCUS applied to steam reforming (blue H_2)
- H_2 produced via dry biomass gasification

Regarding competition between green and blue H_2 pathways, global project announcements for H_2 projects with ammonia output are heavily skewed towards green H_2 (87%).[2] Given the very large biomass requirements, dry biomass gasification is likely to remain a marginal option.[86]

In setting saturation rates, we assume the following split between green and blue H_2 pathways for ammonia synthesis: in the central case, green H_2 is assumed to supply approximately 80% of the H_2 feedstock, consistent with the IEA's Net Zero scenario.[85] In the extended case, green H_2 fully outcompetes blue H_2, reflecting limited carbon removal effectiveness and stringent pricing of residual CO_2 and methane emissions.[43] In the restricted case, we assume an equal split between green and blue H_2.

H_2 and synthetic gas

As H_2 is the key precursor in the production of ammonia, we assume the relative competitiveness of decarbonization options to match that of ammonia and apply the same saturation rates.

Organic chemicals and polymers

Organic chemicals and polymers comprise products such as methanol, olefins, and aromatics, which serve as key precursors for plastic resins. Production pathways vary by product. Methanol, a precursor to formaldehyde and various plastics, is synthesized from synthesis gas, which is typically produced via steam reforming of natural gas or coal gasification. Olefins, such as ethylene and propylene, are generated through steam cracking of naphtha or ethane, both of which are outputs of the refining sector (see Refining). Aromatics, including benzene, toluene, and xylene, are generally produced via catalytic reforming of naphtha. These platform chemicals function as intermediates that are subsequently converted into a broad range of polymers and downstream products.[87,88]

Decarbonizing organic chemicals and polymers is particularly challenging because carbon is required as a material feedstock. Deep decarbonization therefore entails substantial process redesign, replacing not only fossil-based process heat but also fossil feedstocks. We first assess methanol, followed by olefins and aromatics, as green H_2-based methanol plays a central role in decarbonization pathways for the latter.

Methanol

In the conventional production process, methanol is produced through the hydrogenation of CO and CO_2 contained in syngas, which is derived from natural gas or coal using steam reforming.[89] Energy input and emissions are concentrated in the steam reforming step.[89] Methanol synthesis itself is exothermic but requires process temperatures of 200–300°C to maintain reaction temperatures and pressures. Process heat is typically generated from the feedstock.[90] Decarbonization options include:[86,87]

- Synthetic carbon pathways using green H_2 and captured or biogenic CO_2 (yielding "green methanol")
- Synthetic carbon pathways using blue H_2 and captured or biogenic CO_2 (yielding "blue methanol")
- CCUS in steam reforming (yielding "blue methanol")
- Dry biomass gasification

The competition between green H_2 and blue H_2 and CCUS pathways is highly dependent on the effectiveness of carbon removal, the presence of methane leakages, and the pricing of fossil inputs, carbon, and methane emissions.[43] Due to the extremely high amount of biomass that would be required, dry biomass gasification is likely to play a subordinate role.[86]

In setting saturation rates, we assume the following splits between green and blue H_2 in methanol synthesis. In the central case, green H_2 is assumed to supply approximately 80% of the H_2 feedstock used in methanol production, consistent with the predominance of electrolytic H_2 in the IEA's Net Zero scenario.[85] In the extended case, green H_2 is assumed to fully displace blue H_2. In the restricted case, we assume an equal split between green and blue H_2. Across all scenarios, process heat in methanol production is assumed to continue to be generated primarily from the feedstock. Consequently, the upstream H_2 supply mix directly determines the overall energy composition of decarbonized methanol synthesis. This structurally mirrors our assumptions for nitrogen-based chemicals.

Olefins and aromatics

For olefins and aromatics, it is important to distinguish between the decarbonization of feedstocks and the decarbonization of process heat. Process heat can account for up to 40% of total emissions.[90] In products such as ethylene, up to 35% of energy consumption occurs outside the high-temperature steam cracking step.[87] While process heat in the conventional production setup is often generated from feedstocks or through the combustion of by-products on site, this configuration may change under a decarbonized process design.[87,90]

Decarbonization options include:[86,87,90]

- Direct electrification technologies for process heat (e.g., resistive heating, electric steam crackers)
- Methanol-to-olefins (MTO) or methanol-to-aromatics (MTA) pathways using green methanol (feedstock and process heat)
- Methanol-to-olefins (MTO) or methanol-to-aromatics (MTA) pathways using blue methanol (feedstock and process heat)
- CCUS in steam cracking (feedstock and process heat)

Direct electrification through resistive heating is a high-maturity option for replacing process heat in lower-temperature separation steps. For the very high temperatures required in steam cracking (electric steam crackers), maturity is low and may require substantial process redesign.[90] The Methanol-to-Olefins (MTO) and Methanol-to-Aromatics (MTA) routes allow producers to synthesize these platform chemicals from alternative carbon sources such as natural gas, coal, or CO_2, rather than naphtha.[91] From today's perspective, CCUS often exhibits comparatively low marginal abatement costs, but requires large-scale CO_2 transport and storage infrastructure[87] and is complicated by the low CO_2 concentration in steam cracker flue gases (4–7%), which increases capture costs relative to more concentrated streams such as those in steam reforming.[88]

Based on these considerations, we assume the following technology split. In the central case, process heat is assumed to continue to be generated primarily from feedstocks. We assume the split between green H_2 (green MTO/MTA) and CCUS (through steam cracking with CCUS and blue MTO/MTA pathways) to be the same as for methanol. This yields a saturation rate of approximately 80%. In the extended case, green H_2 fully outcompetes CCUS. In the restricted case, lower-temperature process heat (up to 35%) is electrified via resistive heating, with the remaining energy input (high-temperature process heat and feedstock) split equally between green H_2 and CCUS pathways. This results in a saturation rate of approximately 30%.

Based on data from Methanol Institute[92] and Methanol Market Services[93] we assume methanol production to account for approximately 8% of total output within organic chemicals, with the remainder covered by olefins and aromatics.

Other inorganic chemicals

Other inorganic chemicals (beyond H_2, ammonia, and synthetic gas) include products such as soda ash, chlor-alkali chemicals, sulfuric acid and carbon black. In our database, approximately half of estimated energy consumption in 2050 within the other inorganic chemicals segment relates to soda ash.

Soda ash is produced from limestone and brine, using ammonia as a recycled catalyst. Emissions and energy consumption are concentrated in the lime calcination step. In this step, calcium carbonate is calcined to generate quicklime, which releases CO_2 as process emissions and requires process temperatures of 950–1100°C.[94] While this process is also used in the production of lime (see non-metallic minerals), electricity plays a more prominent role, resulting in a thermal energy share of 75%[94] compared to 92% for lime.[86] Decarbonization options are described more extensively in the non-metallic minerals section. Chlor-alkali production is an electrochemical process for which full electrification is commercialized at scale.[90] We therefore assume chlor-alkali production to not be addressable for green H_2. Sulfuric acid is today produced mainly as a byproduct of refining processes, which are expected to decline.[95] The shortfall could be replaced through sulfur mining or with sulfuric acid generated as a byproduct in the processing of copper, gypsum, or cement.[95,96] We therefore assume sulfuric acid to also not be materially addressable for green H_2. Carbon black today is produced primarily from oil or natural gas in a furnace black process, which results in significant process emissions. Decarbonization options include direct electrification through plasma technology, CCUS and feedstock substitution with biogas, biomass-based pyrolysis oil or e-methane. An other option is to replace the furnace black process with methane pyrolysis, which produces solid carbon black and H_2, but needs high-temperature process heat, which again needs to be decarbonized. H_2 is relevant primarily to decarbonize process heat in methane pyrolysis (where the H_2 generated in the pyrolysis rather than externally sourced green H_2 could be used to sustain reactor temperatures) or in a furnace black process with CCUS or feedstock substitution.[97] As the primary decarbonization

lever is feedstock substitution, we assume the role of (externally sourced) green H_2 in carbon black production to be negligible.

Based on the above, green H_2 potential is concentrated in soda ash. We assume the same decarbonization options and saturation rates as for lime (see non-metallic minerals), while adjusting the non-addressable electricity share to 25%. This results in saturation rates of 7.5% for the central case, 30% for the extended case, and 0% for the restricted case.

Summary

Based on our subsector analysis, we set saturation rates as weighted averages of the subsector saturation rates (Supplementary Table 7).

Supplementary Table 7 Saturation assumptions for green H_2 in Chemicals

Saturation scenario	Saturation rate	Rationale
Restricted	35%	Equal split between green and blue H_2 in ammonia and methanol (applied to H_2 feedstock, which dominates energy input); more limited role in olefins and aromatics due to electrification of lower-temperature heat (up to 35% of total energy input) and CCUS competition in steam cracking; no material role in other inorganic chemicals.
Central	70%	Green H_2 supplies ≈80% of H_2 feedstock in ammonia and methanol (consistent with the supply mix in the IEA's Net Zero H_2 scenario), analogous split applied to MTO/MTA and steam-cracking pathways; negligible role in chlor-alkali and sulfuric acid; limited but positive role in soda ash.
Extended	90%	Green H_2 fully outcompetes blue H_2/CCUS in ammonia, methanol, H_2/syngas, and olefins/aromatics; biomass remains marginal; chlor-alkali and sulfuric acid remain non-addressable; soda ash reaches 30% saturation.

Note: Sectoral saturation rates derived by weighting subsector assumptions with estimated 2050 energy shares in the database (46% organic chemicals and polymers, 35% nitrogen-based chemicals, 8% H_2 and synthetic gas, 12% other inorganic chemicals). Values rounded to 5% increments.

Heat

The heating sector comprises space and water heating in residential buildings as well as heating demand in the commercial and services sectors. An important aspect of the decarbonization of buildings is increasing energy efficiency in new buildings and through retrofits in the existing building stock. Increasing energy efficiency has the double benefit of reducing the amount of energy that needs to be decarbonized and, for example by lowering the heating point, prepares the ground for the adoption of decarbonization technologies such as heat pumps.[98]

Technologies for the decarbonization of heating beyond efficiency include:[99,100]

- Direct electrification via air-source and ground-source heat pumps
- Expansion and decarbonization of district heating systems
- Green H_2 boilers or hybrid heat pump systems
- Solar thermal heating
- Biomass boilers

Electrification through heat pumps is widely regarded as the central pathway for decarbonization of heating in Europe, supported by falling technology costs and high operational efficiencies.[2] For dense urban areas, extension and decarbonization of district heating systems that integrate large-scale renewable as well as waste heat sources can also play an important role.[101] Technical efficiency

in terms of power input for the generation of useful heat can reach more than 275% for individual heat pumps, and more than 300% for decarbonized district heating systems.

Green H_2 could in principle be deployed at the building level through H_2 combustion boilers or H_2 fuel cell micro-combined heat and power (micro-CHP) systems, or at the network level through H_2-fired turbines or CHPs integrated into district heating systems.[49] Large-scale H_2 deployment in building heat is unlikely to be cost-effective or system-efficient relative to electrification-based pathways. In a comprehensive meta-analysis of 54 studies, Rosenow evaluates scenarios that include H_2 for space and water heating and finds that at-scale deployment is generally not supported.[100] Across studies, H_2 heating is associated with higher overall energy system costs, higher consumer heating costs, and in many cases higher lifecycle environmental impacts compared to alternatives such as electric heat pumps and decarbonized district heating. The reported saturation rates for green H_2 in heating range between 0% and 10%, with a median value of 1%.[100]

Solar thermal heating plays an ancillary role in integrated heating systems, where it can reduce system costs by contributing to water heating.[99] Biomass boilers can likewise be integrated into hybrid heating systems combining heat pumps and solar thermal technologies,[99] and may contribute to the decarbonization of heating, particularly in rural areas.[102]

The current state of project deployment reinforces this assessment. Progress in the commercialization and rollout of H_2-ready boilers and fuel cell systems remains very limited.[2] Pilot projects exist, but large-scale infrastructure conversion from natural gas to H_2 has not materialized in most European markets.[2] Still, limited applications may arise in specific contexts, including hybrid H_2 heat pump systems in very cold climates where peak loads are high, and as a complementary fuel in certain district heating configurations.[49] In such cases, green H_2 could provide flexibility or backup capacity rather than serve as a dominant primary heat source.

Supplementary Table 8 reports the saturation rates and assumptions based on this analysis.

Supplementary Table 8 Saturation assumptions for green H_2 in heating

Saturation scenario	Saturation rate	Rationale
Restricted	0%	Electrification and decarbonized district heating dominate; green H_2 remains structurally uncompetitive for space and water heating.
Central	0%	Consistent with the median value of 1% reported in the literature and the absence of large-scale deployment; green H_2 does not achieve material penetration at system level.
Extended	5%	Limited niche applications in hybrid heat pump systems and selected district heating configurations; conservative midpoint within the 0–10% range reported by Rosenow.[100]

Note: Saturation values are rounded to 5% increments.

Heavy-duty transport

Road transport comprises several segments with differing technical requirements and corresponding decarbonization options. We focus exclusively on the heavy-duty segment (trucks), as battery electric vehicles (BEVs) exhibit clear technical and economic advantages over green H_2 applications for two-wheelers, passenger cars, and light-duty vehicles.[103] For heavy-duty vehicles, however, the considerations differ due to higher vehicle weights and longer range requirements.[50] Decarbonization options include:

- Battery electric vehicles (BEVs)
- Fuel cell electric vehicles (FCEVs)
- Green H_2 in internal combustion engines
- E-diesel
- Biofuels

Competition primarily occurs between H_2 fuel cell electric vehicles (FCEVs) and battery electric vehicles (BEVs). Although BEVs remain the most energy-efficient option for decarbonizing heavy-duty transport, as in passenger and light-duty segments, large vehicle classes and long-haul applications may require very large battery capacities.[50] The relative performance of BEVs depends strongly on assumptions regarding battery costs, battery pack lifetimes, and the availability of high-power fast charging.[104] The deployment of high-power charging infrastructure may, in turn, require substantial grid reinforcements.[105] In certain applications and vehicle classes, these constraints may render FCEVs more attractive.[50]

Among green H_2 applications, fuel cells represent the technology closest to commercialization. In contrast, the use of green H_2 in internal combustion engines remains at an early stage. E-diesel, which can serve as a drop-in fuel in existing vehicles, requires fewer adjustments to refueling infrastructure but is less energy-efficient than fuel cells.[50] For the purpose of our analysis, we therefore assume green H_2 to be deployed primarily in FCEVs.

Similar to aviation, biofuels such as biodiesel constitute an additional decarbonization pathway. Today, biofuels such as ethanol are commonly blended with conventional fuels to reduce carbon emissions.[106] In forward-looking scenarios, however, the role of biofuels in heavy-duty transport remains limited, reflecting supply-side constraints and competing uses in other hard-to-abate sectors.[85]

Supplementary Table 9 reports the saturation rates and assumptions based on this analysis.

Supplementary Table 9 Saturation assumptions for green H_2 in heavy-duty transport

Saturation scenario	Saturation rate	Rationale
Restricted	0%	BEVs dominate all heavy-duty segments, including long-haul transport, for example due to continued advances in battery technology and the successful roll-out of megawatt charging infrastructure.
Central	25%	FCEVs are primarily deployed in larger vehicle classes and long-haul routes. This level is broadly consistent with the projected green H_2 share in heavy-duty energy use in the IEA's Net Zero 2025 report.[85]
Extended	35%	Green H_2 penetration exceeds baseline expectations, for example due to grid bottlenecks limiting high-power charging, slower battery cost reductions, or battery material constraints. We assume a 10 percentage point increase relative to the central case, reflecting a stronger role for FCEVs in long-haul applications.

Note: Saturation values refer to final energy demand and are rounded to 5% increments.

Iron & steel

Global iron & steel production is predominantly based on the blast furnace–basic oxygen furnace (BF–BOF) route.[86] In this process, iron ore, coke, and fluxes are fed into the blast furnace (BF), where oxygen is removed from iron ore to produce molten iron. The molten iron is then transferred to the basic oxygen furnace (BOF), where impurities are removed to produce steel. The gaseous by-products of this process (blast furnace gas, coke oven gas, and basic oxygen furnace gas) are utilized on-site in combined heat and power (CHP) plants to generate electricity and heat. These gases exhibit high emission factors (blast furnace gas has nearly four times the emission factor of natural gas).[86]

Decarbonization options for the steel sector, in most cases, require major process redesign compared to the BF–BOF route.

These include the following process options:[86,107,108]

- Use of steel scrap in an electric arc furnace (EAF), replacing iron as input material (secondary steelmaking)
- Direct electrification through electrowinning technologies such as molten oxide electrolysis, where electricity serves as both energy source and reduction agent

- Direct reduction of iron (DRI) and subsequent processing in an EAF. This process relies on the use of natural gas (with CCUS) or green H_2 as a reducing agent in the DRI plant, and electricity in the EAF
- H_2-based direct steel production using flash and plasma reactors instead of an EAF
- CCUS and efficiency improvements (e.g., smelting reduction and top gas recycling) in the BF–BOF process
- Substitution of solid biomass (biochar) in the BF–BOF process

Secondary steelmaking is an important driver of decarbonization, as it reduces the requirement for energy-intensive primary iron production. Today, the share of scrap in steel production amounts to approximately 30%. This share could increase: for 2050, the World Steel Association targets a scrap steel share of 35%, while the IEA projects a share of 55% in its Net Zero 2050 scenario. The scrap share is strictly limited by global scrap supply.[108] Direct electrification technologies such as molten oxide electrolysis remain at relatively low technical maturity compared to other production routes.[86,108] Direct reduction of iron (DRI) using green H_2 is approaching commercial maturity and faces few technical constraints, apart from potential shortages of DR-grade iron ore and challenges in achieving full metallization during the final DR stages.[109] A large majority of green steel projects announced in Europe plan to use green H_2-based direct reduction technology.[110] CCUS and efficiency improvements can markedly improve the emissions performance of the BF–BOF route. However, retrofits such as top-gas recycling are costly,[108] and residual emissions (at least 14%) persist.[86] Substitution of biomass in the BF–BOF process is technically feasible. However, competitiveness depends on biomass supply chain constraints, given the large energy requirements, and the emissions reduction potential is sensitive to life-cycle accounting.[108]

As these processes differ substantially in the type and structure of energy input, we set saturation rates by varying two parameters for which publicly available projection ranges exist: the share of secondary steelmaking and the share of green H_2-based direct reduction in primary steelmaking. Total sectoral H_2 saturation is given by the green H_2 share in primary iron production multiplied by the primary steel share (i.e., one minus the scrap share).

Supplementary Table 10 reports the saturation rates and assumptions based on this analysis.

Supplementary Table 10 Saturation assumptions for green H_2 in iron & steel

Saturation scenario	Saturation rate	Rationale
Restricted	20%	IEA green H_2 share in primary iron production (44%) combined with high scrap share (55%, IEA Net Zero scenario)[?]
Central	40%	BNEF green H_2 share in primary iron production (65%) combined with a moderate scrap share (35%)[111]
Extended	70%	Dominant role of green H_2 in primary iron production (100%) combined with low scrap share (approximately 30%, current global average)[112]

Note: Saturation values rounded to 5% increments.

Non-ferrous metals

The non-ferrous metals sector includes the production of aluminum, copper, lead, zinc, and tin, with aluminum (78%) and copper (18%) accounting for the major share of 2050 estimated energy consumption recorded in our database. We therefore focus on aluminum and copper in our analysis of saturation rates.

Aluminum

Primary aluminum is produced from bauxite in a high-temperature process. First, alumina is refined from bauxite using caustic soda. The alumina is then processed into liquid aluminum in an electrolysis cell. Emissions and energy consumption are concentrated in the electrolysis step, which is

electricity-intensive. However, the full process (including refining) also uses significant thermal energy (about 30% of total energy input) and carbon anodes, which result in substantial process emissions when consumed.[86] Thermal energy use accounts for up to 16% of emissions. Emissions can be reduced through the use of inert anodes, which avoid process emissions but increase electricity consumption per tonne of aluminum by up to 20%.

Beyond process redesign, decarbonization options for the remaining thermal energy input include:[86,113]

- Electrification
- Fuel-switching to green H_2
- Fossil fuels (e.g., natural gas) combined with CCUS

Green H_2 is a viable option in alumina refining, in the furnaces used for aluminum recycling and aluminum casting, and, when not replaced by inert anodes, in the production of carbon anodes.[113] Despite high process temperatures, direct electrification can be a viable option for bauxite processing steps and in aluminum casting. The relevance of CCUS declines when carbon anodes are replaced with inert anodes that do not produce process emissions, but it could still be used in connection with the continued use of natural gas for the generation of process heat.[113] Given the large energy requirements, biomass supply chain constraints and the sensitivity of emissions reduction potential to life-cycle accounting we assume biomass to play a subordinate role in the aluminum sector.

Secondary aluminum production is based on recycled aluminum and therefore skips the refining and electrolysis steps.[86] While overall energy consumption is significantly lower, the potential share of green H_2 in the overall energy mix increases as the share of secondary (recycled) aluminum production rises, since the electricity-intensive steps of the value chain are eliminated. The IEA's Net Zero scenario projects a target share of 55% for secondary aluminum production by 2050.[2]

Copper

Copper production involves flash smelting of concentrate in an oxygen-enriched atmosphere to produce matte and slag, with slag treated in a slag-cleaning furnace to recover entrained copper. The matte is converted to blister copper, refined in anode furnaces to remove residual impurities, cast into anodes, and electrolytically refined to high-purity copper cathodes.[114]

Green H_2 can replace natural gas as a reducing agent in the anode furnace and the slag-cleaning furnace, and substitute for natural gas in the generation of process heat. This substitution can increase specific energy demand by up to 20% compared to natural gas and metallurgical coke but, if H_2 is produced on site, also yields oxygen as a byproduct, which reduces the need for electricity-intensive oxygen production by up to 30%. Beyond process redesign, decarbonization options for the remaining energy input used for process heat generation are analogous to those for aluminum. However, due to melt chemistry constraints and the extremely high temperatures required, direct electrification is considered somewhat less relevant than in other applications.[114]

In the traditional production setup, natural gas and metallurgical coke account for approximately 45% of energy input. Adjusting for increased specific energy demand when switching to H_2 and accounting for the use of the oxygen byproduct, the share increases to 55%.[114]

Summary

In determining saturation rates, we weight the contribution of copper at 18%, consistent with the energy consumption recorded in our database. As the remaining metals account for less than 4% of energy consumption, we simplify by weighting aluminum at 82%. Supplementary Table 11 reports the saturation rates and assumptions based on these considerations.

Supplementary Table 11 Saturation assumptions for green H_2 in non-ferrous metals

Saturation scenario	Saturation rate	Rationale
Restricted	0%	Predominant use of inert anodes and direct electrification of furnaces in aluminum; use of direct electrification and CCUS for major off-gas streams in copper
Central	25%	Realization of 50% of addressable potential in primary aluminum (30%), secondary aluminum (66%), and copper (55%), assuming a 55% secondary aluminum share. Remainder covered through direct electrification.
Extended	50%	Realization of full addressable potential in primary aluminum (30%), secondary aluminum (66%), and copper (55%), assuming a 55% secondary aluminum share

Note: Saturation values rounded to 5% increments.

Non-metallic minerals

The non-metallic minerals sector includes the production of cement, ceramics, glass, lime, gypsum and plaster. Cement (45%), ceramics (23%), glass (22%) and lime (6%) encompass the major share of estimated energy consumption for 2050 (as recorded in our database) for the sector.

Across all major sub-sectors, emissions originate from a combination of high-temperature process heat and, to varying degrees, process-related chemical reactions. The relative importance of these two components differs across cement, lime, ceramics and glass, which in turn shapes the relative role of green H_2 in deep decarbonization pathways.

Cement

The cement production process includes raw material processing, a calcination kiln that produces clinker and final product finishing that processes clinker into cement. This occurs at extremely high process heats. Emissions and energy consumption are concentrated in the calcination step. In this step calcium carbonate is calcined to generate quicklime, which releases CO_2 as process emissions, in addition to emissions from process heat.[86] Approximately 90% of energy input is high-temperature process heat (1,400°C, the remainder is electricity).

We separate the analysis into two components: decarbonization of process emissions and decarbonization of process heat.

To fully avoid process emissions in the kiln, possible options include chemical lime synthesis and the use of alternative materials such as belite cement or magnesium oxides – all of which are of low technical maturity.[86] In this context, CCUS occupies a unique position, as it can directly capture and store these process emissions. Possible approaches include calcium looping, direct separation and oxyfuel processes (see Supplementary Figure 12 for a cost reference). Importantly, these approaches significantly increase required energy inputs in the form of electricity (oxyfuel and direct separation) and electricity and thermal energy (calcium looping). Moreover, CCUS does not eliminate all emissions, with effectiveness ranging from 65 to 96% depending on the technology.[86,115] This is a notable disadvantage of CCUS when it comes to fuel and process heat emissions – which, in contrast to process emissions, could be removed fully by fuel-switching – and means that the competitiveness of CCUS is tied strongly to carbon costs on residual carbon emissions.

Decarbonization of process heat can be achieved through fuel switching to biomass or waste, green H_2, or direct electrification (e.g., plasma torches). While direct electrification is, in general, more economical (see Supplementary Figure 12), in the cement context—characterized by extremely high process heat requirements—its technological maturity remains significantly lower than fuel switching to biomass or green H_2.[86] Notably, many kilns already use thermal energy biomass (17%) and alternative fuels (36%). However, many of these alternative fuels are carbon-based, including plastics (51%), industrial waste (19%) or tyres (12%).

We assume that processes that are already electrified (8-13%) or using biomass (17% of thermal energy) are not addressable for green H_2. For the remainder, we assume that green H_2 competes with

biomass and fossil fuels and direct electrification through plasma torches. For the central case, we assume an equal split between these technologies (reflecting the elevated uncertainty in the relative competition between these technologies, low overall technical maturities and the lack of reliable third party projections), yielding a H_2 share of approximately 20% of total energy input. For the extended case, we assume green H_2 to dominate the remaining energy mix, yielding a share of approximately 70% of total energy input. For the restricted case we assume that green H_2 is fully outcompeted by alternative technologies.

Lime

Lime production, as well as its decarbonization options, broadly follows that of cement, with a somewhat higher share of thermal energy (92% to 97%) relative to electricity.[86] As in cement, a significant share of emissions arises from calcination, implying that fuel switching to green H_2 addresses combustion emissions but not process CO_2. For lime we assume the same saturation rates as for cement.

Ceramics

Ceramics include several final products ranging from bricks to tiles and refractories. While materials and processes differ across products, they follow a similar structure, including preparation and shaping of raw materials, drying and firing and final treatment. Preparation and drying are low-temperature processes (up to 90°C), while kiln firing occurs at temperatures between 1,000 and 1,300°C and incurs the largest share of energy input.[86]

Ceramics production results in process emissions, which on average amount to 17%[86] but can reach up to 30% for bricks and roof tiles.[116] Similar to, albeit to a lesser degree than cement, this implies that CCUS would be required to abate these emissions fully.

Decarbonization options for process heat include:

- Direct electrification via heat pumps (drying and final treatment), spark-plasma sintering or other electrification technologies (firing)
- Fuel-switching to green H_2
- Fossil fuels (e.g., natural gas) combined with CCUS
- Fuel switching to biomass

Compared to cement, a larger share of ceramics emissions is combustion-related, which increases the technical relevance of fuel switching versus CCUS. At the same time, for process steps outside the kiln, electrification options (such as heat pumps) are comparably mature,[86] introducing stronger competition between green H_2 and direct electrification in these process steps, given the economic advantages of heat pumps over H_2 firing (see Supplementary Figure 12).

In the present set-up, thermal energy input makes up approximately 65-75% of total energy input. We assume that direct electrification to be the dominant decarbonization route for the preparation and drying steps (approx. 25-30% of total energy input). This yields a remaining energy input of 38-43%. In the central case, we assume green H_2, biomass and direct electrification to compete equally, resulting in a green H_2 saturation rate of approximately 14%. As for cement, we assume that in the extended case, green H_2 dominates the remaining energy input (38-43%), and that in the restricted case green H_2 is fully outcompeted.

Glass

As in ceramics, materials and processes vary between glass product types but follow a similar structure. High-purity and other materials are mixed and then melted and refined in a glass furnace. This is followed by downstream processes that include forming, annealing or surface treatment based on the glass type. Energy input is concentrated in the glass furnace step, which occurs at high process temperatures. Glass production incurs process emissions amounting to approximately 16% of total emissions.[86,117]

Options for decarbonizing process heat include:[86,117]

- Direct electrification via heat pumps (drying and final treatment), spark-plasma sintering or other electrification technologies (firing)
- Full electric melting
- Hybrid melting (combining electric boosting with gas combustion)
- Fuel-switching to green H_2
- Fossil fuels (e.g., natural gas) combined with CCUS
- Fuel switching to biomass

H_2 can be employed for all glass types using existing production processes. While electric melting can reach high efficiencies (up to 85%), it can be applied only to around 80% of glass types. The fluctuating composition of biogas can disrupt production consistency, which limits its use in certain glass applications. Oxy-fuel combustion, which burns fuel with purified oxygen, can reduce energy consumption by 10–20% and is synergetic with CCUS, as it reduces exhaust volumes and increases CO_2 concentrations in the off-gas. Oxy-fuel combustion is already employed in the production of some specialized glasses.[117] Technical maturity is high across all technologies, although electric melting today is restricted mainly to small and medium size furnaces (<300 tonnes per day).

Based on these considerations, we assume green H_2 to be employed mainly in the glass furnace step, where it competes with electric melting and biogas and is relevant, in particular for specialty glass applications that require a consistent fuel mix and for larger-scale applications.

Thermal energy in the glass furnace accounts for approximately 84% of total energy inputs. In the central case, we assume green H_2, biomass and direct electrification to compete equally, resulting in a green H_2 saturation rate of approximately 30%. As for cement and ceramics, we assume that in the extended case, green H_2 dominates the remaining energy input (84%), and that in the restricted case green H_2 is fully outcompeted.

To set overall saturation rates, we weight cement, lime, ceramics and glass to their respective shares in our database, and take the average for the remaining 4% of energy input. Supplementary Table 12 reports the saturation rates and assumptions based on this analysis.

Supplementary Table 12 Saturation assumptions for green H_2 in non-metallic minerals

Saturation scenario	Saturation rate	Rationale
Restricted	0%	Direct electrification, biomass and CCUS outperform green H_2 across cement, lime, ceramics and glass.
Central	20%	Weighted average across sub-sectors based on process-step addressability and equal competition in remaining high-temperature applications. Sub-sector saturation rates amount to approx. 18% in cement and lime, 14% in ceramics, 28% in glass and 20% in the remaining 4% of energy use, yielding 20% overall (rounded)
Extended	70%	Green H_2 dominates remaining addressable thermal energy across sub-sectors (cement and lime ≈74%, ceramics ≈43%, glass ≈81%, remaining 4% ≈68%), yielding a weighted average of 70% (rounded)

Note: Saturation values rounded to 5% increments.

Other

The "Other" category comprises all installations that cannot be clearly assigned to one of the hard-to-abate industry groups explicitly covered in this analysis. It includes three main types of facilities: manufacturing plants (e.g., automotive, electronics, furniture), agro-industrial plants (notably sugar production), and mining, quarrying, and upstream metals and minerals processing operations

(including iron ore and magnesite extraction and processing). Within this category, sugar production accounts for more than 20% of estimated energy consumption in 2050, while mining, quarrying and related upstream processing activities account for approximately 12%. Representative facilities include LKAB's iron ore operations in Kiruna, Sweden, magnesite mining and processing facilities operated by RHI and Magnesitas Navarras in Austria and Spain, and large sugar processing plants such as the Suedzucker facility in Zeitz, Germany.

Manufacturing plants

Manufacturing plants include plants from the automotive industry as well as producers of furniture and wood products. In the automotive sector, half of all energy consumption is already electricity. The remaining thermal energy is mainly low-to-medium temperature process heat, with metal casting and processing steps (e.g., in the body shop and in powertrain assembly) being the highest temperature processes at 430-750°C.[118]

Agro-industrial plants

Agro-industrial plants include plants for the manufacture of sugar, starch and other food processing plants. Sugar and starch processing plants frequently operate lime kilns that decompose calcium carbonate into CO_2 and quicklime for juice purification, which require high-temperature process heat (see non-metallic minerals section).[119] Sugar plants also include high-temperature drying of beet pulp requires process heat in the range of approximately 500–750°C and can account for up to 50% of plant-level energy consumption when installed.[119] However, these energy needs can also be met using biomass derived from process residues. By comparison, the lime kiln accounts for roughly 5% of total energy input in a typical sugar plant.[119]

Mining, quarrying and upstream metals and minerals processing

Mining and quarrying operations, including iron ore pelletizing, sintering and magnesite processing, require high-temperature process heat and therefore represent the primary applications in which green H_2 may play a role. Even with a switch to green H_2, however, both magnesite processing and lime kilns continue to generate process emissions from carbonate decomposition, implying that CCUS remains relevant for full decarbonization.

Summary

In this heterogeneous category, energy consumption broadly includes electricity, low- and medium-temperature process heat, and select high-temperature processes (in particular iron ore processing, magnesite processing and lime kilns in sugar and starch processing plants). Decarbonization options therefore differ across applications and include:

- Direct electrification of low- and medium-temperature heat (e.g., steam-generating heat pumps and mechanical vapor recompression)
- Fuel-switching to green H_2 for high-temperature process heat in mineral processing and lime kilns
- CCUS applied to high-temperature processes with process emissions
- Fuel-switching to biomass from process residues (e.g., beet pulp in sugar production)

We assume that low- and medium-temperature heat demand in manufacturing as well as in non-thermal components of sugar and mining operations is largely electrified. After excluding these electrifiable shares, slightly more than 30% of total energy consumption within the "Other" category remains associated with high-temperature processing in mining, quarrying, upstream mineral processing, and selected agro-industrial units. This residual high-temperature segment defines the technical potential for green H_2 deployment in this category. Supplementary Table 13 reports the saturation rates and assumptions based on this analysis.

Supplementary Table 13 Saturation assumptions for green H_2 in the "Other" category

Saturation scenario	Saturation rate	Rationale
Restricted	0%	Low- and medium-temperature heat electrified; high-temperature processes decarbonized via CCUS and biomass where applicable.
Central	5%	Green H_2 deployed in approximately half of high-temperature iron ore and magnesite processing; remaining high-temperature units rely on CCUS. Sugar lime kilns decarbonized via biomass or CCUS.
Extended	10%	Green H_2 deployed in most high-temperature iron ore and magnesite processing and in lime kilns (corresponding to roughly 1% of total energy in the "Other" category).

Note: Saturation values rounded to 5% increments.

Power

Decarbonization of electricity generation is expected to occur mainly through the deployment of renewable generation like wind and solar, which replace fossil-based thermal power generation. The main challenge in this process is the decarbonization of the dispatchable generation required to meet consumption peaks and ensure system reliability.[120] Possible technology pathways include the replacement of fossil generation through:[121,122]

- Green H_2 (co-)firing in repurposed natural gas plants
- Dispatchable renewable generation like biomass and hydropower
- Natural gas plants with CCUS
- Replacement of dispatchable generation with energy storage solutions (such as large-scale battery systems)

The generation and re-electrification of H_2 is subject to substantial energy losses.[2] As such, H_2 power generation is generally only considered as an option for the decarbonization of dispatchable power, and not electricity systems at large. This is consistent with our definition of the addressable installation base, which includes only natural gas peaker plants that could be retrofitted to run on green H_2 (see Offtaker database in the Methods section and Supplementary Note 9). Assuming a typical capacity factor of around 15%,[123] these plants correspond to slightly more than 10% of total EU electricity generation.

Natural gas with CCUS allows existing thermal infrastructure to continue providing firm capacity, although its long-term viability depends on the effectiveness of carbon removal, and the pricing of residual carbon and methane emissions. Biomass and hydropower function as key renewable dispatchable sources: biomass can supply reliable peak capacity and achieve emission reductions exceeding 85% when substituting for fossil fuels; pumped hydropower in particular is a cornerstone for seasonal balancing. Both biomass and hydropower are broadly deployed commercially but further expansions are restricted by biomass avaialbility, geographic conditions and weather-dependent inflows. Large-scale battery systems are highly effective in managing short-term, hourly variability and shifting solar surpluses to evening peak demand, but they remain less suitable for addressing long-term seasonal imbalances compared to thermal or hydropower-based options.[124]

In its Net Zero scenario, the IEA projects green H_2 generation to make up approximately 1% of total power generation in 2050 (equivalent to around 10% of dispatchable generation).[85] Oshiro and Fujimori find that, depending on the stringency of emissions targets, this share ranges from 0 to 2% of total generation (equivalent to up to around 20% of dispatchable generation, with slightly below 1% in the default scenario).[122] While there are no binding commitments on an EU level, some EU member states have set ambitious targets for the use of H_2 in the power sector: Germany's draft power plant strategy requires all newly built natural gas power plants to run on green H_2 by 2045, in effect resulting in a full replacement of natural gas with green H_2 over time as legacy plants retire.[64]

Based on the considerations above, we set saturation rates relative to the existing dispatchable generation base, defined here as natural gas peaker plants that could technically be retrofitted to run on green H_2. Saturation rates and assumptions are reported in Supplementary Table 14.

Supplementary Table 14 Saturation assumptions for green H_2 in dispatchable power generation

Saturation scenario	Saturation rate	Rationale
Restricted	0%	Dispatchable power is provided exclusively by renewable dispatchable generation, energy storage systems, or natural gas power plants with CCUS.
Central	10%	A share of today's natural gas-based dispatchable generation (10%, equivalent to around 1% of total electricity generation) switches to H_2. This aligns with the IEA's Net Zero scenario[85] and projections in the academic literature.[122]
Extended	100%	All natural gas-based dispatchable generation today (100%, equivalent to around 10% of total electricity generation) switches to H_2. This assumes EU-wide adoption of H_2-ready dispatchable plants and gradual retirement of legacy gas units.

Note: Saturation values refer to the share of dispatchable generation (defined as natural gas peaker plants with an assumed capacity factor of 15%) that switches to green H_2. Values are rounded to 5% increments.

Pulp & paper

The pulp & paper sector includes the production of pulp, cartonboard, and various paper products (corrugated and non-corrugated paper, tissue, newsprint, etc.). Pulp is produced from wood either mechanically, chemically (kraft process), or from recycled paper. Mechanical pulping is electricity-intensive, whereas chemical pulping relies more strongly on thermal energy. Much of this thermal energy is internally supplied through the combustion of black liquor, a biogenic by-product of the pulping process.[86]

Following pulping, fibers are processed and formed into paper through successive mechanical treatment and drying steps. The drying section represents the most energy-intensive stage of paper production and requires substantial amounts of low- to medium-temperature steam.[86] In most applications, required process temperatures remain below 200°C.[86]

In chemical (kraft) pulping, the recovery cycle includes a lime kiln in which calcium carbonate is calcined to regenerate quicklime, which releases CO_2 as process emissions. However, as the carbon originates from biogenic feedstock, these emissions are typically classified as biogenic rather than fossil.[125] One tonne of pulp requires approximately 0.25 tonnes of lime.[126] Based on an energy consumption of 3.71 GJ per tonne of lime (see Extended Data Table 6), the lime kiln accounts for approximately 13% of the energy use within the recovery cycle. In an integrated pulp & paper mill, this corresponds to about 10% of total energy input excluding black liquor (or about 3–4% when black liquor is included).[86]

For decarbonizing remaining process heat demand, options include:[86,127]

- Direct electrification (e.g., steam-generating heat pumps or electric boilers)
- Fuel-switching to green H_2
- Fossil fuels (e.g., natural gas) combined with CCUS
- Fuel-switching to biomass

Energy efficiency measures can be applied extensively across the sector, particularly in drying processes and steam system optimization. Chemical pulping is largely energy self-sufficient due to the use of black liquor in recovery boilers.[86] As of 2022, approximately 40% of global energy consumption in the pulp & paper sector was covered by bioenergy, most prominently black liquor.[128]

For the remaining energy consumption, direct electrification—primarily through industrial heat pumps and electric boilers—appears technically feasible for most low- and medium-temperature heat applications and is often economically favorable due to higher system efficiencies.[128] Green H_2 can in principle be integrated through the retrofit of existing natural gas boilers and high-temperature lime kilns,[127] but its role is likely limited to selected high-temperature applications or cases where electrification is constrained.

Based on these considerations, we set saturation rates for green H_2 in the pulp & paper sector as follows. In both the central and restricted cases, we assume that self-sufficient chemical pulping plays a dominant role in pulp production, that low-temperature processes are predominantly electrified, and that the remaining high-temperature processes (mainly the lime kiln in the recovery cycle) are decarbonized through biomass substitution. For the extended case, we assume these high-temperature processes to be decarbonized with green H_2. Saturation rates and assumptions are reported in Supplementary Table 15.

Supplementary Table 15 Saturation assumptions for green H_2 in pulp & paper

Saturation scenario	Saturation rate	Rationale
Restricted	0%	Predominant use of energy self-sufficient chemical pulping and electrification of low-temperature process heat. Residual fossil demand addressed through efficiency improvements and biomass substitution.
Central	0%	As in the restricted case, given limited structural need for H_2 in predominantly low-temperature heat applications.
Extended	10%	Conversion of lime kiln in the recovery process to green H_2.

Note: Saturation values rounded to 5% increments. Since the energy consumption factors used to estimate pulp & paper energy demand (Extended Data Table 6) exclude black liquor, saturation rates are defined relative to energy inputs excluding black liquor. The 10% value therefore corresponds to the lime kiln share relative to non-biogenic energy inputs. We deliberately do not distinguish between the restricted and central cases, as the structural role for green H_2 in predominantly low-temperature heat applications appears limited across most decarbonization pathways.

Refining

The refining sector today is dominated by the refining of crude oil into fuels: about 75% of products produced in European refineries today are related to fuels for the transport sector such as gas oil, diesel oil, motor gasoline or kerosene.[129] Further products, such as liquefied petroleum gas or petroleum coke, decline with the decarbonization of industry and building heat.

Yet some refinery processes are likely to persist even in deep decarbonization scenarios. This includes the production of naphtha, lubricants or raw materials for the chemical industry. Refinery processes are also likely to change, as naphtha, the main feedstock for chemicals such as aromatics, ethylene or propylene, is today co-produced with fuels for the transport sector.[130] As a consequence, future refinery configurations are expected to resemble chemical plants rather than conventional fuel refineries, with a stronger focus on naphtha, aromatics, and other chemical intermediates.

Options to decarbonize these remaining processes include:[130,131]

- Synthetic carbon pathways using green H_2 and captured or biogenic CO_2
- Synthetic carbon pathways using blue H_2 and captured or biogenic CO_2
- Bio-based feedstocks such as bio-naphtha

Decarbonization occurs primarily through feedstock replacement. For instance, fossil naphtha for the production of olefins or aromatics can be replaced through a methanol-to-olefins (MTO) production route that builds on green or blue H_2 (see organic chemicals and polymers in the chemicals section). Alternatively, fossil feedstocks can be replaced by biomass-based feedstocks such as bio-naphtha.[132] RED III requires at least 60% of industrial H_2 use to consist of renewable fuels of non-biological origin (RFNBO, conceptually equivalent to green H_2) by 2035.[10]

Due to large structural shifts in refinery processes in the context of the decarbonization of transport and industry, setting saturation rates for the refining sector is challenging. We use Eurostat's product break-down for an approximation. To that purpose, we assume that of today's refinery portfolio, the production of (decarbonized) naphtha, bitumen, lubricants, and some other industrial oil products (e.g., spirits, waxes) are required as upstream inputs even in full decarbonization scenarios. We assume bitumen and lubricants (23%) to be produced via a bio-feedstock route, and the remaining 77% to be decarbonized through a synthetic carbon pathway using biogenic or atmospheric CO_2 and H_2 (e.g., via methanol). We assume 60% of this, corresponding to the EU's RED III target, to be produced from green H_2.[10] For the central case, we raise this share to 80%, and for the extended case to 100%, assuming increasing competitiveness of green relative to blue H_2, for example due to methane leakage penalties. Multiplying these shares yields green H_2 saturation levels of approximately 46%, 62%, and 77% of refinery H_2 demand, respectively (see Supplementary Table 16).

Supplementary Table 16 Saturation assumptions for green H_2 in refining

Saturation scenario	Green H_2 share of refinery H_2 demand	Rationale
Restricted	45%	Green H_2 supplies 45% of refinery H_2 demand by 2050. Its use is largely limited to compliance with EU mandates, while blue H_2 remains cost-competitive in non-bitumen and lubricant processes and continues to account for a substantial share of supply.
Central	60%	Green H_2 reaches 60% of refinery H_2 demand by 2050. Both green and blue H_2 are deployed in parallel across non-bitumen and lubricant processes, reflecting moderate cost convergence and diversified decarbonization strategies within integrated refinery–chemical complexes.
Extended	75%	Green H_2 supplies 75% of refinery H_2 demand by 2050. This assumes that green H_2 becomes structurally more competitive than blue H_2, driven by declining renewable electricity costs, rising natural gas prices, and additional methane leakage penalties, resulting in dominance of green H_2 in non-bitumen and lubricant processes.

Note: Saturation values rounded to 5% increments.

Shipping

Decarbonizing the shipping sector remains structurally challenging because the global fleet currently relies almost entirely on fossil fuels and vessels exhibit long technical lifetimes and slow fleet turnover. Decarbonization will therefore require large-scale fuel and vessel substitution, and the development of associated bunkering infrastructure remain major constraints.[133]

The principal decarbonization options include:[50,133]

- Direct electrification using batteries
- E-fuels generated from green H_2 (e.g., ammonia, e-methanol, e-methane, e-diesel)
- E-fuels generated from blue H_2 (e.g., ammonia, e-methanol, e-methane, e-diesel)
- Biofuels (e.g., biodiesel, biomethanol)

For short-range vessels and inland shipping, direct electrification via batteries can be a viable option, as the requirement for energy stored onboard is significantly lower.[50] All candidate fuels are expected to reach commercial maturity by around 2030.[134] Within e-fuels, ammonia and methanol

are comparable in terms of overall efficiency and, in contrast to cryogenic liquid H_2, easier to handle in transport and storage. Both fuels face specific challenges: methanol requires a source of concentrated CO_2, which makes its cost dependent on the availability of low-cost CCUS, while ammonia is highly toxic and can produce nitrous oxide, a greenhouse gas, when combusted.[50] As for aviation, e-fuels can also be generated from blue H_2, which is produced from natural gas using CCUS. Biofuels are compatible with existing ships and infrastructure, making them a feasible option for replacing fossil fuels in the short term. However, similar to biofuels for aviation, supply is subject to constraints and may not be sufficient to meet long-term demand.[133]

At present, most (more than 55%) new ship orders equipped with alternative fuel technology still use fossil-based technologies including liquefied natural gas (LNG) or liquefied petroleum gas (LPG), 23% are battery or hybrid-battery based, and 19% use H_2-based e-fuels, primarily methanol.[133] Future projections diverge substantially with respect to the relative shares of biofuels and H_2-derived e-fuels. In a review of projections from eight public sector and commercial sources, Lloyd's Register finds both biofuel-dominant and H_2-dominant scenarios. Within the H_2-dominant scenarios, fuels derived from green H_2, excluding blue ammonia, account on average for 63% of maritime fuel demand. By contrast, within the biofuel-dominant scenarios, the corresponding share of fuels derived from green H_2 amounts to 16%. Across all scenarios, the share of H_2 derived fuels (including green and blue H_2, ammonia and methanol) averages approximately 47%.[135]

Based on the discussion above, we set saturation rates as follows: For the central case, we assume an overall share of H_2-derived fuels of 47% (the average across all scenarios recorded by LLoyd's Registers)[135] and that, consistent with our assumptions for the aviation and chemicals sectors, 80% of of these are generated from green rather than blue H_2, yielding a saturation rate of 35%. This value is also consistent with the 35% e-fuel target defined for aviation under the EU ReFuelEU framework, which we use as an additional policy anchor. For the extended case, we follow the IEA's Net Zero scenario (80% share of H_2-derived e-fuels relative to biofuels) and again assume 80% of these to be generated from green H_2, yielding a 60% saturation rate (see Supplementary Table 17).

Supplementary Table 17 Saturation assumptions for green H_2 in shipping

Saturation scenario	Saturation rate	Rationale
Restricted	0%	Maritime transport continues to rely predominantly on advanced biofuels and efficiency improvements, while H_2-based e-fuels do not achieve large-scale deployment. Sustainable biomass supply is assumed to remain sufficient, and infrastructure constraints together with high fuel production costs limit e-fuel uptake.
Central	35%	H_2-based e-fuels reach 35% penetration of maritime fuel demand by 2050. This reflects a balanced fuel mix in which biofuels and e-fuels are deployed in parallel, while battery-electric vessels serve short-distance and coastal routes.
Extended	60%	Green H_2-based e-fuels supply 60% of maritime fuel demand by 2050 (anchored to IEA projection). This assumes that constrained sustainable biomass availability reduces long-term biofuel competitiveness, while large-scale renewable H_2 production and fuel synthesis infrastructure are successfully deployed. Battery-electric vessels remain limited to selected short-distance applications.

Note: Saturation values rounded to 5% increments.

2.3 SN7: Demand projections under different carbon price regimes

As discussed in Supplementary Note 5, we rely on cost estimates from Odenweller and Ueckerdt [42] for simulation purposes. These have built-in assumptions on carbon pricing, which are based on the work of Sitarz et al, [75] who estimate the marginal ETS carbon prices required for meeting EU policy goals as set forwards in the Fit for 55 package. [136] While this trajectory is consistent with carbon prices following the tightening of the ETS cap through the Market Stability Reserve and Fit for 55 reforms, their model does foresee a very significant increase of carbon prices (see Supplementary Figure 13).

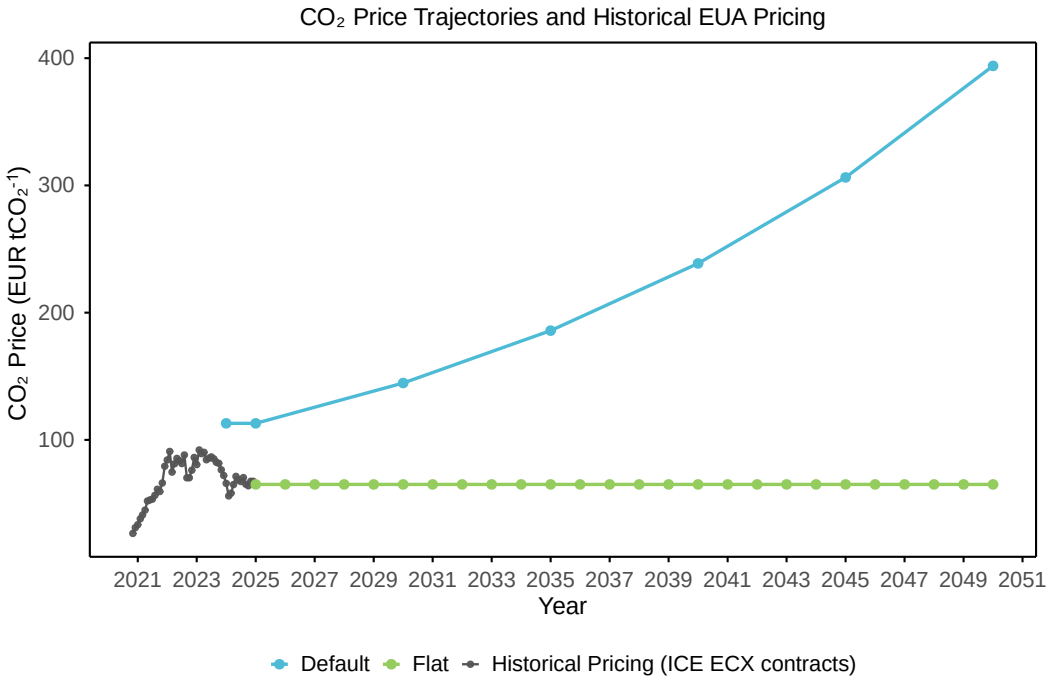

Supplementary Figure 13 Carbon price projections in EUR/t CO_2 equivalent. Default carbon price projections used in the baseline simulation presented in the main article are based on Sitarz et al. [75] Flat carbon prices are based on the average realized carbon price in 2024. Historical carbon prices are based on ICE ETX contracts and are drawn from S&P Capital IQ. Note that default carbon prices escalate significantly beyond the current level reflecting the carbon pricing required to achieve the EU's Fit for 55 policy goals.

To assess the model's sensitivity to carbon price assumptions and investigate the impact of carbon pricing policy on green H_2 diffusion, we simulate an alternative environment, whereby the carbon price remains constant at the average secondary market value realized in 2024 (approximately 65 EUR per tonne of CO_2 equivalent). The results of this simulation are reported in Supplementary Figure 14.

Results show that the model is sensitive to carbon pricing policy. While the results presented in the main article show substantial diffusion of green H_2, despite shortfalls versus policy targets, diffusion takes off before 2050 only under progressive H_2 cost assumptions. In the *mean* cost + *central* saturation case, the gap between the 2050 policy target and estimated diffusion amounts to 48.5 Mt, or 97%. This underscores that for achieving stated targets and limiting the requirement for further policy interventions, an ambitious carbon pricing regime is critical.

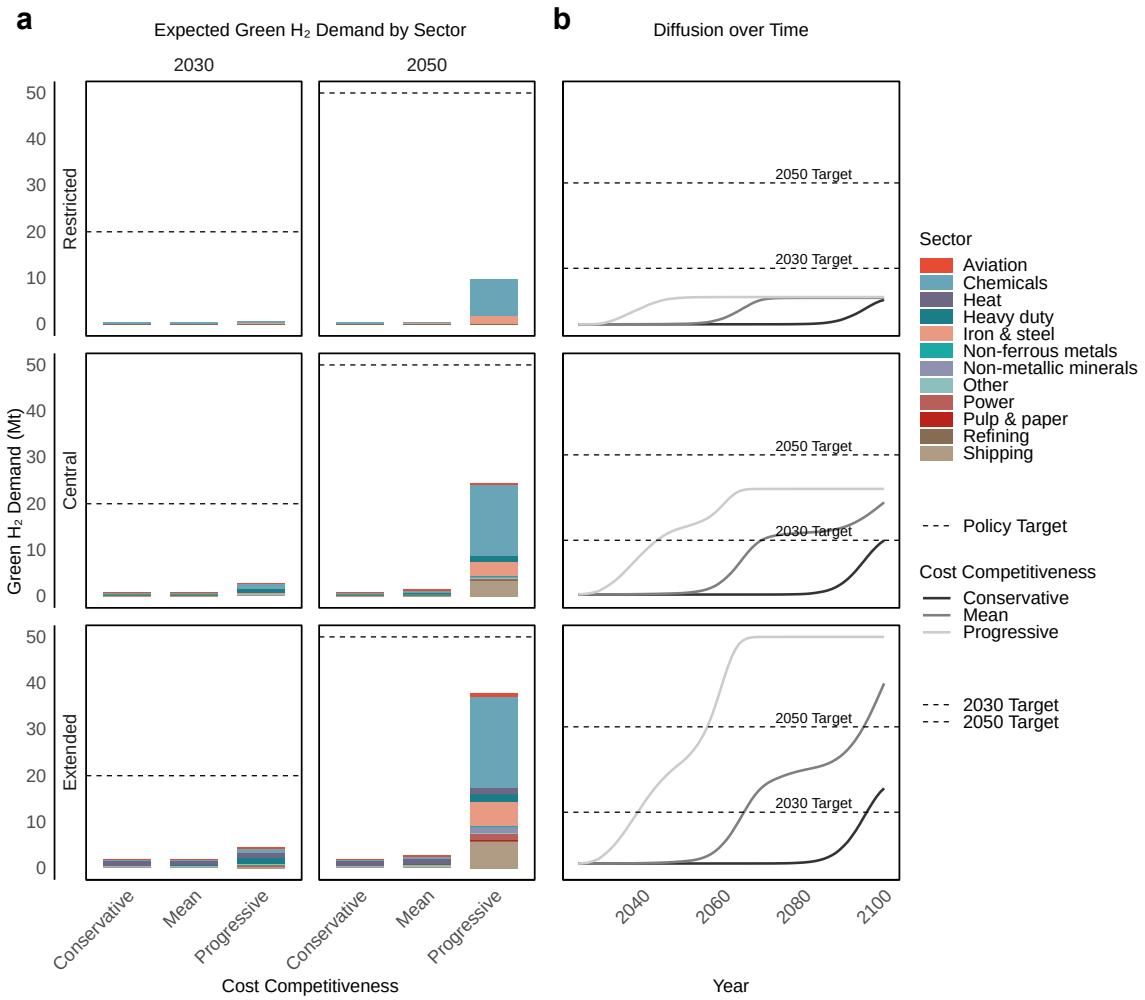

Supplementary Figure 14 Baseline projections of expected green H_2 before policy interventions assuming flat carbon prices. Expected green H_2 demand in 2030 and 2050 under combinations of green H_2 cost trajectories (conservative, mean, progressive) and saturation assumptions (restricted, central, extended). **a** Each box shows cumulative H_2 diffusion in million tonnes (Mt) across sectors, colored according to sector classification. Dashed lines indicate policy targets of 20 Mt green H_2 demand by 2030, and 50 Mt (10% of final energy demand) by 2050. **b** Time series of green H_2 diffusion between 2024 and 2100 disaggregated by saturation level. Green H_2 cost trajectories are shown in varying shades of grey. Under flat carbon prices, demand is almost fully surppressed until 2050.

2.4 SN8: Policy effectiveness under alternative baseline demand projections

For clarity, the main article only reports the policy effectiveness analysis against the baseline demand projection that uses the *mean* cost and *central* saturation case. This scenario can be thought of as the "median" scenario when it comes to projected green H_2 demand. Supplementary Figure 15 and Supplementary Figure 16 report the result of the same policy interventions presented in the main paper (a CfD controlling for sector, cost and size (Supplementary Figure 15) and an EHB-style auction(Supplementary Figure 16)).

Supplementary Figure 15 reports the differences in annual green H_2 demand and policy cost effectiveness for all possible specifications of the baseline projections. The results reported in the main paper – for the central saturation and mean cost competitiveness scenario – hold across most specifications of the baseline. Targeting high-centrality offtakers on average increases annual green H_2 demand and cost-effectiveness in the restricted and central saturation scenarios. This is consistent with the patterns presented in the main article. In the extended saturation case, however, the result does not hold for policy effectiveness (and in the case of betweenness centrality, annual demand). In contrast, targeting high-centrality offtakers can result in an increased policy cost per unit of induced green H_2 demand.

This diverging result can be tied back to the underlying economics of the sectors included in the extended scenario. This case extends non-zero saturation rates to several sectors, where green H_2 is expected to remain structurally uncompetitive in the medium to long term (e.g., heating). This results in CfD interventions targeting these sectors incurring high policy costs. This disproportionately penalizes the high-centrality targeting strategies, as centrality is structurally correlated with demand volumes and highly central offtakers are more likely to adopt when targeted by the CfD. These additional costs are not offset by increases in demand. This is also consistent with the pattern observed between different cost cases, where, in the extended case, high-centrality targeting performs best in the progressive cost scenario, where the cost differential is more limited even for uncompetitive sectors.

This result carries a relevant policy implication: When extended broadly, to sectors where the cost competitiveness of green H_2 is especially low (e.g., heating), cost-linked policy interventions that target offtakers with high spatial spillover potential might result in an increase in H_2 demand, but at prohibitive policy cost.

Results for the EHB-style auction setting show the same patterns as in the controlled setting. (Supplementary Figure 16).

In the main article, we represent results for an EHB-style auction setting that is augmented with a spatial spillover component, weighted at 10%. Supplementary Figure 17 reports results for a range of weights. Consistent with the results from above, augmenting the auction with a spatial spillover component only improves policy outcomes up to a certain extent: For weights above 20%, the additional policy costs that come from targeting offtakers with low cost competitiveness outweigh the spatial spillover benefits. Accordingly, to optimize policy cost efficiency, adjusting the auction design to include a demand-side component (e.g., spatial spillover potential), is preferable to fully replacing cost competitiveness as a criterion.

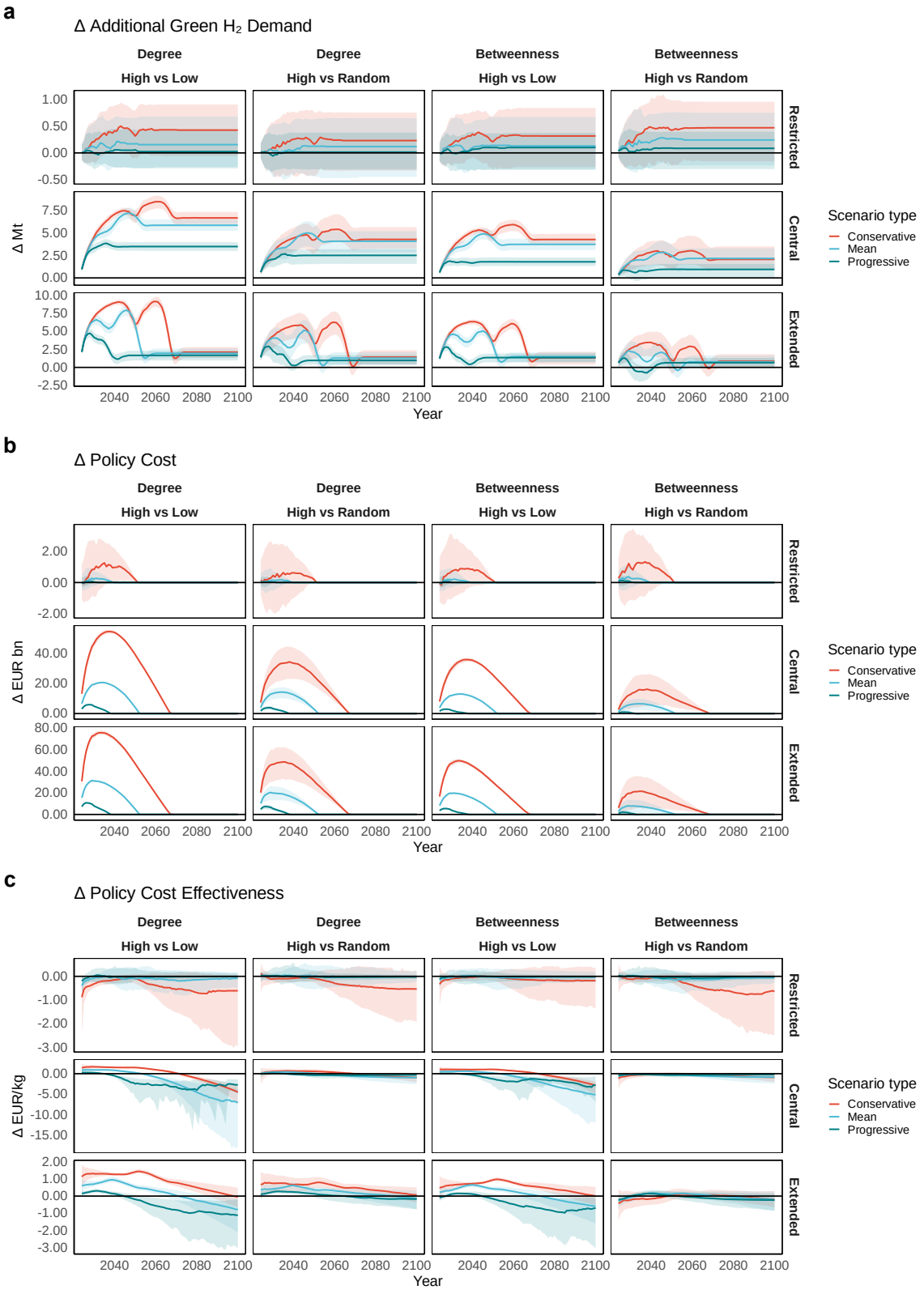

Supplementary Figure 15 Expected green H_2 and cost effectiveness for demand-side policy interventions targeted on spatial spillover potential: Results for different baseline specifications. Differences in policy outcomes between spatially-informed (high spillover potential or centrality) and spatially-neutral policy intervention (CfD) controlling for sector, cost and size. Results are disaggregated by centrality metric and saturation scenario. Solid lines denote the median difference across 250 simulation runs for conservative (red line), mean (blue line) and progressive (green line) cost competitiveness scenario. Ribbons refer to the inter-quartile distance. **a** Difference in annual green H_2 demand (Mt). **b** Difference in annual policy cost (EURbn) over time. Policy cost is estimated as the difference between green H_2 (derivative) cost and incumbent fossil cost, and incurred when a targeted offtaker adopts. **b** Difference in policy cost effectiveness trajectories over time, measured as the ratio of cumulative policy cost to cumulative H_2 demand (EUR per kg H_2)

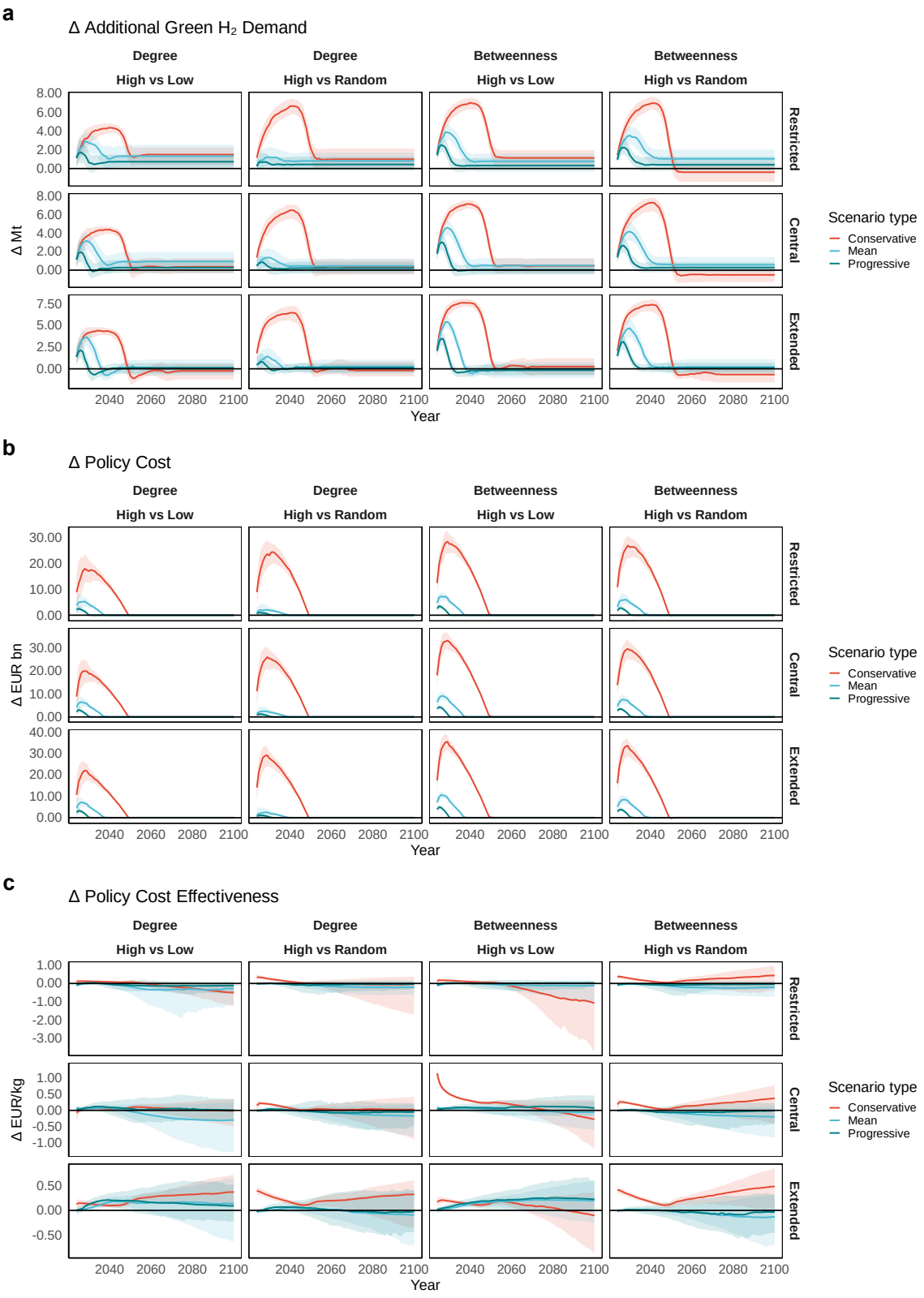

Supplementary Figure 16 Expected green H_2 and cost effectiveness for demand-side policy interventions targeted on spatial spillover potential: Results for different baseline specifications. Differences in policy outcomes between spatially-informed (high spillover potential or centrality) and spatially-neutral policy intervention (EHB-style auction setting). Results are disaggregated by centrality metric and saturation scenario. Solid lines denote the median difference across 250 simulation runs for conservative (red line), mean (blue line) and progressive (green line) cost competitiveness scenario. Ribbons refer to the inter-quartile distance. **a** Difference in annual green H_2 demand (Mt). **b** Difference in annual policy cost (EURbn) over time. Policy cost is estimated as the difference between green H_2 (derivative) cost and incumbent fossil cost, and incurred when a targeted offtaker adopts. **b** Difference in policy cost effectiveness trajectories over time, measured as the ratio of cumulative policy cost to cumulative H_2 demand (EUR per kg H_2)

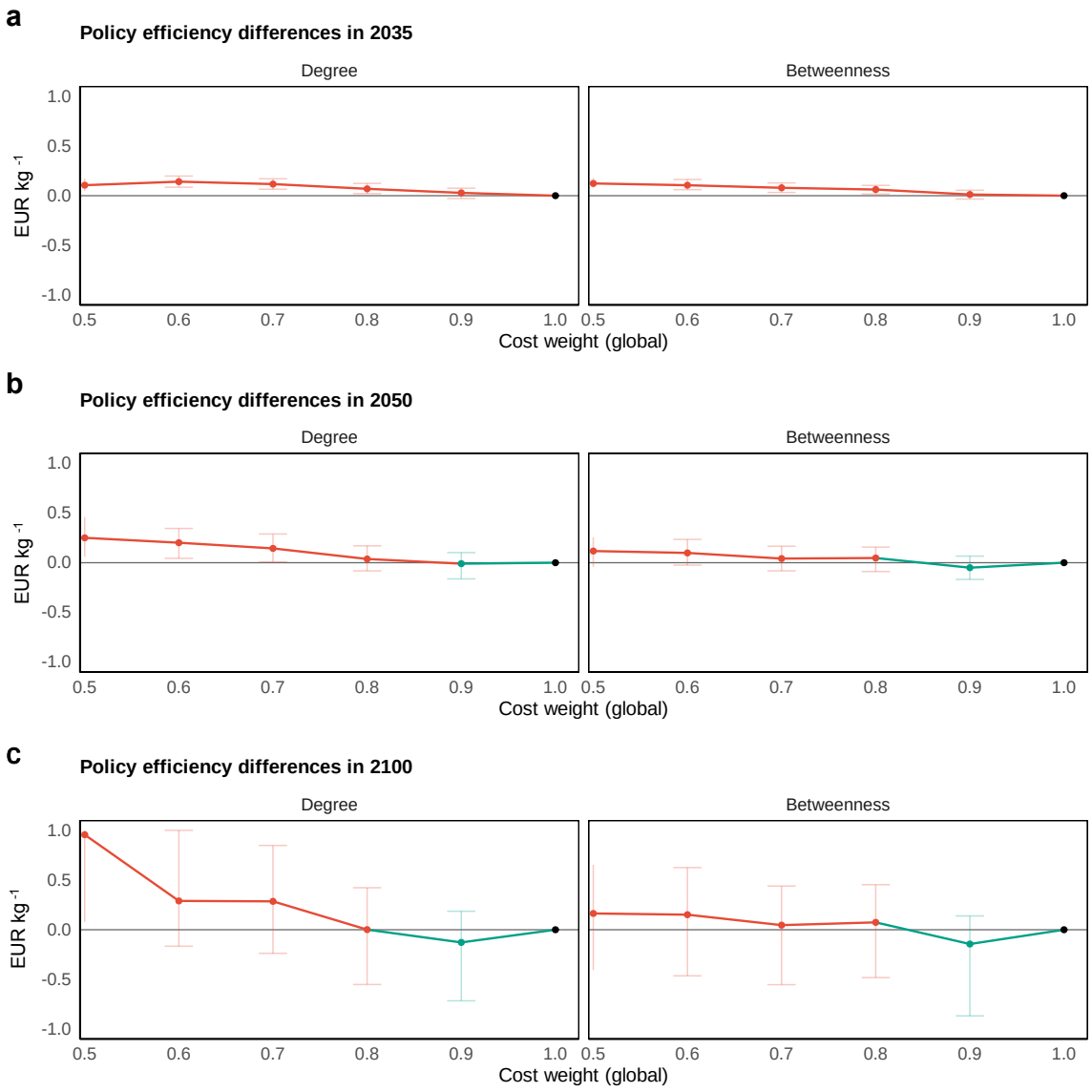

Supplementary Figure 17 Policy efficiency differences in an EHB-style auction setting for different weight to the spatial spillover component a Policy efficiency differences in 2030, disaggregated by centrality metric. Points show the median policy efficiency across 250 simulations, the error bars show the interquartile distance. **b** Policy efficiency differences for 2050. **c** Policy efficiency differences for the end of the simulation in 2100. Augmenting an EHB-style auction with a spatial spillover component can improve policy efficiency at moderate weights. At weights exceeding 20% (2100) the additional policy cost from targeting offtakers with unfavorable cost structure offsets the positive effect of spatial spillovers. Results also demonstrate the importance of policy commitment: Positive effects only materialize between 2030 and 2050.

3 Supplementary Note to Methods

3.1 SN9: Build-up of sectoral offtaker databases

Hard-to-abate industries

The database for hard-to-abate sectors includes industries that could use green H_2 as feedstock or for fuel and process heat in high temperature processes. We start from installations covered under the EU Emissions Trading System (EU ETS). The data is based on the latest available ETS registry data as per 31 December 2024, covering verified emissions and emissions allocation up to 2023.

Geographic coordinates for installations are generally determined using a hierarchical geocoding approach. We favor the open source OSM overpass API for geocoding, but use the Google Maps API when geocoding on the basis of installation names. Details per sector are provided below.

1. Installations are geocoded based on a combination of installation name, account holder name and country, using the Google Maps API. For this step, Google Maps is favored over the open source OSM overpass API due to greater availability of installation names and greater robustness towards diverging spellings. Note that the Google Maps API defaults to the country centroid if no information on installation and account holder name are available. To take this into account, all installations geocoded to the country centroid after this step are set again to missing value.
2. Installations that remain unresolved are geocoded based on combination of full address, city and country, using the OSM overpass API.
3. Installations that remain unresolved are geocoded based on combination of postal code, city and country, using the OSM overpass API.
4. Installations that remain unresolved are geocoded based on combination of city and country, using the OSM overpass API.
5. The remaining 35 unresolved installations are geocoded manually.

To check the geocoding's robustness, the coordinates are matched with the coordinates included in Jan Abrell's database for the European Transaction Log.[137] In 769 cases the distance between coordinates exceeds 20km, in 2099 10km. For these cases, the conflict is resolved through manual review. Adjusted coordinates are flagged as manual in the database.

Industry classification approaches vary widely between different databases. Each installation in the ETS registry includes an activity code. Additionally, a NACE Economic activity is added from Abrell's database for the European Transaction Log.[137] The European Commission Directorate General for Climate Action's emissions benchmark database again uses a diverging list of industries.[138] To ensure consistency, we match each NACE activity code to one or a set of industries included in the benchmark. We filter the database to include installations in the EU that are classified as active in the ETS registry and have a positive, non-zero carbon credit allocation in 2023. Under the EU ETS, a positive allocation indicates that an installation has verified activity levels and benchmarked emissions in the reference period. Installations with zero allocation typically fall into categories that are not relevant for H_2 adoption decisions in the period we study, such as facilities that are shut down, below allocation thresholds, temporarily inactive, or no longer producing benchmarked output. Including these sites would introduce locations that face no meaningful compliance or abatement incentives, thereby adding noise to the network analysis. Further, we exclude installations classified as "Maritime operator holding" or "Aircraft operator" via the ETS registry activity code, as emissions data for shipping and aviation is attributed to headquarters or registered offices of the operator, and are therefore not reflective of activity footprint at port and airport locations. Shipping and aviation sectors are covered separately in the data collection process. The ETS registry activity codes do not distinguish between combustion installations associated with industrial activity and combustion installations for the power generation sector. We therefore identify power generation installations through the NACE Economic activity classification "Power generation" and exclude them from the dataset. We cover the power sector separately in the data collection process.

The EU ETS registry includes installation-level data for verified carbon emissions and carbon credit allocations for the years 2017 to 2023. While carbon credits are allocated to individual installations based on production activity and a benchmark emissions factor, neither production activity nor benchmark emissions factor are explicitly disclosed in the database. We estimate production activity by dividing the carbon credit allocations for 2023 by the industry-level benchmark emissions factor. The benchmark emissions factor is based on the European Commission Directorate General for Climate Action's[138] update of benchmark values for the years 2021-2025 of phase for of the EU ETS. The emissions factors are reported in Extended Data Table 5.

We then estimate H_2-specific energy consumption as the product of activity levels, and specific H_2 energy consumption factors in terms of fuel and feedstock. The specific H_2 energy consumption factors used in the calculation are reported in Extended Data Table 6. Factors are drawn from Neuwirth et al,[139] Kiemel et al[140] and for some chemical subsectors, the IEA.[141] For some sectors, we aggregate specific energy consumption factors, weighted by activity levels. Lower heating value of H_2 is drawn from NREL.[142] Assumptions and sourcing are fully documented in the database.

Aviation

The aviation sector database includes aviation routes for passenger flights that either start or end within the EU. Since cargo-only flights account for only 4% of the aviation sector's emissions, we omit them for simplicity.[143] We collect data on aviation routes and passenger numbers from country-specific statistics collected by Eurostat.[144] Geographic coordinates for departure and arrival airports are assigned using the Google Maps API. Coordinates are validated manually and missing coordinates added. Manual interventions are flagged in the database. Distances for each aviation route are calculated using the Haversine formula. Missing distances are imputed using mean distances for each departure airport. In contrast to the industrial sector, H_2 is not used in its gaseous form, but needs to be converted into e-kerosene before being used in an aircraft. In this paper, we take the simplifying assumption that e-kerosene plants are collocated with airports, and H_2 demand consequently occurs at the departure airport. We calculate passenger-kms by multiplying passenger numbers with the route distances. To calculate H_2 energy consumption we use an estimate of 1.45 MJ per passenger-km (0.01208 kg H_2 per passenger-km at lower heating value) from AirBP and Lufthansa reported by Beck et al.[145]

Shipping

The shipping sector database includes maritime and inland waterway routes. We derive data for maritime routes from country-specific statistics collected by Eurostat.[146] These records include port level information for the departure port and country or region-level information for the arrival port. We assume the arrival port to be the principal sea port in the respective country or region. We subsequently merge the data into a combined dataset that includes data for all maritime routes that either start or end within the EU, as well as 2023 tonnage numbers. Records with missing or ambiguous information are excluded. Geographic coordinates for departure and arrival ports are assigned using the Google Maps API. Coordinates are validated manually and missing coordinates added. Manual interventions are flagged in the database. Distances for each aviation route are calculated using the Haversine formula. Missing distances are imputed using mean distances for each departure port. Tkms are calculated by multiplying tonnage by route distances, capped at 25,000 km to reflect limits on tank capacity. The cap is calculated for Panamax carriers, assuming an average tank capacity of 1.75 million gallons, a daily consumption of 63 thousand gallons, and an average travel speed of 24 knots, yielding an estimate of approximately 29,500 km.[147] We round this estimate down to 25,000km to to be conservative and reflect the presence of vessels smaller than the Panamax. Data for inland waterway routes is derived from two Eurostat datasets. We first draw tkm information on a NUTS-2 level.[148] We then dis-aggregate this across ports, using total port handling volumes of inland ports.[149] For the Netherlands, handling volumes are not reported on a port level; we therefore attribute handling volumes to the principal port in each NUTS-2 region. For six further NUTS-2 regions reporting tkm figures but no handling port we manually add the principal port in the respective NUTS-2 region for use in the disaggregation.

To calculate H_2-specific energy consumption we use an estimate of 0.4 MJ per tkm (0.0033 kg H_2 per tkm at lower heating value) from the German Environmental Agency reported by Beck et al.[145]

Heavy-duty transport

The heavy-duty transport database considers only potential H_2 demand from heavy-duty transport, as other applications are expected to be decarbonized through alternative pathways, most prominently through the use of battery electric vehicles.[50] We assume demand to occur at fuel stations within 10 kms of a major road. Fuel station and road networks in the EU are extracted using the OSM overpass API. Heavy-duty vehicles are assumed to be likely to refuel in the vicinity of major road networks. Accordingly, the sample of relevant fuel stations is reduced to stations that are within 10km of a major road, tagged as "motorway" or "trunk". The resulting dataset is filtered to remove duplicate entries and retain unique records for each station. As fuel stations are extracted using the OSM overpass API, they natively include coordinates. Note that for the purposes of the network analysis and the simulation, heavy duty-offtakers are aggregated on a NUTS-3 level to avoid disproportionate impact on the network structure. For this purpose, the "aggregated heavy-duty offtaker" is geo-located at the fuel station closest to the centroid of the NUTS-3 region. As a basis for estimating H_2-specific energy consumption, road transport volumes in tkm are extracted from national road transport statistics collected by Eurostat.[150] We then distribute tkms equally across fuel stations in each country. To calculate H_2-specific energy consumption we use an estimate of 0.0775 kg H_2 per km reported by Beck et al,[145] based on the Hyundai XCIENT fuel cell truck.[151] The Hyundai XCIENT reports maximum gross vehicle weight as 36t, with an empty vehicle weight of approximately 10t. The European Commission's report on emissions from new heavy-duty vehicles reports average payloads, excluding vehicle weight, of long haul heavy-duty vehicles from approximately 7.5 to 14.5t. For our calculations, we assume a gross vehicle weight of approximately 30t, which yields a H_2-specific energy consumption of 0.00258kg H_2 per tkm.

Power

We collect data on power plants, including capacity, curtailment, and geographic coordinates, from the JRC Open Power Plants database.[152] We opt to use this dataset instead of the commercial S&P Capital IQ dataset used for the empirical analysis to keep the offtaker database fully open source and because for this purpose information on commissioning years is not required. he JRC Open Power Plants database natively includes coordinates for power plants. The dataset is filtered to include only natural gas plants located in Europe with valid geographic information. H_2-specific energy consumption is calculated based on plant capacity and energy output. H_2-based power generation is assumed to be limited to flexible "peaker" plants. To estimate energy output, availability is assumed to be 90 percent, resulting in 7884 full load hours. Following the U.S. Government Accountability Office's definition of a peaker plant, the capacity factor is set to 15 percent.[123]

Heat

We collect data on residential heat consumption in GWh from the EU Hotmaps project[153] on a NUTS-3 level, and convert it to kg H_2 at lower heating value. We then merge this dataset with an open-source city location and population file.[154] City locations are extracted from Geonames, an open-source city location and population file that natively includes coordinates.[154] Finally, we disaggregate heat consumption to a city level based on population data. For computational feasibility, we only consider cities with a population greater than 10,000 for our analysis.

References

[1] European Commission. A hydrogen strategy for a climate-neutral europe (2020). URL https://eur-lex.europa.eu/legal-content/EN/TXT/?uri=CELEX%3A52020DC0301. Accessed: 2025-09-30

[2] IEA. Global hydrogen review 2024 (2024). URL https://www.iea.org/reports/global-hydrogen-review-2024/hydrogen-production. Accessed: 2025-09-30

[3] European Commission. European hydrogen bank (2025). URL https://energy.ec.europa.eu/topics/eus-energy-system/hydrogen/european-hydrogen-bank_en. Accessed: 2025-07-10

[4] European Commission, Directorate-General for Climate Action. If25 hydrogen auction (2026). URL https://cinea.ec.europa.eu/document/download/923767e1-73a3-47c8-8ed6-510b80a1e7a3_en?filename=Q%26A_IF25Hydrogen.pdf. Accessed: 2026-02-10

[5] Clean Hydrogen Partnership. Hydrogen valleys (2024). URL https://www.clean-hydrogen.europa.eu/get-involved/hydrogen-valleys_en. Accessed: 2026-02-10

[6] European Commission, European Climate, Infrastructure, and Environment Executive Agency. Calls - regular grants (2026). URL https://cinea.ec.europa.eu/programmes/innovation-fund/calls-regular-grants_en. Accessed: 2026-02-10

[7] European Commission. EU just transition platform (2025). URL https://ec.europa.eu/regional_policy/funding/just-transition-fund/just-transition-platform/about_en. Accessed: 2025-07-10

[8] European Parliament and Council of the European Union. Regulation (EU) 2023/2405 of the european parliament and of the council of 18 october 2023 on ensuring a level playing field for sustainable air transport (ReFuelEU aviation) (text with EEA relevance) (2023). URL https://eur-lex.europa.eu/eli/reg/2023/2405/oj/eng. Accessed: 2025-07-10

[9] European Parliament and Council of European Union. Regulation (eu) 2023/1805 of the european parliament and of the council of 13 september 2023 on the use of renewable and low-carbon fuels in maritime transport, and amending directive 2009/16/ec (text with eea relevance) (2023). URL https://eur-lex.europa.eu/eli/reg/2023/1805/oj/eng. Accessed: 2025-09-30

[10] European Parliament and Council of the European Union. Directive (EU) 2023/2413 of the european parliament and of the council of 18 october 2023 amending directive (EU) 2018/2001, regulation (EU) 2018/1999 and directive 98/70/ec as regards the promotion of energy from renewable sources, and repealing council directive (EU) 2015/652 (2023). URL https://eur-lex.europa.eu/eli/dir/2023/2413/oj/eng. Accessed: 2025-07-10

[11] Clean Hydrogen Partnership. Ipcei hydrogen (2026). URL https://ipcei.observatory.clean-hydrogen.europa.eu/. Accessed: 2025-02-10

[12] European Commision. Law. Approved ipceis in the hydrogen value chain (2024). URL https://competition-policy.ec.europa.eu/state-aid/ipcei/approved-ipceis/hydrogen-value-chain_en. Accessed: 2026-02-10

[13] Bundeministerium für Wirtschaft und Energie. Co2-differenzverträge erklärt (2026). URL https://www.klimaschutzvertraege.info/thema/allgemeine_informationen_ksv. Accessed: 2026-02-10

[14] H2 Global Stiftung. The h2 global mechanism (2025). URL https://www.h2-global.org/the-h2global-instrument. Accessed: 2025-07-10

[15] World Bank. Scaling hydrogen financing for development (2024). URL https://documents1.worldbank.org/curated/en/099022024121527489/pdf/P1809201780da10e518c061a2e73041a6fc.pdf?utm. Accessed: 2026-02-10

[16] J. Burgess. European hydrogen industry digests failure of second eu auction (2026). URL https://www.spglobal.com/energy/en/news-research/latest-news/energy-transition/012226-european-hydrogen-industry-digests-failure-of-second-eu-auction. Accessed: 2026-02-10

[17] M. Jansen, P. Beiter, I. Riepin, F. Müsgens, V.J. Guajardo-Fajardo, I. Staffell, B. Bulder, L. Kitzing, Policy choices and outcomes for offshore wind auctions globally. Energy Policy **167**, 113000 (2022)

[18] Wind Europe. The netherlands run another successful auction based on non-price criteria (2022). URL https://windeurope.org/news/the-netherlands-run-another-successful-auction-based-on-non-price-criteria/. Accessed: 2026-02-10

[19] A. Grubler, C. Wilson, G. Nemet, Apples, oranges, and consistent comparisons of the temporal dynamics of energy transitions. Energy research & social science **22**, 18–25 (2016)

[20] C. Wilson, Up-scaling, formative phases, and learning in the historical diffusion of energy technologies. Energy Policy **50**, 81–94 (2012)

[21] T. Arvanitopoulos, C. Wilson, C. Morton, Decarbonising residential heating: local conditions and spatial spillovers driving heat pump uptake. Energy Policy **206**, 114787 (2025)

[22] N.B. Irwin, Sunny days: Spatial spillovers in photovoltaic system adoptions. Energy Policy **151**, 112192 (2021)

[23] M. Graziano, K. Gillingham, Spatial patterns of solar photovoltaic system adoption: the influence of neighbors and the built environment. Journal of Economic Geography **15**(4), 815–839 (2015)

[24] S. Losacker, J. Horbach, I. Liefner, Geography and the speed of green technology diffusion. Industry and Innovation **30**(5), 531–555 (2023)

[25] B. Noll, B. Steffen, T.S. Schmidt, The effects of local interventions on global technological change through spillovers: A modeling framework and application to the road-freight sector. Proceedings of the National Academy of Sciences **121**(29), e2215684120 (2023)

[26] S. Zhou, B.D. Solomon, M.A. Brown, The spillover effect of mandatory renewable portfolio standards. Proceedings of the National Academy of Sciences **121**(25), e2313193121 (2024)

[27] A. Grübler, N. Nakićenović, D.G. Victor, Dynamics of energy technologies and global change. Energy policy **27**(5), 247–280 (1999)

[28] M. Dejonghe, T. Van de Graaf, R. Belmans, From natural gas to hydrogen: Navigating import risks and dependencies in northwest europe. Energy Research & Social Science **106**, 103301 (2023)

[29] C. Doblinger, K. Surana, D. Li, N. Hultman, L.D. Anadón, How do global manufacturing shifts affect long-term clean energy innovation? a study of wind energy suppliers. Research Policy **51**(7), 104558 (2022)

[30] K. Surana, C. Doblinger, L.D. Anadon, N. Hultman, Effects of technology complexity on the emergence and evolution of wind industry manufacturing locations along global value chains. Nature Energy **5**(10), 811–821 (2020)

[31] J. Huenteler, J. Ossenbrink, T.S. Schmidt, V.H. Hoffmann, How a product's design hierarchy shapes the evolution of technological knowledge—evidence from patent-citation networks in wind power. Research Policy **45**(6), 1195–1217 (2016)

[32] R. Zhu, T. Ma, J. Feng, Diffusion of electric vehicles–the spillover effect of charging facilities and government demonstrations for neighbouring and peer regions. Energy Economics p. 109164

(2026)

[33] D. Fadly, F. Fontes, Geographical proximity and renewable energy diffusion: An empirical approach. Energy Policy **129**, 422–435 (2019)

[34] K. Luo, Y. Qiu, K. Surana, Network structure matters: how coordination and cooperation mechanisms drive solar-battery co-adoption. Environmental Research Letters **21**(1), 014039 (2026)

[35] C. Roberts, G. Nemet, Systematic historical analogue research for decision-making (SHARD): Introducing a new methodology for using historical case studies to inform low-carbon transitions. Energy Research & Social Science **93**, 102768 (2022)

[36] A. Malhotra, T.S. Schmidt, Accelerating low-carbon innovation. Joule **4**(11), 2259–2267 (2020)

[37] N. Mac Dowell, N. Sunny, N. Brandon, H. Herzog, A.Y. Ku, W. Maas, A. Ramirez, D.M. Reiner, G.N. Sant, N. Shah, The hydrogen economy: A pragmatic path forward. Joule **5**(10), 2524–2529 (2021)

[38] F. Kourougianni, A. Arsalis, A.V. Olympios, G. Yiasoumas, C. Konstantinou, P. Papanastasiou, G.E. Georghiou, A comprehensive review of green hydrogen energy systems. Renewable Energy p. 120911 (2024)

[39] F. Neumann, E. Zeyen, M. Victoria, T. Brown, The potential role of a hydrogen network in europe. Joule **7**(8), 1793–1817 (2023)

[40] B.C. Erdener, B. Sergi, O.J. Guerra, A.L. Chueca, K. Pambour, C. Brancucci, B.M. Hodge, A review of technical and regulatory limits for hydrogen blending in natural gas pipelines. International Journal of Hydrogen Energy **48**(14), 5595–5617 (2023)

[41] K. Topolski, E.P. Reznicek, B.C. Erdener, C.W. San Marchi, J.A. Ronevich, L. Fring, K. Simmons, O.J.G. Fernandez, B.M. Hodge, M. Chung, Hydrogen blending into natural gas pipeline infrastructure: Review of the state of technology. Tech. rep., National Renewable Energy Laboratory (2022). URL https://www.osti.gov/biblio/1893355. Accessed: 2025-09-30

[42] A. Odenweller, F. Ueckerdt, The green hydrogen ambition and implementation gap. Nature Energy **10**(1), 1–14 (2025)

[43] F. Ueckerdt, P.C. Verpoort, R. Anantharaman, C. Bauer, F. Beck, T. Longden, S. Roussanaly, On the cost competitiveness of blue and green hydrogen. Joule **8**(1), 104–128 (2024)

[44] Liebreich, Michael. Liebreich: Clean hydrogen's missing trillions (2023). URL https://about.bnef.com/blog/liebreich-clean-hydrogens-missing-trillions/. Accessed: 2025-09-30

[45] A. Ason, J. Dal Poz. Contracts for difference: The instrument of choice for the energy transition (2024). URL https://www.oxfordenergy.org/wpcms/wp-content/uploads/2024/03/Contracts-for-difference.pdf. Accessed: 2025-09-30

[46] European Commission. Hydrogen valleys facility (tender no. cleanh2/2024/op/0002) (2024). URL https://ec.europa.eu/info/funding-tenders/opportunities/portal/screen/opportunities/tender-details/424246ca-5b16-41b0-8bd0-355c769a396a-CN. Accessed: 2025-07-10

[47] European Commission. Commission Delegated Regulation (EU) 2023/1184 of 10 February 2023 supplementing directive (eu) 2018/2001 of the european parliament and of the council by establishing a union methodology setting out detailed rules for the production of renewable liquid and gaseous transport fuels of non-biological origins (2023). URL https://eur-lex.europa.eu/legal-content/EN/TXT/?uri=CELEX%3A32023R1184. Accessed: 2025-09-30

[48] N. Farrell, Policy design for green hydrogen. Renewable and Sustainable Energy Reviews **178**, 113216 (2023)

[49] J. Rosenow, Is heating homes with hydrogen all but a pipe dream? an evidence review. Joule **6**(10), 2225–2228 (2022)

[50] T.J. Wallington, M. Woody, G.M. Lewis, G.A. Keoleian, E.J. Adler, J.R.R.A. Martins, M.D. Collette, Green hydrogen pathways, energy efficiencies, and intensities for ground, air, and marine transportation. Joule **8**(8), 2190–2207 (2024)

[51] G. Nemet, J. Greene, F. Müller-Hansen, J.C. Minx, Dataset on the adoption of historical technologies informs the scale-up of emerging carbon dioxide removal measures. Communications Earth & Environment **4**(1), 397 (2023)

[52] A. Odenweller, F. Ueckerdt, G.F. Nemet, M. Jensterle, G. Luderer, Probabilistic feasibility space of scaling up green hydrogen supply. Nature Energy **7**(9), 854–865 (2022)

[53] P.J. Heptonstall, R.J.K. Gross, A systematic review of the costs and impacts of integrating variable renewables into power grids. Nature Energy **6**(1), 72–83 (2021)

[54] W. Gorman, J.M. Kemp, J. Rand, J. Seel, R. Wiser, N. Manderlink, F. Kahrl, K. Porter, W. Cotton, Grid connection barriers to renewable energy deployment in the united states. Joule **9**(2) (2025)

[55] R. Way, M.C. Ives, P. Mealy, J.D. Farmer, Empirically grounded technology forecasts and the energy transition. Joule **6**(9), 2057–2082 (2022)

[56] European Commission. Report from the commission to the european parliament, the council, the european economic and social committee and the committee of the regions: 2024 report on energy subsidies in the EU (2024). URL https://eur-lex.europa.eu/legal-content/EN/TXT/?uri=COM:2025:17:FIN. Accessed: 2025-09-30

[57] N. Apergis, H. Fahmy, Geopolitical risk and energy price crash risk. Energy Economics **140**, 107975 (2024)

[58] T. Van de Graaf, I. Overland, D. Scholten, K. Westphal, The new oil? the geopolitics and international governance of hydrogen. Energy Research & Social Science **70**, 101667 (2020)

[59] S. Yu, Y. Fan, Z. Shi, J. Li, X. Zhao, T. Zhang, Z. Chang, Hydrogen-based combined heat and power systems: A review of technologies and challenges. International Journal of Hydrogen Energy **48**(89), 34906–34929 (2023)

[60] J.A. Kuiper, V.C. Tidwell, A.B. Orr, J.J. Quinn, K. Quinter, V. Koritarov, D.A. Ladner, Modeling power plant siting opportunities and constraints in the eastern interconnection. Tech. rep., Argonne National Laboratory (ANL), Argonne, IL (United States) (2022). https://doi.org/10.2172/1861485. URL https://www.osti.gov/biblio/1861485

[61] J.P. Jimenez-Navarro, K. Kavvadias, F. Filippidou, M. Pavičević, S. Quoilin, Coupling the heating and power sectors: The role of centralised combined heat and power plants and district heat in a european decarbonised power system. Applied Energy **270**, 115134 (2020)

[62] IEA. Cogeneration and renewables (2011). URL https://iea.blob.core.windows.net/assets/f88eee81-deba-4abf-9fb8-34ba2b8cb9d6/CoGeneration_RenewablesSolutionsforaLowCarbonEnergyFuture.pdf. Accessed: 2026-02-10

[63] IEA. Cogeneration and district energy (2009). URL https://iea.blob.core.windows.net/assets/5c02850f-e951-4f4b-abae-f55cc29275f8/CogenerationandDistrictEnergy.pdf. Accessed: 2026-02-10

[64] A. Abuzayed, M. Liebensteiner, N. Hartmann, Hydrogen-ready power plants: Optimizing pathways to a decarbonized energy system in germany. Applied Energy **395**, 126228 (2025)

[65] M.R. Edwards, Z.H. Thomas, G.F. Nemet, S. Rathod, J. Greene, K. Surana, K.M. Kennedy, J. Fuhrman, H.C. McJeon, Modeling direct air carbon capture and storage in a 1.5°C climate

future using historical analogs. Proceedings of the National Academy of Sciences **121**(20), e2215679121 (2024)

[66] E.M. Rogers, *Diffusion of Innovations* (Free Press, New York, 1963)

[67] M. Hobday, The project-based organisation: an ideal form for managing complex products and systems? Research policy **29**(7-8), 871–893 (2000)

[68] E. Von Hippel, "sticky information" and the locus of problem solving: implications for innovation. Management science **40**(4), 429–439 (1994)

[69] Rolls Royce. Our businesses) (2026). URL https://www.rolls-royce.com/about/our-businesses.aspx. Accessed: 2026-02-10

[70] GE Vernova. Businesses) (2026). URL https://www.gevernova.com/. Accessed: 2026-02-10

[71] European Commission – Joint Research Centre. General equilibrium model – economy, energy, environment (GEM-E3) (2024). URL https://web.jrc.ec.europa.eu/policy-model-inventory/explore/models/model-gem-e3/. Accessed: 2025-01-10

[72] L. Davis, C. Hausman, Market impacts of a nuclear power plant closure. American Economic Journal: Applied Economics **8**(2), 92–122 (2016)

[73] M. Ram, M. Child, A. Aghahosseini, D. Bogdanov, A. Lohrmann, C. Breyer, A comparative analysis of electricity generation costs from renewable, fossil fuel and nuclear sources in g20 countries for the period 2015-2030. Journal of cleaner production **199**, 687–704 (2018)

[74] K.Y. Liang, S.L. Zeger, Longitudinal data analysis using generalized linear models. Biometrika **73**(1), 13–22 (1986)

[75] J. Sitarz, M. Pahle, S. Osorio, G. Luderer, R. Pietzcker, EU carbon prices signal high policy credibility and farsighted actors. Nature Energy **9**(6), 691–702 (2024)

[76] J. Ling, H. Yang, G. Tian, J. Cheng, X. Wang, X. Yu, Direct reduction of iron to facilitate net-zero emissions in the steel industry: A review of research progress at different scales. Journal of Cleaner Production **441**, 140933 (2024)

[77] D.R. Nhuchhen, S.P. Sit, D.B. Layzell, Alternative fuels co-fired with natural gas in the pre-calciner of a cement plant: Energy and material flows. Fuel **295**, 120544 (2021)

[78] Danish National Energy Agency. Technology data for industrial process heat (2026). URL https://ens.dk/en/analyses-and-statistics/technology-data-industrial-process-heat. Accessed: 2026-02-10

[79] R.M.L. Novaes, M.M.R. Moreira, S.M. Arantes, L.C. Bachion, T.A.D. Hernandes, Dealing with the iluc risk of biofuel production for the energy transition. Energy Policy **210**, 115035 (2026)

[80] J. Fargione, J. Hill, D. Tilman, S. Polasky, P. Hawthorne, Land clearing and the biofuel carbon debt. Science **319**(5867), 1235–1238 (2008)

[81] L. Dray, A.W. Schäfer, C. Grobler, C. Falter, F. Allroggen, M.E. Stettler, S.R. Barrett, Cost and emissions pathways towards net-zero climate impacts in aviation. Nature Climate Change **12**(10), 956–962 (2022)

[82] J. Holladay, Z. Abdullah, J. Heyne, Sustainable aviation fuel: Review of technical pathways. Tech. rep., USDOE Office of Energy Efficiency and Renewable Energy (EERE) (2020)

[83] D.R. Vardon, B.J. Sherbacow, K. Guan, J.S. Heyne, Z. Abdullah, Realizing "net-zero-carbon" sustainable aviation fuel. Joule **6**(1), 16–21 (2022)

[84] S. van Ewijk, W. McDowall, Diffusion of flue gas desulfurization reveals barriers and opportunities for carbon capture and storage. Nature Communications **11**(1), 4298 (2020)

[85] IEA. Net zero roadmap: A global pathway to keep the 1.5 °c goal in reach. (2023). URL https://iea.blob.core.windows.net/assets/8ad619b9-17aa-473d-8a2f-4b90846f5c19/NetZeroRoadmap_AGlobalPathwaytoKeepthe1.5CGoalinReach-2023Update.pdf. Accessed: 2026-02-10

[86] A. Gailani, S. Cooper, S. Allen, A. Pimm, P. Taylor, R. Gross, Assessing the potential of decarbonization options for industrial sectors. Joule **8**(3), 576–603 (2024)

[87] C.M. Woodall, Z. Fan, Y. Lou, A. Bhardwaj, A. Khatri, M. Agrawal, C.F. McCormick, S.J. Friedmann, Technology options and policy design to facilitate decarbonization of chemical manufacturing. Joule **6**(11), 2474–2499 (2022)

[88] IEA. Technology roadmap - energy and ghg reductions in the chemical industry via catalytic processes (2013). URL https://iea.blob.core.windows.net/assets/d0f7ff3a-0612-422d-ad7d-a682091cb500/TechnologyRoadmapEnergyandGHGReductionsintheChemicalIndustryviaCatalyticProcesses.pdf. Accessed: 2026-02-10

[89] P. Gabrielli, L. Rosa, M. Gazzani, R. Meys, A. Bardow, M. Mazzotti, G. Sansavini, Net-zero emissions chemical industry in a world of limited resources. One Earth **6**(6), 682–704 (2023)

[90] D.S. Mallapragada, Y. Dvorkin, M.A. Modestino, D.V. Esposito, W.A. Smith, B.M. Hodge, M.P. Harold, V.M. Donnelly, A. Nuz, C. Bloomquist, et al., Decarbonization of the chemical industry through electrification: Barriers and opportunities. Joule **7**(1), 23–41 (2023)

[91] T. Cordero-Lanzac, A.G. Gayubo, A.T. Aguayo, J. Bilbao, The mto and dto processes as greener alternatives to produce olefins: A review of kinetic models and reactor design. Chemical Engineering Journal **494**, 152906 (2024)

[92] Methanol Institute. Production of methanol worldwide from 2017 to 2022 (in million metric tons). Statista (2022). URL https://www.statista.com/statistics/1323406/methanol-production-worldwide/. Graph. Retrieved March 11, 2026

[93] Methanol Market Services Asia (MMSA). Distribution of methanol supply worldwide in 2020, by region. Statista (2021). URL https://www.statista.com/statistics/1323622/distribution-of-methanol-supply-worldwide-by-region/. Graph. Retrieved March 11, 2026

[94] M. Rumayor, A. Dominguez-Ramos, A. Irabien, Toward the decarbonization of hard-to-abate sectors: a case study of the soda ash production. ACS Sustainable Chemistry & Engineering **8**(32), 11956–11966 (2020)

[95] M. Maslin, L. Van Heerde, S. Day, Sulfur: A potential resource crisis that could stifle green technology and threaten food security as the world decarbonises. The Geographical Journal **188**(4), 498–505 (2022)

[96] S.J. Faucher, M.R. Shaner, S.T. Omelchenko, G. Anikeeva, I.S. McKay, Gypsum as a feedstock for low-cost, decarbonized portland cement and sulfuric acid. ACS Sustainable Chemistry & Engineering **13**(11), 4290–4301 (2025)

[97] F. Rosner, T. Bhagde, D.S. Slaughter, V. Zorba, J. Stokes-Draut, Techno-economic and carbon dioxide emission assessment of carbon black production. Journal of Cleaner Production **436**, 140224 (2024)

[98] A. Levesque, S. Osorio, S. Herkel, M. Pahle, Rethinking the role of efficiency for the decarbonization of buildings is essential. Joule **7**(6), 1087–1092 (2023)

[99] IEA. Heating (2026). URL https://www.iea.org/energy-system/buildings/heating#home-heating-technologies. Accessed: 2026-02-10

[100] J. Rosenow, A meta-review of 54 studies on hydrogen heating. Cell Reports Sustainability **1**(1) (2024)

[101] H. Lund, P.A. Østergaard, P. Sorknæs, S. Nielsen, I.R. Skov, M. Yuan, J.Z. Thellufsen, B.V. Mathiesen, S.M. Benson, A. Jentsch, et al., District heating in clean energy systems. Nature Reviews Clean Technology **1**(8), 532–546 (2025)

[102] V. Soltero, R. Chacartegui, C. Ortiz, R. Velázquez, Potential of biomass district heating systems in rural areas. Energy **156**, 132–143 (2018)

[103] P. Plötz, Hydrogen technology is unlikely to play a major role in sustainable road transport. Nature electronics **5**(1), 8–10 (2022)

[104] B. Nykvist, O. Olsson, The feasibility of heavy battery electric trucks. Joule **5**(4), 901–913 (2021)

[105] M. Bampaou, K.D. Panopoulos, An overview of hydrogen valleys: Current status, challenges, and their role in increased renewable energy penetration. Renewable and Sustainable Energy Reviews **207**, 114923 (2025)

[106] T. Verger, U. Azimov, O. Adeniyi, Biomass-based fuel blends as an alternative for the future heavy-duty transport: A review. Renewable and Sustainable Energy Reviews **161**, 112391 (2022)

[107] X. Wu, J. Meng, X. Liang, L. Sun, D. Coffman, A. Kontoleon, D. Guan, Technological pathways for cost-effective steel decarbonization. Nature pp. 1–9 (2025)

[108] Z. Fan, S.J. Friedmann, Low-carbon production of iron and steel: Technology options, economic assessment, and policy. Joule **5**(4), 829–862 (2021)

[109] W. Kim, I. Sohn, Critical challenges facing low carbon steelmaking technology using hydrogen direct reduced iron. Joule **6**(10), 2228–2232 (2022)

[110] LeadIT. Green steel tracker. leadership group for industry transition (2025). URL https://www.industrytransition.org/trackers/green-steel-tracker/download-green-steel-dataset/. Accessed: 2026-02-10

[111] Bloomberg New Energy Finance. Scaling up hydrogen. the case for low-carbon steel (2024). URL https://assets.bbhub.io/media/sites/25/2024/01/Scaling-Up-Hydrogen-The-Case-For-Low-Carbon-Steel-Bloomberg-New-Economy.pdf. Accessed: 2026-02-10

[112] IEA. Steel (2026). URL https://www.iea.org/energy-system/industry/steel. Accessed: 2026-02-10

[113] L. Zore. Decarbonization options for the aluminium industry (2024). URL https://publications.jrc.ec.europa.eu/repository/handle/JRC136525. Accessed: 2026-02-10

[114] F.T. Röben, N. Schöne, U. Bau, M.A. Reuter, M. Dahmen, A. Bardow, Decarbonizing copper production by power-to-hydrogen: A techno-economic analysis. Journal of Cleaner Production **306**, 127191 (2021)

[115] G. Clark, M. Davis, A. Kumar, The development of a framework to compare carbon capture and storage technologies as a means of decarbonizing cement production. Renewable and Sustainable Energy Reviews **214**, 115556 (2025)

[116] Cermaneunie. Ceramic roadmap to 2050 (2021). URL https://www.cerameunie.eu/media/zyqdwwwp/ceramic-roadmap-to-2050.pdf. Accessed: 2026-02-10

[117] M. Zier, P. Stenzel, L. Kotzur, D. Stolten, A review of decarbonization options for the glass industry. Energy Conversion and Management: X **10**, 100083 (2021)

[118] A. Giampieri, J. Ling-Chin, Z. Ma, A. Smallbone, A. Roskilly, A review of the current automotive manufacturing practice from an energy perspective. Applied Energy **261**, 114074 (2020)

[119] CEFS. Cefs climate neutrality toolbox (2023). URL https://cefs.org/wp-content/uploads/2023/06/CEFS-Climate-Neutrality-Toolbox-2.pdf. Accessed: 2026-02-10

[120] S.J. Davis, N.S. Lewis, M. Shaner, S. Aggarwal, D. Arent, I.L. Azevedo, S.M. Benson, T. Bradley, J. Brouwer, Y.M. Chiang, et al., Net-zero emissions energy systems. Science **360**(6396), eaas9793 (2018)

[121] J.E. Bistline, G.J. Blanford, The role of the power sector in net-zero energy systems. Energy and Climate Change **2**, 100045 (2021)

[122] K. Oshiro, S. Fujimori, Limited impact of hydrogen co-firing on prolonging fossil-based power generation under low emissions scenarios. Nature Communications **15**(1), 1778 (2024)

[123] U.S. Government Accountability Office. Electricity: Information on peak demand power plants (2024). URL https://www.gao.gov/assets/gao-24-106145.pdf. Accessed: 2025-01-10

[124] IEA. Managing the seasonal variability of electricity demand and supply (2024). URL https://www.iea.org/reports/managing-the-seasonal-variability-of-electricity-demand-and-supply. Accessed: 2026-02-10

[125] S. Ingvarsson, M. Odenberger, F. Johnsson, The chemical pulp mill as a flexible prosumer of electricity. Energy conversion and Management: X **20**, 100401 (2023)

[126] K. Kuparinen, E. Vakkilainen, Green pulp mill: renewable alternatives to fossil fuels in lime kiln operations. BioResources **12**(2), 4031–4048 (2017)

[127] F.H. Joyo, B. Nastasi, D.A. Garcia, Decarbonization pathways for the pulp and paper industry: A comprehensive review. Renewable and Sustainable Energy Reviews **223**, 116070 (2025)

[128] IEA. Paper (2023). URL https://www.iea.org/energy-system/industry/paper. Accessed: 2026-02-10

[129] Eurostat. Oil and petroleum products - a statistical overview (2025). URL https://ec.europa.eu/eurostat/statistics-explained/index.php?title=Oil_and_petroleum_products_-_a_statistical_overview. Accessed: 2026-02-10

[130] M. Zanon-Zotin, L.B. Baptista, R. Draeger, P.R. Rochedo, A. Szklo, R. Schaeffer, Unaddressed non-energy use in the chemical industry can undermine fossil fuels phase-out. Nature Communications **15**(1), 8050 (2024)

[131] A. Nurdiawati, F. Urban, Decarbonising the refinery sector: A socio-technical analysis of advanced biofuels, green hydrogen and carbon capture and storage developments in sweden. Energy Research & Social Science **84**, 102358 (2022)

[132] S.P. Pyl, C.M. Schietekat, M.F. Reyniers, R. Abhari, G.B. Marin, K.M. Van Geem, Biomass to olefins: Cracking of renewable naphtha. Chemical engineering journal **176**, 178–187 (2011)

[133] DNV. Energy transition outlook 20255. maritime forecast to 2050 (2026). Accessed: 2026-02-10

[134] Ricardo Energy & Environment. Study on the readiness and availability of low- and zero-carbon ship technology and marine fuels. Report prepared for the International Maritime Organization (IMO) (2023). URL https://wwwcdn.imo.org/localresources/en/MediaCentre/WhatsNew/Documents/MEPC80.INF10.pdf. Accessed 10 February 2026

[135] C. Eaucci, C. McKinlay, A. Karan. The future of maritime fuels (2023). URL https://maritime.lr.org/l/941163/2023-09-04/86cyj/941163/1693881339KV19NyGO/LR_Fuel_Mix_Report_v1.pdf. Accessed: 2026-02-10

[136] Council of the European Union. Fit for 55 (2025). URL https://www.consilium.europa.eu/en/policies/fit-for-55/. Accessed: 2025-09-30

[137] J. Abrell. Documentation for the european union transaction log database (2021). Database documentation

[138] European Commission, Directorate-General for Climate Action. Update of benchmark values for the years 2021–2025 of phase iv of the EU ETS (2021). URL https://climate.ec.europa.eu/system/files/2021-10/policy_ets_allowances_bm_curve_factsheets_en.pdf. Accessed: 2025-01-10

[139] M. Neuwirth, T. Fleiter, P. Manz, R. Hofmann, The future potential hydrogen demand in energy-intensive industries-a site-specific approach applied to germany. Energy Conversion and Management **252**, 115052 (2022)

[140] S. Kiemel, R. Miehe, S. Glöser-Chahoud, A. Sauer, Proposed method for identifying industrial hydrogen demands–structural basics of a transferable procedure model. Journal of Cleaner Production **457**, 142299 (2024)

[141] European Commission - The Joint Research Centre: EU Science Hub. Energy and ghg reductions in the chemical industry via catalytic processes: Annexes (2013). URL https://iea.blob.core.windows.net/assets/fc71e0ab-aef1-4d06-b9c2-caf293a91c6e/Technology_Roadmap_Catalytic_Processes_Annexes.pdf. Accessed: 2025-01-10

[142] NREL. Hydrogen conversion factors and fact cards (revised) (2013). URL https://docs.nrel.gov/docs/gen/fy08/43061.pdf. Accessed: 2025-09-30

[143] E.S. Sman, B. van der Peerlings, L.A. Söffing, R.W.H. Brouwer, M.W. Adler, A. Jongeling, C. Behrens, M. Kieffer, Destination 2050 – roadmap. Tech. rep., Netherlands Aerospace Center (NLR) (2025). URL https://reports.nlr.nl/server/api/core/bitstreams/3051bcd9-5af9-4ac7-b39f-15fedd533980/content. Accessed: 2025-07-10

[144] Eurostat. Detailed air passenger transport routes by country (avia_par). https://ec.europa.eu/eurostat/databrowser/explore/all/transp?sort=category&lang=en&subtheme=avia.avia_go&display=list (2024). Accessed: 2025-01-10

[145] S. Beck, D. Fischer, A methodological framework for geospatial modelling of hydrogen demand in cities. Energy Informatics **6**(Suppl 1), 21 (2023)

[146] Eurostat. Detailed tables per reporting country (main ports) by direction, partner entity, type of cargo, and nationality of vessel registration – annual data (2024). URL https://ec.europa.eu/eurostat/databrowser/view/mar_go_am_se/default/table?lang=en. Accessed: 2025-01-10

[147] Freightwaves. How many gallons of fuel does a container ship carry? (2020). URL https://www.freightwaves.com/news/how-many-gallons-of-fuel-does-a-container-ship-carry. Accessed: 2025-09-30

[148] Eurostat. Transport by type of good (country/regional flows from 2007 onwards) (2025). URL https://ec.europa.eu/eurostat/databrowser/view/iww_go_atygofl/default/table?lang=en&category=iww.iww_go.iww_go_a. Accessed: 2025-09-30

[149] Eurostat. Freight loaded and unloaded in ports for inland waterway transport (2024). URL https://ec.europa.eu/eurostat/databrowser/product/page/IWW_GO_APORT. Accessed: 2025-01-10

[150] Eurostat. Territorialised road freight transport, by transport coverage – annual data (2024). URL https://ec.europa.eu/eurostat/databrowser/view/road_tert_go/default/table?

lang=en&category=road.road_tert. Accessed: 2025-01-10

[151] Hyundai Truck and Bus. Hyundai XCIENT (2020). URL https://hyundaihm.com/wp-content/uploads/2020/10/XCIENT-Fuel-Cellcatalog_print.pdf. Accessed: 2025-09-30

[152] I. Gonzalez Hidalgo, K. Kanellopoulos, M. De Felice, A. Bocin, JRC Open Power Plants Database (JRC-PPDB-OPEN). Tech. rep., European Commission, Joint Research Centre (JRC) (2019)

[153] Hotmaps. Heat density map (final energy demand for heating and dhw) of residential buildings in EU28 + switzerland, norway and iceland for the year 2015 (2020). URL https://gitlab.com/hotmaps/buildings/heat/heat_res_curr_density/-/blob/master/data/heat_res_curr_density_LAU2_ID_NUMBER.csv. Accessed: 2025-01-10

[154] GeoNames. cities.json (2021). URL https://github.com/lmfmaier/cities-json. GitHub repository, Accessed: 2024-12-31